

Copyright

by

Andrew Michael Moore

2010

**The Thesis Committee for Andrew Michael Moore
Certifies that this is the approved version of the following thesis:**

Shear Behavior of Prestressed Concrete U-beams

**APPROVED BY
SUPERVISING COMMITTEE:**

Supervisor:

Oguzhan Bayrak

James O. Jirsa

Shear Behavior of Prestressed Concrete U-beams

by

Andrew Michael Moore, BSCE

Thesis

Presented to the Faculty of the Graduate School of

The University of Texas at Austin

in Partial Fulfillment

of the Requirements

for the Degree of

Master of Science in Engineering

The University of Texas at Austin

December 2010

Dedication

This thesis is dedicated to my parents for their unending patience, love and support.

Acknowledgements

This research was made possible by the generous support of the Texas Department of Transportation. In particular, thanks to Dean Van Landuyt, Project Director, as well as the rest of the Project Monitoring Committee: John Holt, Graham Bettis, and Amy Eskridge. The second phase of this project was made possible by the donation of U-beam test specimens from the Precast Concrete Manufacturers' Association of Texas. Without whose help we would have not been able to pursue an effective solutions to the problems uncovered during this research.

Special thanks go to all of the students at Ferguson Lab whom postponed work on their own projects to help on concrete pours among other things. In particular, thanks to Alejandro Avendaño for helping through many shear tests and long days. Also thanks to all those directly involved with the U-beam project: Catherine Hovell, Dave Dunkman, and David Wald. It has been a pleasure working with all of you.

Dr. Bayrak deserves special recognition for allowing me to work on this research project for the past two years, and more importantly play in the lab's woodshop. Also thanks to the staff at Ferguson Lab: Blake Stasney, Dennis Fellip, Eric Schell, Mike Watson, Barbara Howard and Jessica Hanten. Particularly thanks to Andrew Valentine for, among many other things, the 2 AM wakeup calls on cast days.

Thanks to my parents, without your continued love, support and example this would not have been possible. Finally, thanks to Zoe Gannon for keeping me sane and for making my time away from the lab so much more enjoyable.

December 3, 2010

Abstract

Shear Behavior of Prestressed Concrete U-beams

Andrew Michael Moore, M.S.E.

The University of Texas at Austin, 2010

Supervisor: Oguzhan Bayrak

An experimental study was conducted at the Ferguson Structural Engineering Laboratory in order to investigate the shear behavior of 54-inch deep prestressed concrete U-beams. The primary goal of this research was to improve the design and detailing of the skewed end-blocks commonly used in these beams. As U-beams had been in service for several decades without incident, it was anticipated that there would be little need for change in the design, and the findings of the research would involve a slight tweaking to improve the overall performance.

Unfortunately, during the first phase of shear testing (testing of the current design standard) it was found that the U-beam was not reaching the code calculated shear capacity. During this phase of testing the premature failure mechanism was isolated as the breakdown of the web-to-flange interface in the end region of the girder.

Therefore, the second phase of testing sought to prevent the breakdown of this boundary by three options: (1) increasing the web width while maintaining current levels of mild reinforcement, (2) increasing the web width while also increasing the amount of

reinforcement crossing the web-to-flange boundary, or (3) by increasing the amount of reinforcement at the boundary while maintaining the current web width.

Two acceptable solutions to the premature failure method were developed and tested during this phase both of which included an increase in the amount of mild reinforcement crossing the web-to-flange interface (with and without an increase in web width). The research into refining of these new details is ongoing as part of the Texas Department of Transportation's Research Project number 0-5831.

Table of Contents

CHAPTER 1 INTRODUCTION.....	1
1.1 Overview.....	1
1.2 Project Objectives.....	2
1.3 Organization.....	3
CHAPTER 2 LITERATURE REVIEW.....	5
2.1 Overview.....	5
2.2 University of Texas Prestressed Concrete Shear Database.....	5
2.3 Need for Research.....	6
2.4 Recent Prestressed Concrete Shear Research.....	10
2.5 Summary.....	11
CHAPTER 3 EXPERIMENTAL PROGRAM.....	12
3.1 Overview.....	12
3.2 Test Specimen Design.....	12
3.3 Test Specimen Fabrication at Ferguson Laboratory (Beams 1-4).....	35
3.4 Test Specimen Fabrication at Precast Plant (Beam 5).....	48
3.5 Material Properties.....	50
3.6 Shear Testing.....	54
3.7 Summary.....	65
CHAPTER 4 PHASE I TEST RESULTS.....	66
4.1 Introduction.....	66

4.2	Phase I Test Results	67
4.3	Critical Evaluation of Phase I Beam Design.....	76
4.4	Summary.....	80
CHAPTER 5 PHASE II TEST RESULTS AND DISCUSSION.....		81
5.1	Introduction.....	81
5.2	Phase II Test Results.....	83
5.3	Understanding Differences between Phase I and Phase II Beams.....	93
5.4	Further Comparison of Beams 4 and 5	93
5.5	General Examination of Web-to-Flange Interface Failure	97
5.6	Summary.....	102
CHAPTER 6 SUMMARY, CONCLUSIONS AND RECOMMENDATIONS.....		104
6.1	Summary.....	104
6.2	Conclusions and Recommendations	105
6.3	Future Work	107

APPENDIX A.....	108
APPENDIX B.....	132
APPENDIX C.....	138
APPENDIX D.....	147
APPENDIX E.....	157
APPENDIX F.....	175
REFERENCES.....	181
VITA	183

List of Tables

Table 3-1: Summary of details for Beams 1 through 5.....	13
Table 3-2: Concrete mixture design.....	50
Table 3-3: Concrete compressive strengths	51
Table 3-4: Transverse reinforcing bar properties.....	51
Table 3-5: Helical and Linear Elastic Modulus' for Prestressing Strand	52
Table 4-1: Service level shear cracking observed in Beams 1 through	70
Table 5-1: Summary of Phase II Shear Testing	100

List of Figures

Figure 2-1: UTPCSDB Member Type Histogram	7
Figure 2-2: U-Beam Layout with Full Strand Profile	7
Figure 2-3: UTPCSDB Width of Bottom Flange to Width of Web	8
Figure 2-4: UTPCSDB Overall Member Height Histogram	9
Figure 2-5: UTPCSDB Concrete Compressive Strength Histogram	10
Figure 3-1: U-Beam geometry	14
Figure 3-2: Standard end block reinforcement layout	15
Figure 3-3: R-Bar	17
Figure 3-4: X-Bar	17
Figure 3-5: S-Bar	17
Figure 3-6: S-Bar	17
Figure 3-7: C-Bar	17
Figure 3-8: C-Bar	17
Figure 3-9: U-Beam Shear Reinforcement Plan	18
Figure 3-10: Rendering and cross section of Beam 1	19
Figure 3-11: Beams 1, 2 and 3 end region web cross section	20
Figure 3-12: Beam 1 primary shear reinforcement (R bars) layout	21
Figure 3-13: Prestressing strand pattern for Beams 1 through 4	22
Figure 3-14: Rendering and cross section of Beam 2	23
Figure 3-15: Beam 2 primary shear reinforcement (R bars) layout	24
Figure 3-16: Rendering and cross section of Beam 3	25
Figure 3-17: Beam 3 primary shear reinforcement (R bars) layout	26
Figure 3-18: Beam 3 debonding pattern	27

Figure 3-19: Sample of debonded U-beams in the State of Texas	28
Figure 3-20: Debonding and sealing of strand.....	28
Figure 3-21: Rendering of Beam 4	29
Figure 3-22: Beam 4 rebar layout	30
Figure 3-23: Beam 4 North reinforcement profile	31
Figure 3-24: Beam 4 South reinforcement profile	31
Figure 3-25: Rendering of Beam 5	32
Figure 3-26: Beam 5 reinforcement layout.....	33
Figure 3-27: Beam 5 end region web cross section	34
Figure 3-28: Beam 5 strand layout.....	34
Figure 3-29: Ferguson Laboratory prestressing bed	35
Figure 3-30: Assembly of mild steel reinforcement with sideforms in-place	36
Figure 3-31: Beam 4 rebar cage assembly	37
Figure 3-32: Gang-stressing plate being monitored during stressing	38
Figure 3-33: Modified formwork from Hamilton Forms (Dunkman 2009)	39
Figure 3-34: Custom interior void from Hamilton Forms	39
Figure 3-35: Design of wooden interior void for Beam 4	40
Figure -3-36: Construction of wooden interior void.....	41
Figure 37: Wooden interior void during construction prior to plywood skin installation	42
Figure 3-38: U-beam casting procedure:.....	43
Figure 3-39: “Sure Cure” match curing system.....	44
Figure 3-40: Thermocouple locations.....	45
Figure 3-41: Prestress Transfer.....	47
Figure 3-42: Construction sequence of Beam 5.....	49

Figure 3-43: Unprotected foil strain gauge on strand	53
Figure 3-44: Shear test frame mounted on elevated strong floor at FSEL	55
Figure 3-45: Loading configuration for all beams	57
Figure 3-46: External post-tensioning stirrups	58
Figure 3-47: Locations and uses of instrumentation during shear testing	59
Figure 3-48: Encapsulated foil strain gauge for rebar and installed gauges	60
Figure 3-49: Two inch linear potentiometer	61
Figure 3-50: (A) Linear potentiometer measuring deflection during shear testing and (B) Correction of deflection readings for deflection at support	62
Figure 3-51: Strand slip gauge	62
Figure 3-52: Shear deformation setup	63
Figure 3-53: 1,000-kip load cells	64
Figure 3-54: Description of reported shear values	64
Figure 4-1: Beam 2 North, Web-to-Flange Interface Failure Crack	72
Figure 4-2: Beam 3 South, Web-to-Flange Interface Failure Crack	73
Figure 4-3: Summary of Phase I Shear Tests (Hovell, et al. 2010)	75
Figure 4-4: Transverse reinforcement crossing the web-to-flange interface	78
Figure 4-5: Location of Shear Deformation and Internal Strain Gauges	79
Figure 4-6: Graph of Diagonal Shear Deformation Gauge Beam 3 South	80
Figure 5-1: Description of beam designs tested in Phase II of Research	82
Figure 5-2: Phase II service level cracking behavior	84
Figure 5-3: Interior of Beam 4 Showing Web-to-Flange Interface Failure	87
Figure 5-4: Beam 4 South Cracking at Maximum Applied Load	88
Figure 5-5: Strain gauge location in reference to Figure 5-6	89

Figure 5-6: Beam 4 South Strain Gauge Data from Transverse Shear Reinforcement	89
Figure 5-7: Beam 5 North cracking at failure	90
Figure 5-8: Beam 5 post-failure	91
Figure 5-9: Beam 5 post-failure showing large permanent displacement	91
Figure 5-10: Tested verses Calculated Capacities, Phase II Beams (Hovell, et al. 2010)	92
Figure 5-11: Cracking Comparison for Beam 4 South and Beam 5 (Hovell, et al. 2010)	94
Figure 5-12: Bottom clear-cover in Beam 5	95
Figure 5-13: Manual Installation of Rebar Chairs for Beam 5	96
Figure 5-14: Rebar Tie Wire Holding Reinforcement for proper cover from	96
Figure 5-15: Web-to-Flange Interface Failure	98
Figure 5-16: Variables affecting the susceptibility of prestressed concrete beams to failures at the web-to-flange interface	99
Figure 5-17: Clamping force illustration (Birkeland and Birkeland 1966)	102

CHAPTER 1

Introduction

1.1 OVERVIEW

The primary objective of this research project is to improve the design and detailing of the skewed end-blocks in the Texas Department of Transportation's (TxDOT) Prestressed Concrete U-beam (hereafter referred to as U-beams). These pretensioned beams have been in service for nearly two decades. Few structural problems had been reported over this time, and no major structural changes were anticipated at the inception of this research project. However it was expected that a few minor changes could be made in an effort to improve the constructability and serviceability of these beams.

Unfortunately, the results from shear tests performed on the first two beams indicated that the current U-beam design could not reach the calculated shear capacity. After an exhaustive analysis of the results, the decision was made to thoroughly investigate the overall shear performance of the U-beams as an alternative to the study of the behavior of skewed end-blocks. Thus three additional beams were constructed and tested in an effort to:

- Understand the effect of debonded strands on shear performance.
- Develop a solution for the poor shear performance of the current U-beam design by incorporating both geometric and reinforcing bar changes to the design.

- Develop an alternative solution for the poor shear performance by incorporating changes to the reinforcement while maintaining the current geometry.

1.2 PROJECT OBJECTIVES

The objective of this research is to understand the structural behavior of the U-beam in relation to:

- Curing temperature concerns
- End-block geometry
- Behavior at release (bursting and spalling)
- Behavior under shear loading

This thesis is focused on the behavior under shear loading while the other aspects of the behavior of these beams will be covered in future thesis and/or dissertations..

1.2.1 Project Direction

The shear tests on the first two beam specimens resulted in failures below the calculated shear capacity. These first two beams contained fully bonded strands along the beam length in an effort to maximize the bursting stresses and to prevent a flexural failure during shear testing.

The third beam specimen focused on shear behavior of a U-beam containing debonded strands. TxDOT allows up to 75% of strands to be debonded in the end-region of a prestressed beam. In order to model a typical girder, a sampling of U-beams currently in service was taken. The third beam followed the average of this sampling in an effort to understand the shear behavior of typical U-beams currently in service.

The results of the first three shear tests indicated that the premature shear failure resulted from a breakdown along the web-to-bottom flange boundary in the end region of the beam. This information was used to develop three new end-region details designed to prevent failure along this horizontal interface. It was understood that some combination of increasing the web thickness and increasing the steel crossing the web-to-bottom flange boundary would be necessary in order to produce a beam which behaved adequately under shear loading. Therefore three options were tested:

- Thickened web walls with minimal increase in the transverse reinforcement crossing the web-to-bottom flange boundary.
- Thickened web walls with a large increase to the transverse reinforcement.
- Maintaining the current web width with a large increase in transverse reinforcement.

Only Two of the three solutions tested were deemed as viable options because the solution in which thicker webs and low transverse reinforcement was used did not reach the calculated shear capacity. The results of these tests as well as a discussion on the merits of each solution are presented in this thesis.

1.3 ORGANIZATION

In chapter two past research on the shear behavior of prestressed concrete girders is presented. It should be noted that although there is extensive research on the shear behavior of prestressed members, the shear performance of members with multiple webs has received limited attention in experimental research.

Chapter three describes the experimental program which was developed to study the behavior of the U-Beams. This includes the design of each specimen and the instrumentation and testing equipment used during this project.

The findings of the shear tests performed on the U-Beams are divided into Phase I and Phase II results (chapters four and five respectively). In Phase I, the behavior of the U-Beam design currently being used by the Texas Department of Transportation is reviewed while Phase II testing includes redesigns of the U-Beam in order to improve the beam's performance under shear loading. Chapter six completes the discussion on the behavior of U-beams with a comprehensive evaluation on the findings of the research presented in this thesis.

CHAPTER 2

Literature Review

2.1 OVERVIEW

A large number of technical reports are available that summarize the structural behavior of prestressed members under shear loading. Due to the ease of access to these papers (which are listed in Section 2.4) there will be no repetition of their results here. Instead, the need for research into the shear behavior which is particular to the U-Beam is the focus of this review.

2.2 UNIVERSITY OF TEXAS PRESTRESSED CONCRETE SHEAR DATABASE

The University of Texas Prestressed Concrete Shear Database (UTPCSDB) contains the results of 506 shear tests conducted from 1954 to 2008 from universities across the country (Avendaño, Shear Strength and Behavior of Prestressed Concrete Beams 2008). This database is currently being expanded to include another 405 tests conducted in Japan as part of an auxiliary research project by Eisuke Nakamura. These results along with 47 more tests (including those conducted during this research project) conducted at the University of Texas since the database was first published now make up a database of 958 shear tests on prestressed concrete members. The findings of this database are outside of the scope of this research and are expected to be published at a later date by Mr. Nakamura, but the database does provide valuable insight into the need for research which prompted the study of the U-Beams.

2.3 NEED FOR RESEARCH

Many of the shear design equations used in modern structural design practice were calibrated with the results of the tests performed on members of small size. In recent years, there has been an emphasis on research seeking to validate these sectional shear equations on full scale specimens. The vast majority of the research to date has involved rectangular or I-shaped members. Although the I-shaped and bulb-tee beams are the most common type of bridge girder sections used in the field, there has been a shift in interest in the last two decades to include box girders, and even more recently U-beams into the catalog for bridge design. These two options have advantages beyond those associated with structural performance, but due to their recent introduction there have been few full-scale tests performed on these specimens. Therefore by the nature of its rarity, the research discussed herein is of utmost importance in understanding the behavior of members with two webs, or more specifically the standardized Texas U54-beam.

As illustrated in Figure 2-1 the vast majority of the research to date has involved members with only one web. In this context, the term “research” is (and will be) used to abbreviate “research on shear behavior of precast prestressed concrete beams.” The twenty-nine tests on multi-webbed girders shown here were conducted as part of this research project, and the results of the shear tests on the box-beams will be published upon this project’s completion. The recent shear tests at the University of Texas makeup the entirety of tests on multi-webbed members available in the literature. This makes them of paramount importance in understanding the behavior of such structural components.

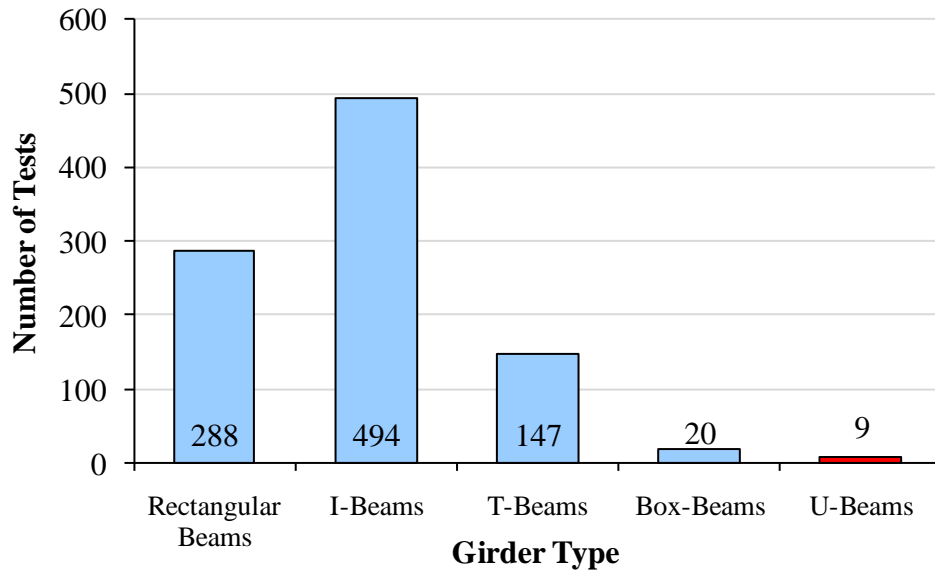


Figure 2-1: UTPCSDB Member Type Histogram (U-Beams in Red)

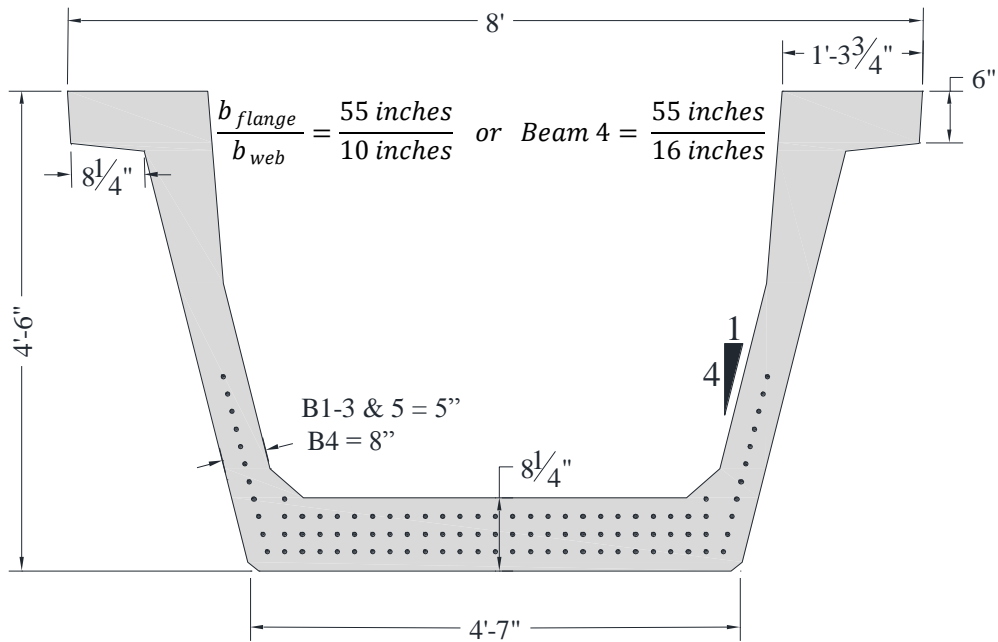


Figure 2-2: U-Beam Layout with Full Strand Profile

The geometry of the U-Beam requires a large bottom flange to contain the ninety-nine total strand positions possible in this design. As a result the ratio of the width of the bottom flange to the web is relatively large (shown in Figure 1-2). The rarity of shear tests performed on specimens with this large ratio is illustrated in Figure 2-3. It should be noted that out of all tests on members whose web to flange ratio exceeds that of the U-Beam only five exceed 24-inches in height.

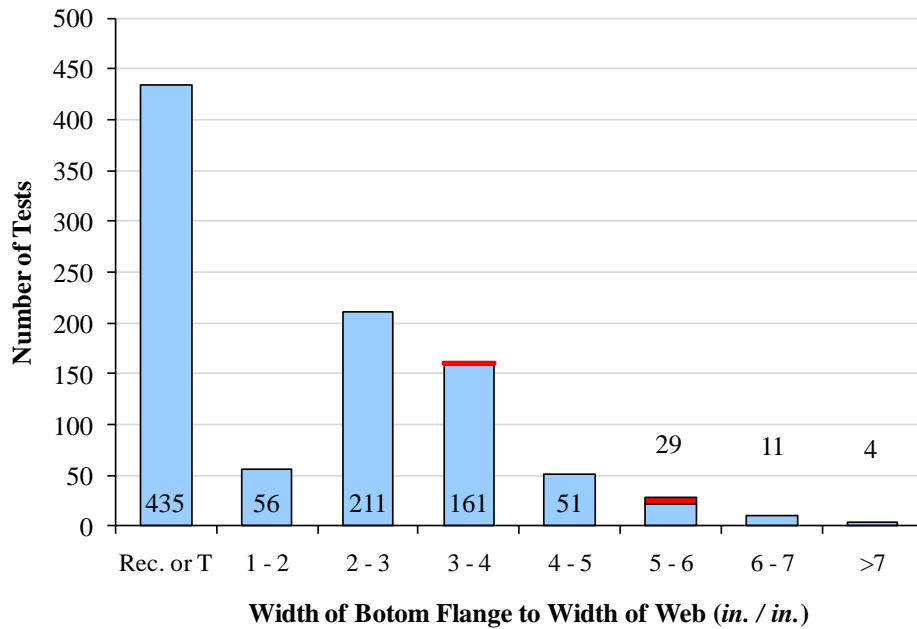


Figure 2-3: UTPCSDB Width of Bottom Flange to Width of Web (U-Beams in red)

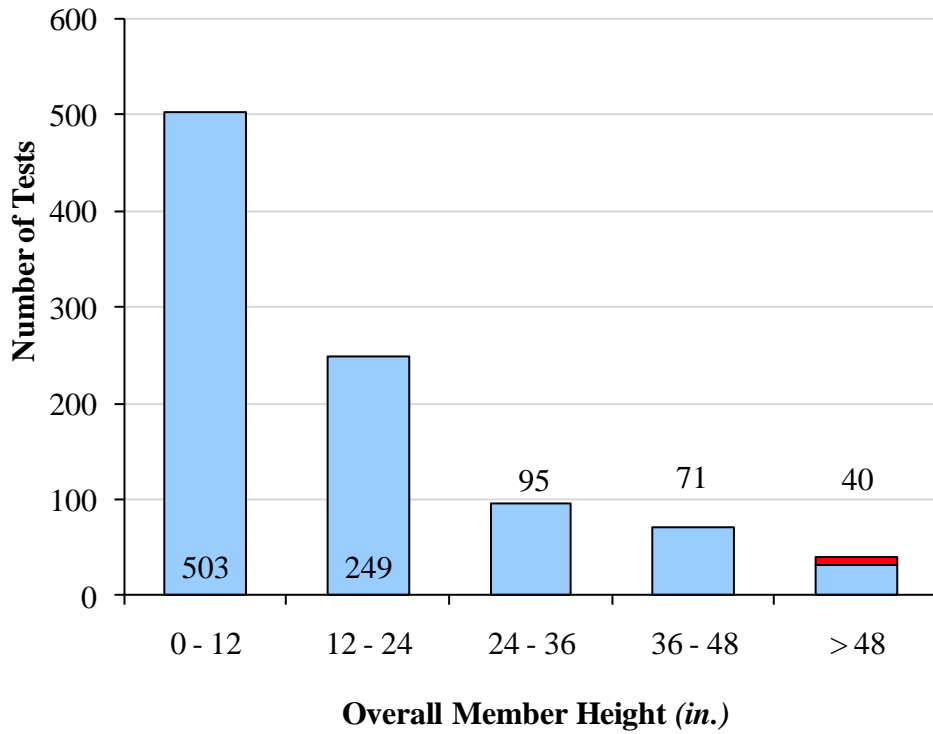


Figure 2-4: UTPCSDB Overall Member Height Histogram (U-Beams in red)

The height (including the deck) of the U-Beams tested in this program is 62.75-inches. As shown in Figure 2-4, the height of the U-Beams tested exceeds all but about 4-percent of the 958 members included in the database. This is another important area of interest because as was stated previously most shear design equations were developed on relatively small scale members and it is important to verify these results on full scale specimens.

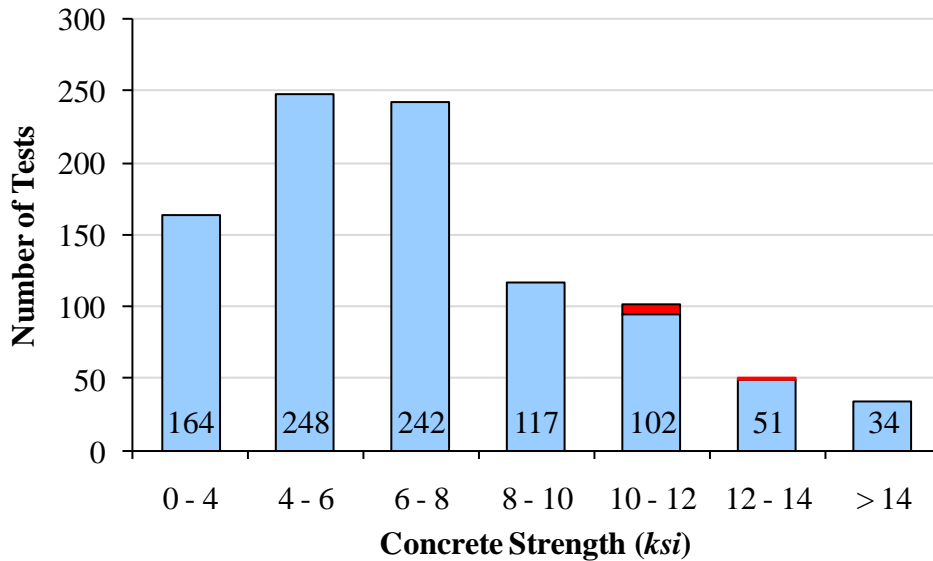


Figure 2-5: UTPCSDB Concrete Compressive Strength Histogram (U-Beams in red)

The average concrete strength of the girders tested in this program was 11,800-psi. Although the shear behavior of high-strength concrete has attracted some recent attention it is still an area which requires additional research. As such the average concrete strength of the U-Beams presented in this thesis fall into the upper 10th percentile of all tests recorded in the database.

2.4 RECENT PRESTRESSED CONCRETE SHEAR RESEARCH

Research on prestressed concrete shear has evolved from the small scale specimens used in the development of the first code equations to the full scale testing of prestressed members. Due to the large number of recent reports on prestressed concrete shear behavior a summary of the behavior of prestressed concrete in shear is not given in this thesis. A listing of the most recent research publications into the shear behavior of

prestressed concrete, is presented and complete references can be found in the bibliography of this thesis:

- Topic: Comprehensive View of Prestressed Concrete Shear Behavior:
 - Avendaño, 2008
 - National Cooperative Highway Research Program Report 579, 2007
 - National Cooperative Highway Research Program Report 549, 2005
 - ACI445R-99, 1999
- Topic: Effect of Debonded Strands on Shear Behavior
 - Llanos, Ross, Hamilton, 2009
- Topic: Non-traditional Shear Failures
 - Nagle, Kuchma 2007

2.5 SUMMARY

To understand the shear performance of U-beams, 958 test results included in the University of Texas Prestressed Concrete Shear Database were examined. This examination demonstrated that there is little data in the literature on the shear behavior of U-Beams. As such, the need for an experimental research program is clear.

CHAPTER 3

Experimental Program



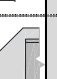








3.1 OVERVIEW

In order to understand the structural behavior of a U-beam it was necessary to test at full scale. Therefore five beams were constructed and tested in shear in order to determine their structural adequacy. Of these five beams, four were constructed at Ferguson Structural Engineering Laboratory (FSEL) and one was constructed at a local precast plant. All U-beams were tested in a load frame specifically designed for this project in order to deliver the large loads needed to ensure shear failure of the specimens.

3.2 TEST SPECIMEN DESIGN

To understand the test specimen design it is necessary to understand the evolution of the research goals. Beams 1 and 2 were constructed to investigate the bursting and shear behavior of two possible skewed end block designs illustrated in Sections 3.2.2 and 3.2.2.1. The results from the first two shear tests were shown to be unconservative when compared to the calculated shear capacities. The scope of the project was therefore modified in order to gain a better understanding of both the cause of the premature shear failure and new reinforcement detailing and/or geometry to improve the performance of future beams. Beams 3 through 5 featured standard square ends and a variety of modifications meant to investigate the effects of strand debonding, web width, and web reinforcement detailing. In Table 3-1, the pertinent details of each test specimen are summarized.

Table 3-1: Summary of details for Beams 1 through 5

Main Parameter under study	Beam	End	Exterior beam geometry	Interior void geometry	End-block description	Web width (single web)	No. of 0.5" Ø strands in btm flange (includes debonded)	No. debonded	Primary shear reinf. within first 5 feet of beam	Primary shear reinf. per web within first 5 feet of beam	Supplementary web-to-flange boundary reinforcement	Supplementary web-to-flange boundary reinforcement	Total web-to-flange boundary reinforcement per web
						<i>in.</i>	<i>No.</i>	<i>No.</i>	<i>no. & spacing</i>	<i>A_{st} /ft.</i>	<i>no. & spacing</i>	<i>A_{st} /ft.</i>	<i>A_{st} /ft.</i>
Influence of skew on structural performance	1	North	Square	Square		5	78	0	#4 @ 4-in.	0.6	0	0	0.6
		South	45° skew	45° skew		5	78	0	#4 @ 4-in.	0.6	0	0	0.6
	2	North	Square	Square		5	78	0	#4 @ 4-in.	0.6	0	0	0.6
		South	45° skew	Square		5	78	0	#4 @ 4-in.	0.6	0	0	0.6
Effect of Debonding	3	North	Square	Square		5	78	36	#4 @ 4-in.	0.6	0	0	0.6
		South	Square	Square		5	78	36	#4 @ 4-in.	0.6	0	0	0.6
Effect of web width and web-to-flange boundary	4	North	Square	Square		8	78	0	#4 @ 3-in.	0.8	0	0	0.8
		South	Square	Square		8	78	0	#4 @ 3-in.	0.8	(3) #5 @ 3-in.	3.72	4.52
	5	North	Square	Square		5	66	0	#5 @ 4-in.	0.93	#6 @ 4-in.	1.32	2.25
		South	Square	Square		5	66	0	#5 @ 4-in.	0.93	#6 @ 4-in.	1.32	2.25

3.2.1 Current Design Standard (2006)

The original concept for the current U-beam dates back to the early 1990's. The design was detailed in a PCI Journal article by Ralls, Ybanez and Panak (1993) and plans were first issued in 1993. The main difference between the current and past standards is a reduction in the reinforcement spacing toward the quarter points of the beam. The reduction in spacing was changed in the last modification to the design standard issued in 2006. Although the transverse reinforcement design has changed slightly, the geometry of the cross-section is the same as the original design (Figure 3-1).

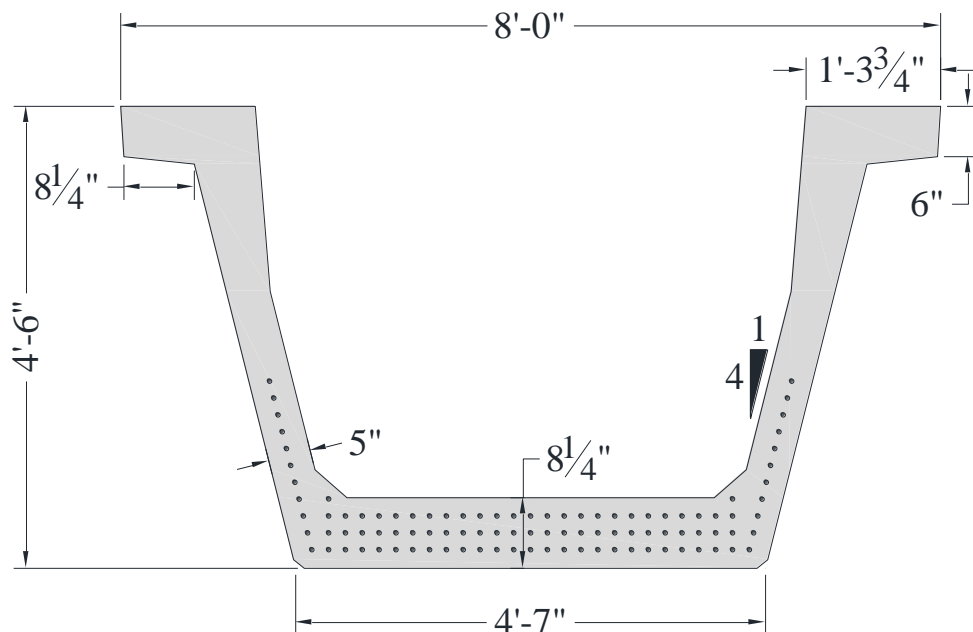
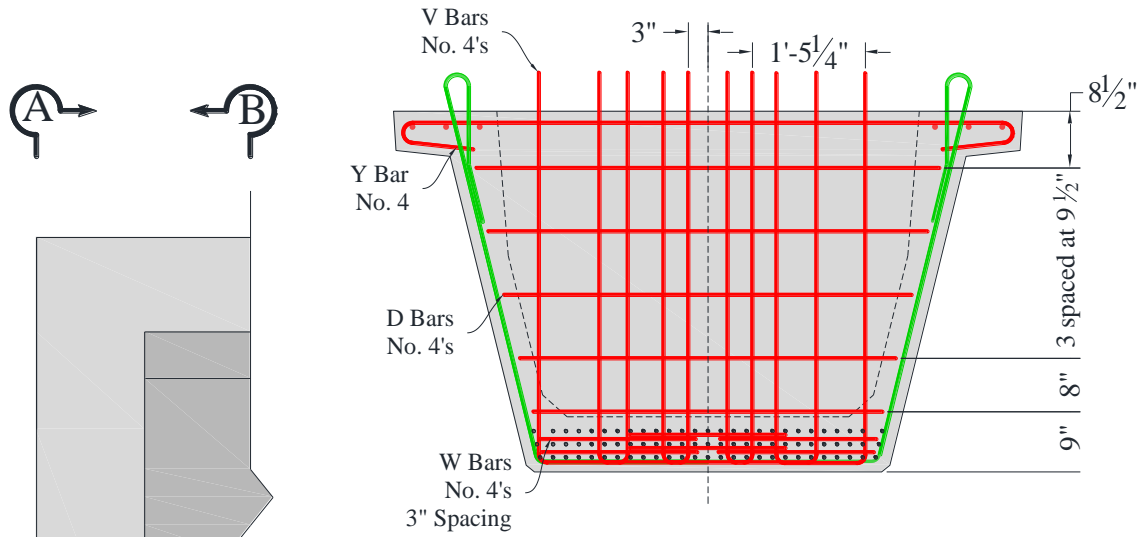


Figure 3-1: U-Beam geometry

All U-beams include a heavily reinforced end block, as well as intermediate diaphragms that act to tie the beam's webs together during transport and construction. The end-block includes two planes of reinforcement as shown in Sections A-A and B-B of Figure 3-2. The end-block also includes bursting reinforcement to resist release stresses (labeled "W bars" in Section A-A of Figure 3-2).

Section A – A



Section B – B

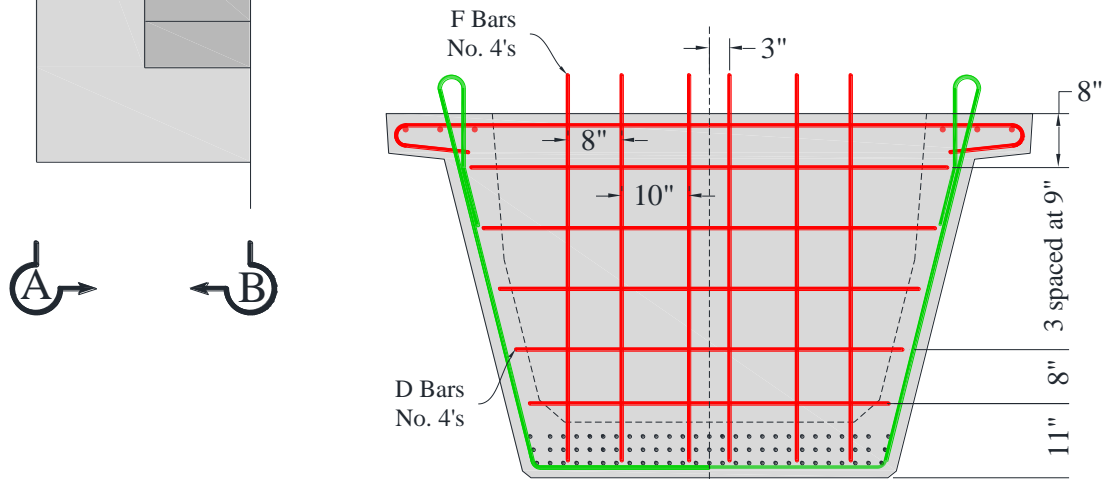


Figure 3-2: Standard end block reinforcement layout

The web reinforcement found along the length of the U-beam consists of R-bars (shown in Figure 3-3) and X-bars (shown in Figure 3-4). The R-bars run the full depth of the web and are lap spliced under the layers of prestressing strand. The R-bars also protrude from the top of the beam to facilitate composite action between the girder and a future bridge deck. X-bars are provided to reinforce the top flange and provide continuity with the webs. The X-bars have little effect on the shear performance of a U-beam and are primarily responsible for preventing damage to the top flange during construction. The transverse layers of reinforcement are spaced on 4-inch centers for the first 6 feet of the beam, 6-inch centers for the next 9 feet, and are eventually increased to a spacing of 8, 10, and 18-inches toward girder midspan (as shown in Figure 3-9). The exact locations of these transitions can be found in the TxDOT standard specifications for U-beams, located in Appendix F.

Over the course of the project, additional reinforcement details were evaluated and are included here to facilitate comparisons. These details included supplemental shear reinforcement (S-bars) and confinement steel (C-bars). The shape and positioning of the S- and C-bars are illustrated in Figure 3-5 through Figure 3-8. Detailed dimensions for all the reinforcing bars can be found in Appendix F.

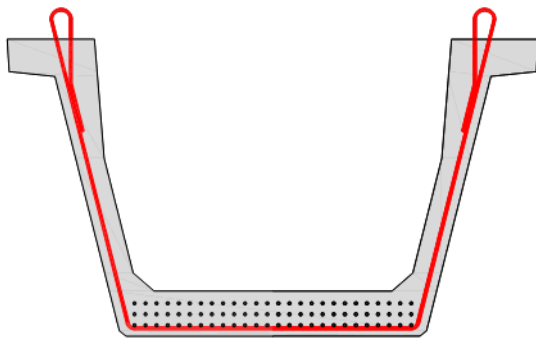


Figure 3-3: R-Bar

No. 4: Beams 1-4
 No. 5: Beam 5
 Standard shape

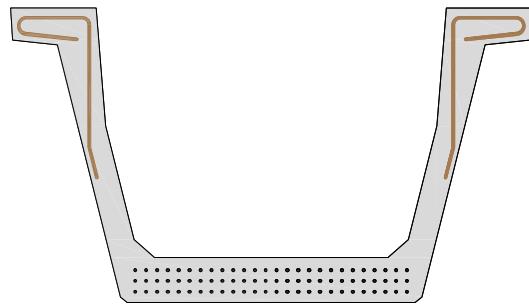


Figure 3-4: X-Bar

No. 4: Beams 1-5
 Standard shape

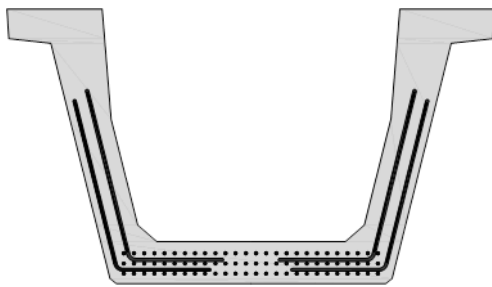


Figure 3-5: S-Bar

No. 5: Beams 4
 Nonstandard shape

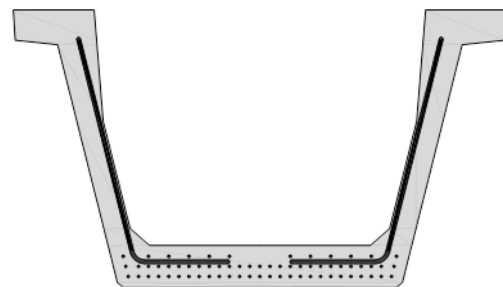


Figure 3-6: S-Bar

No. 6: Beam 5
 Nonstandard shape

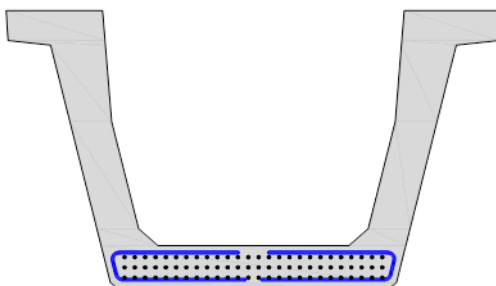


Figure 3-7: C-Bar

No. 4: Beam 4
 Nonstandard shape

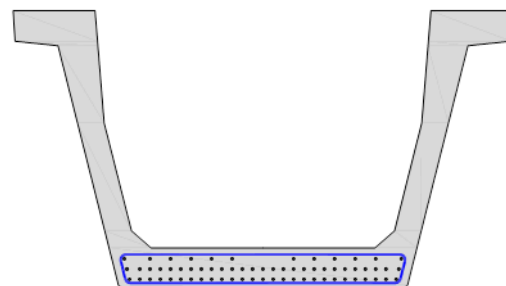


Figure 3-8: C-Bar

No. 4: Beam 4
 Nonstandard shape

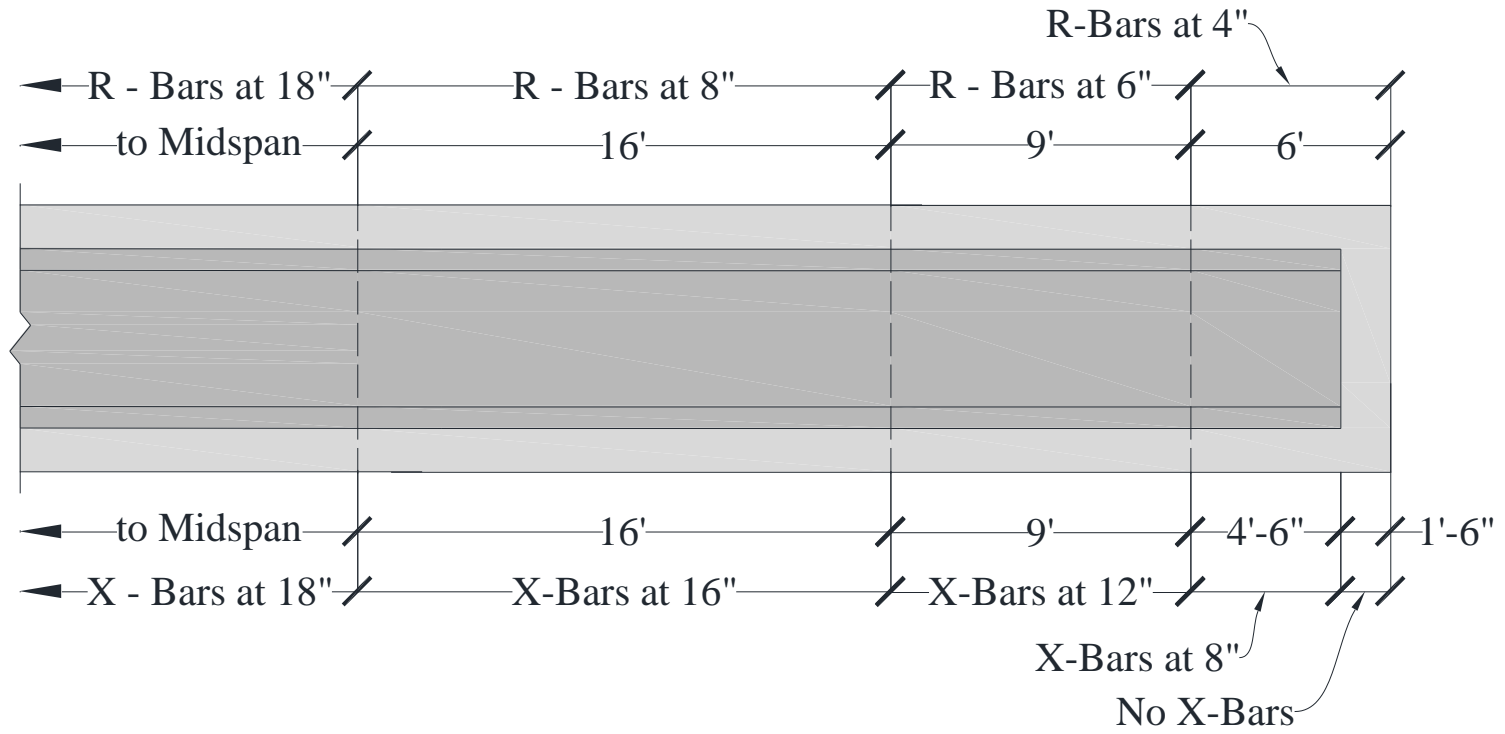


Figure 3-9: U-Beam Shear Reinforcement Plan

3.2.2 Beam 1 Design

Beam 1 was fabricated at Ferguson Structural Engineering Laboratory to evaluate the bursting and shear performance of a standard U-beam with a skewed interior void. The specimen had one 45-degree skewed end block and one square end block as shown in Figure 3-10 and Figure 3-12. The design of this beam focused on evaluating the structural performance of the skewed end-block. The 45-degree skew of this end block is currently allowed in the TxDOT standards, but it is never used due to the need for additional skewed interior void forms. The benefit of this end block configuration is the reduction of concrete mass in the end block. High curing temperatures generated by mass concrete have the potential to induce delayed ettringite formation and/or excessive amounts of internal microcracking in concrete. In general, fresh concrete exposure to high temperatures may lead to a drastically reduced service life.

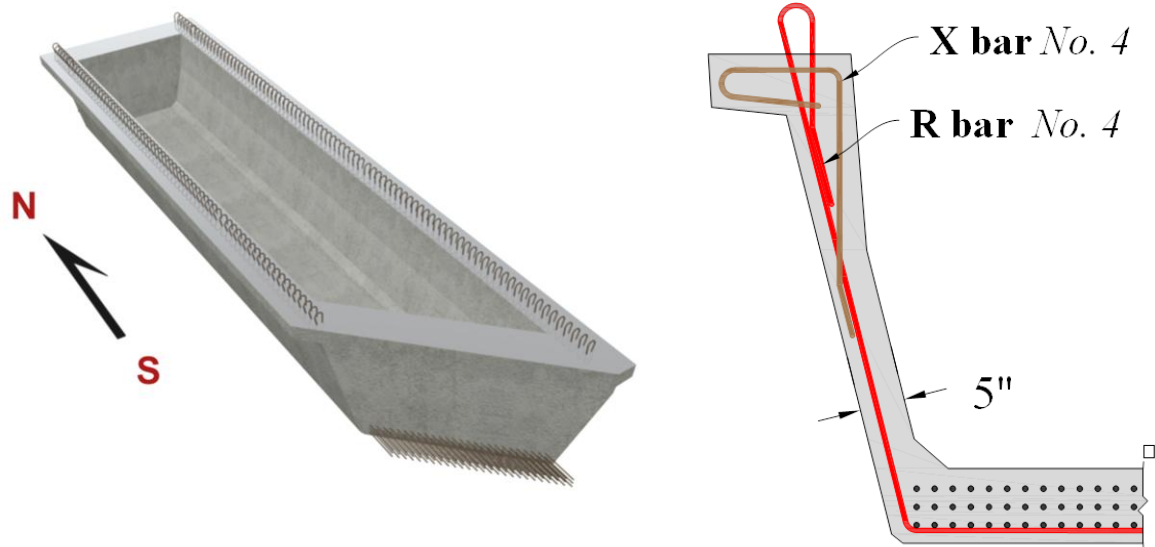


Figure 3-10: Rendering and cross section of Beam 1

The transverse reinforcement layout of Beam 1 followed the current standard design issued by TxDOT (shown in Figure 3-11 and Figure 3-12). This included No. 4 R-bars as the primary shear reinforcement spaced at 4-inches for the first 6.25-feet from the beam face (slight variation for the skewed angle shown in Figure 3-12) after which the spacing was increased to 6-inches for the remainder of the beam.

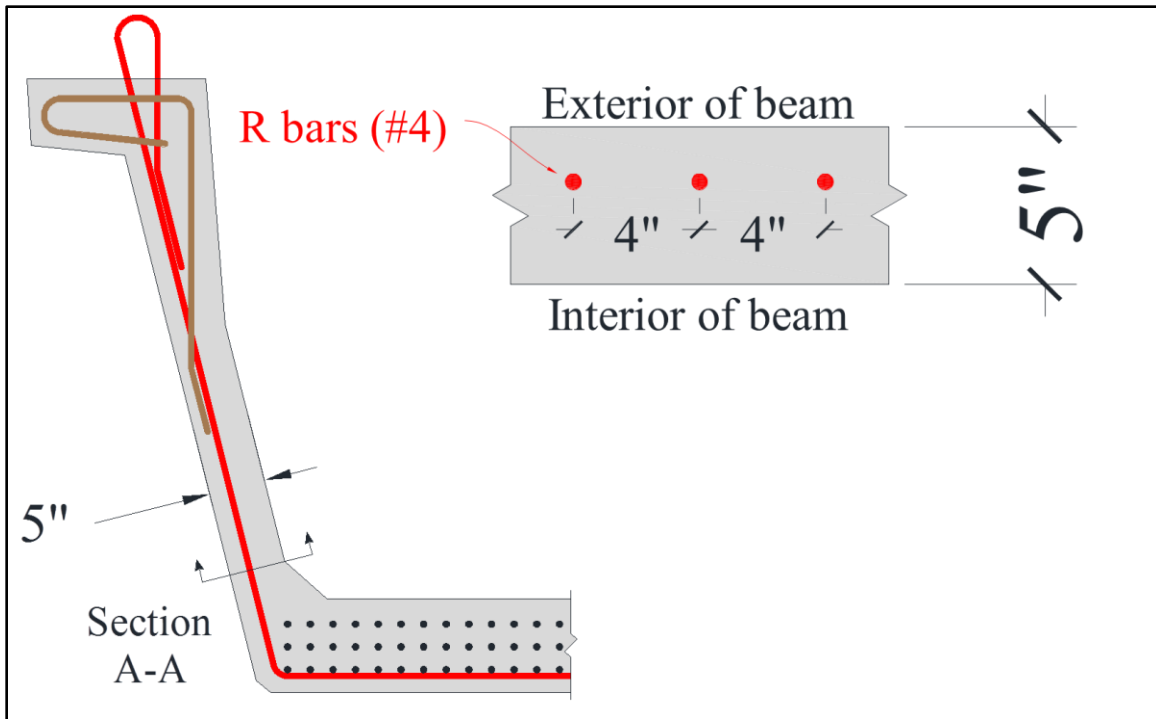


Figure 3-11: Beams 1, 2 and 3 end region web cross section

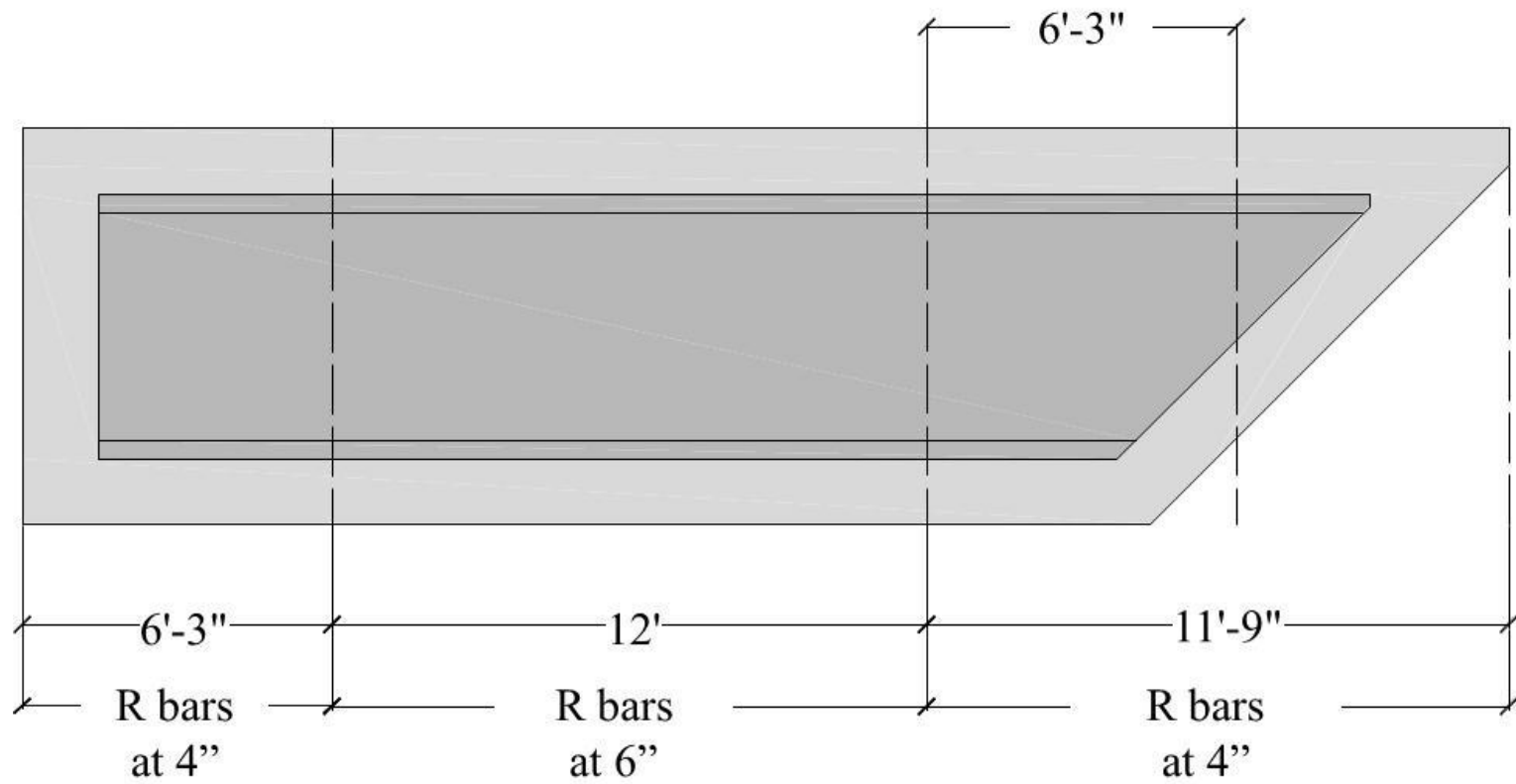


Figure 3-12: Beam 1 primary shear reinforcement (R bars) layout

3.2.2.1 *Beam 1 Flexural Steel Design*

Beam 1 contained 78 0.5-inch prestressing strands as the primary longitudinal reinforcement arranged in three rows of 26 strands (shown in Figure 3-13). This pattern was maintained in Beams 1 through 4 (with the exception of the debonded strands in Beam 3). The large amount of steel insured that: (1) bursting stresses were maximized and (2) flexural failure was prevented during shear testing. Although a relatively large amount of flexural steel was present in these beams they were still consistent with the typical strand patterns (albeit in longer beams) seen in use in Texas. Therefore the strand pattern satisfies the basic design premise that the shear tests of these specimens are meant to represent the end regions of typical U-beams currently in use in the State of Texas.

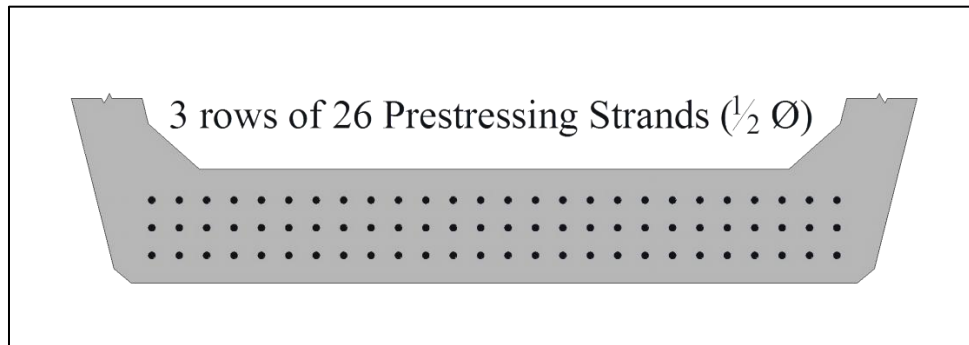


Figure 3-13: Prestressing strand pattern for Beams 1 through 4 (78 total)

3.2.3 Beam 2 Design

Beam 2 was fabricated to provide a direct comparison between the skewed interior void (small end block) and square interior void (large end block shown in Figure 3-14 and Figure 3-15) configurations permitted at skewed ends. Therefore the beam contained the same transverse reinforcement profile as was used in Beam 1 (shown in Figure 3-11) with the exception that the north end contained welded wire reinforcement (WWR) which had a higher yield strength (location of WWR shown in Figure 3-15). The second configuration, with an angled exterior face and square interior face, is the most common configuration for skewed U-beams constructed in the State of Texas. The popularity of the square interior void is rooted in fabricator preferences and has nothing to do with structural adequacy of the detail. As mentioned in Section 3.2.2 this end-block configuration may lead to high curing temperatures that could result in thermal cracking and provide a condition conducive to DEF.

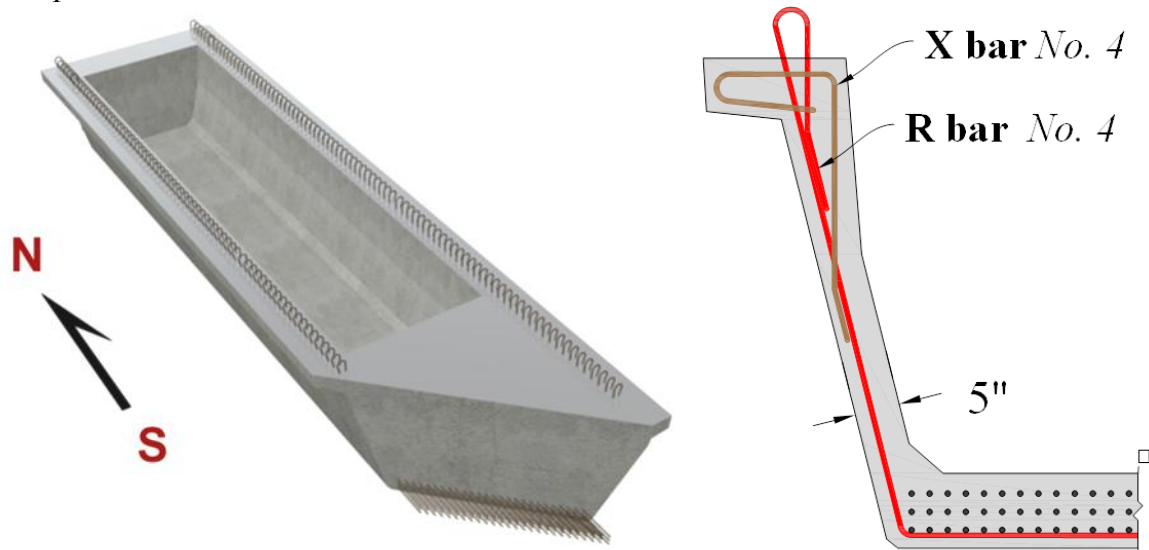


Figure 3-14: Rendering and cross section of Beam 2

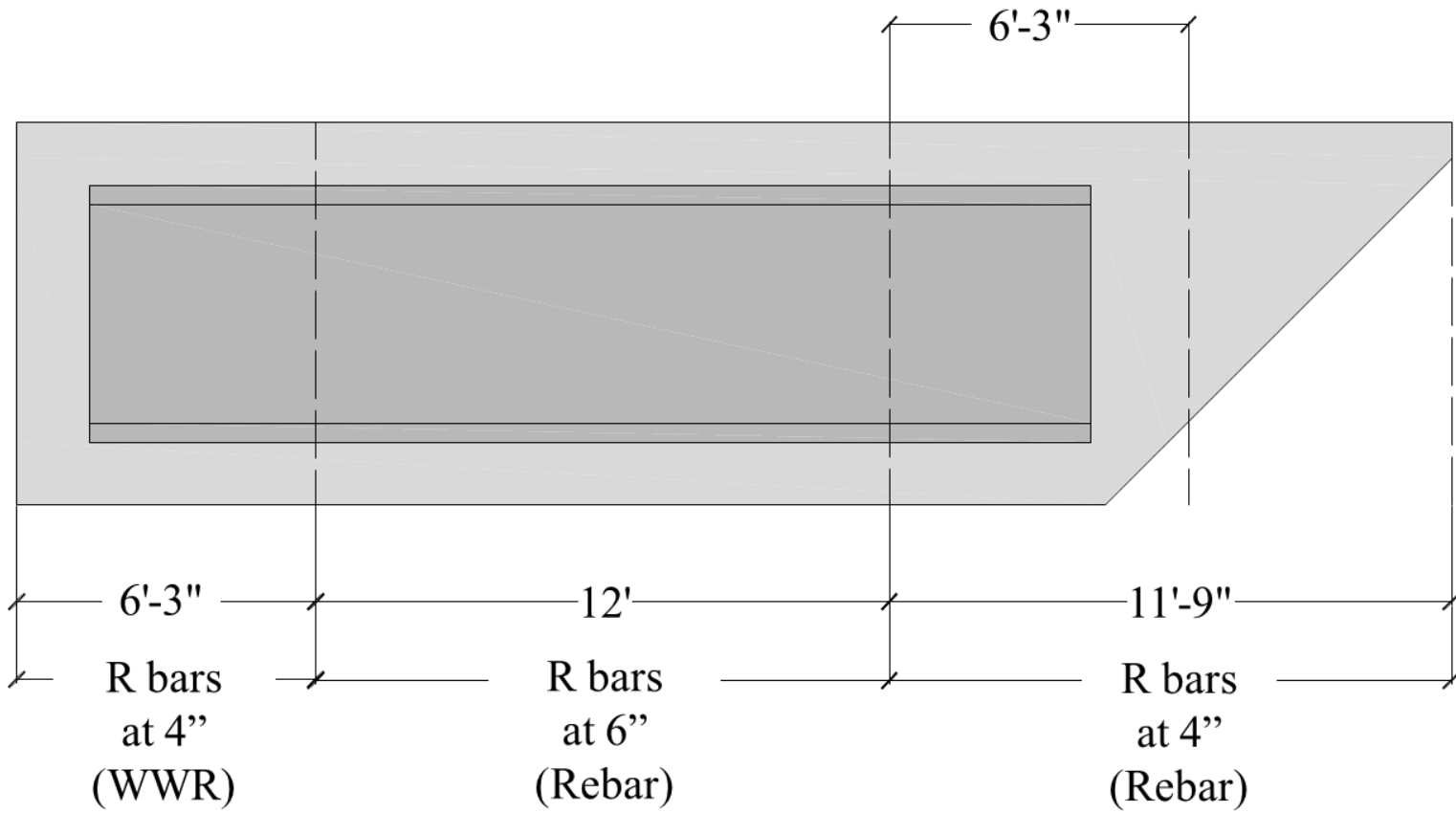


Figure 3-15: Beam 2 primary shear reinforcement (R bars) layout

3.2.4 Beam 3 Design

The ultimate shear strength of Beams 1 and 2 was less than calculated using code provisions for shear capacity, irrespective of the void geometry (detailed results are presented in Chapter 4). The low shear strength raised concerns with regard to in-service U-beams that had a large percentage of tendons debonded. Adequate anchorage of the flexural reinforcement is essential to full development of shear capacity. To further investigate the detrimental effects of strand debonding on standard U-beams, a large percentage of strands were debonded in Beam 3. Square end blocks and standard reinforcement details were implemented, as shown in Figure 3-16 and Figure 3-17.

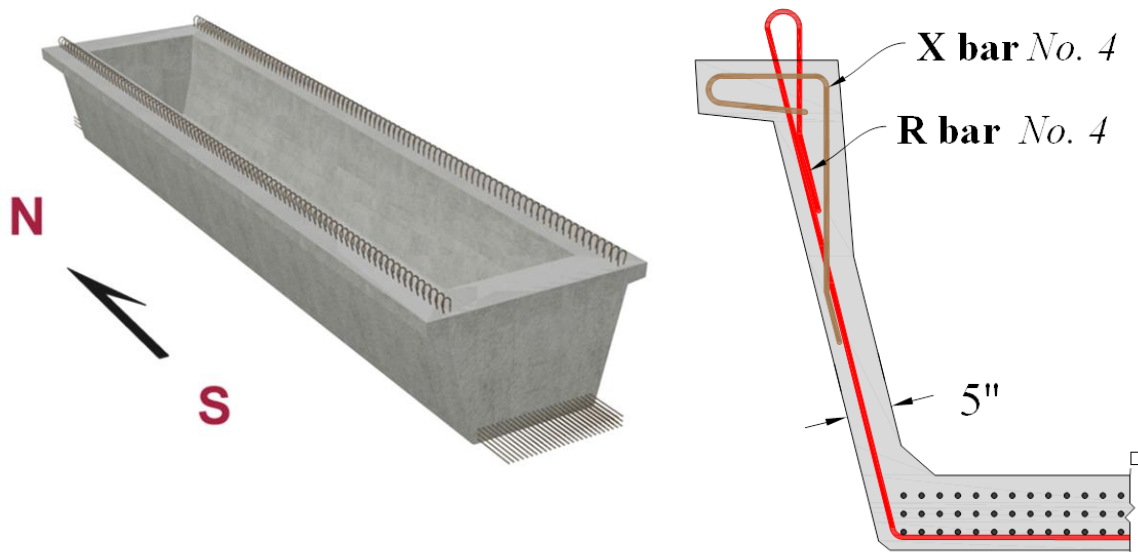


Figure 3-16: Rendering and cross section of Beam 3

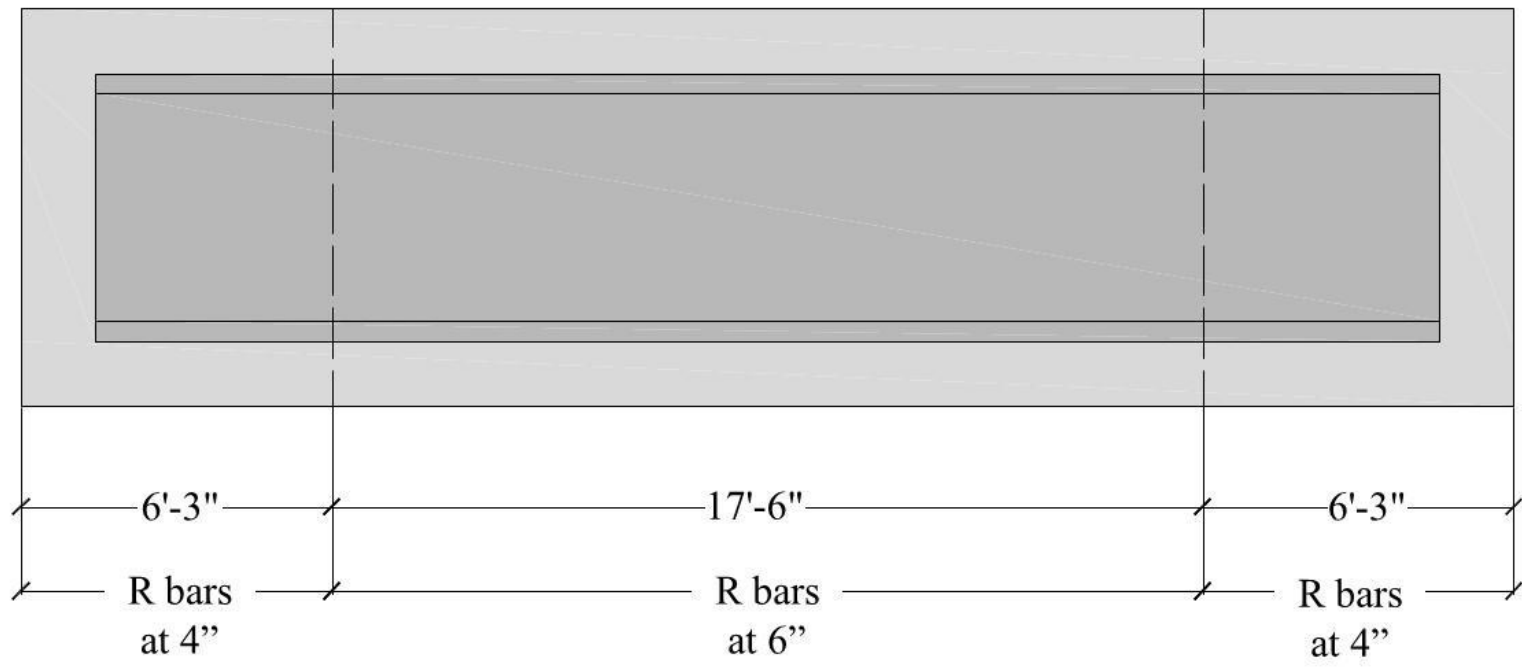


Figure 3-17: Beam 3 primary shear reinforcement (R bars) layout

The pattern of debonding in Beam 3 was configured to represent current practice in the State of Texas. From the debonding pattern shown in Figure 3-18 it is evident that the majority of bonded strands are placed at the center of the cross section *and* the two outermost columns of the strand pattern are fully bonded. TxDOT currently allows a maximum of 75% of the strands to be debonded. For reference, the maximum percentage of debonded strands specified in the 2009 Interim AASHTO LRFD Bridge Design Specifications is 25%. A sample of U-beams currently in service within the State of Texas was reviewed to identify an average strand debonding of 41%. In order to follow standard practice, while still including enough prestressing steel to prevent flexural failure, 46% of the strands within Beam 3 were debonded in a similar pattern to that observed in the field (Figure 3-19).

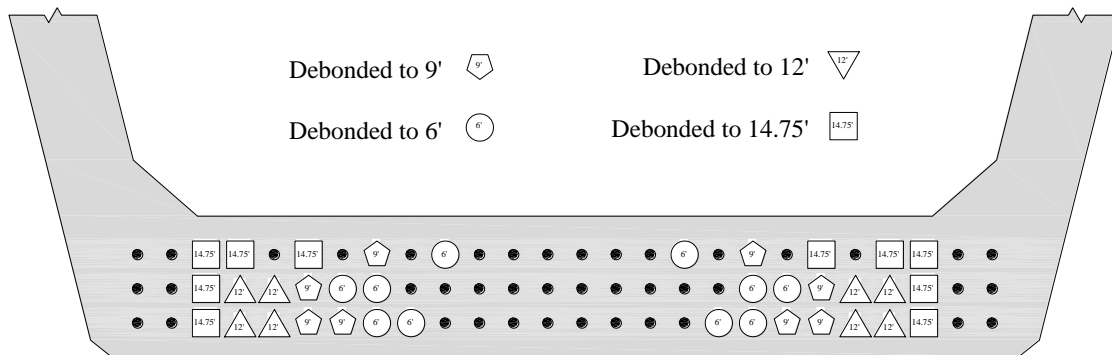


Figure 3-18: Beam 3 debonding pattern

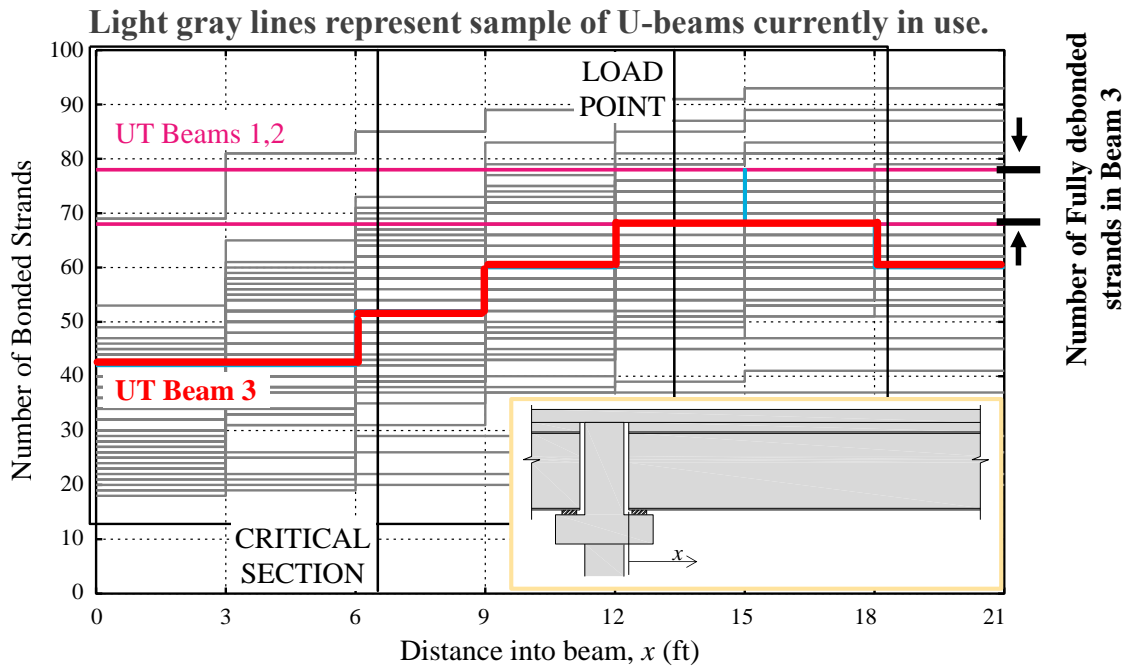


Figure 3-19: Sample of debonded U-beams in the State of Texas (Beam 3 in red)

The bond between the strand and concrete was broken by wrapping and sealing the strands with plastic sleeves and duct tape, as seen in Figure 3-20. This debonding technique is routinely used in all prestressed concrete beam fabrication plants in the State of Texas.



Figure 3-20: Debonding and sealing of strand

3.2.5 Beam 4 Design

Results from the first three beams provided a clear understanding of the deficiencies of the current design standard. Although presented in detail within Chapter 4, premature breakdown of the boundaries between the bottom flange and webs (i.e. web-to-flange interface failure) precluded the standard U-beam from developing the code-calculated shear capacity.

Beam 4 (shown in Figure 3-21) was designed to evaluate the effects of thickened webs, with and without an increase in the amount of transverse steel. Fabrication of Beam 4 required a new interior void form (detailed in Section 3.3.3) and the introduction of S- and C- bars (shown in Figure 3-22, Figure 3-23 and Figure 3-24 but also referenced in Section 3.2.1). The purpose of Beam 4 was to investigate potential solutions to the poor shear performance of Beams 1 through 3 (which complied with the current design standard), while providing a better understanding of the interaction between the steel and concrete contributions to shear strength.

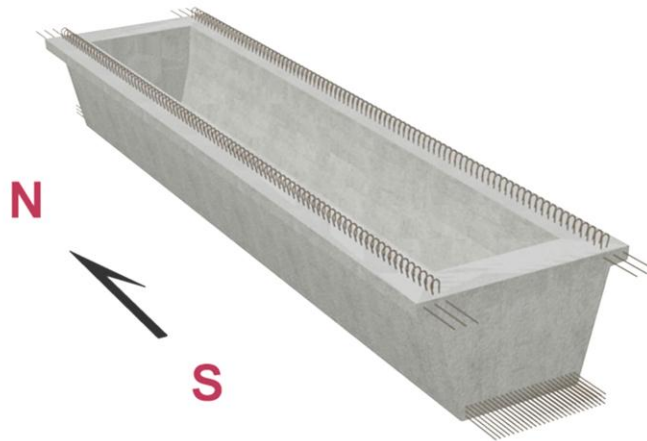


Figure 3-21: Rendering of Beam 4

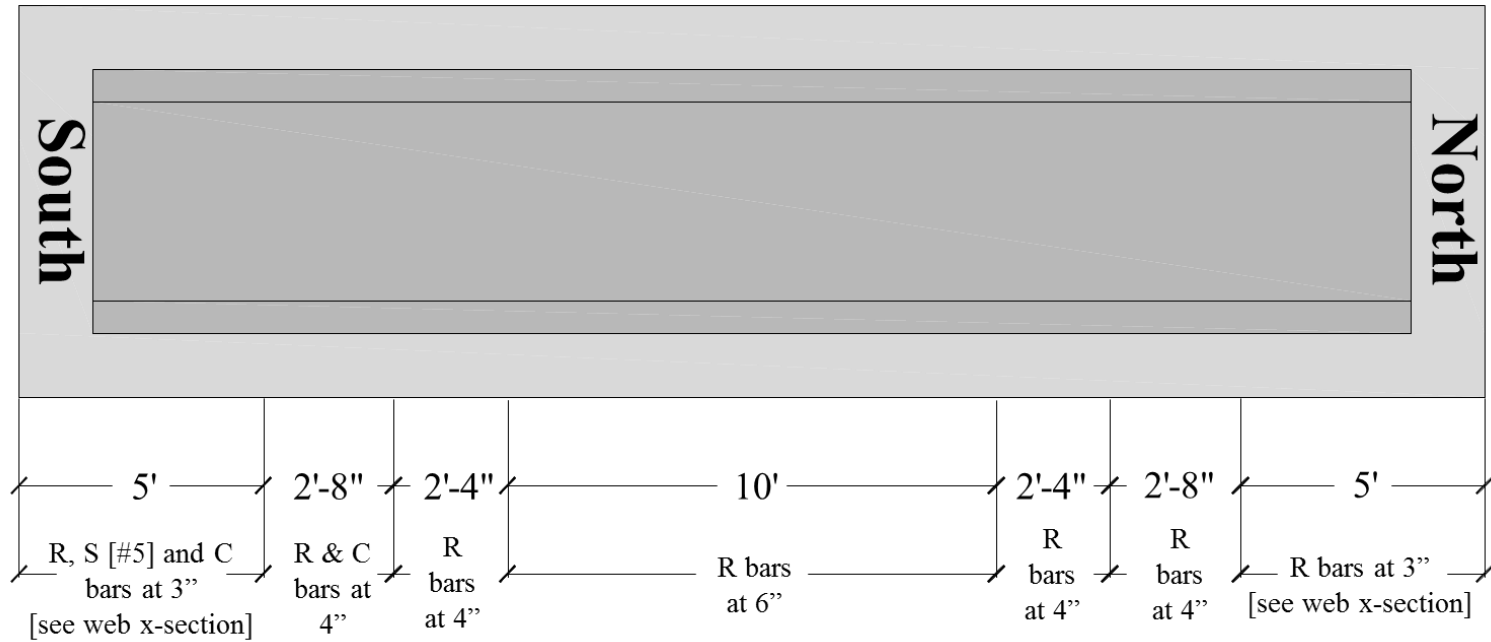


Figure 3-22: Beam 4 rebar layout (*note lack of symmetry in reinforcement layout)

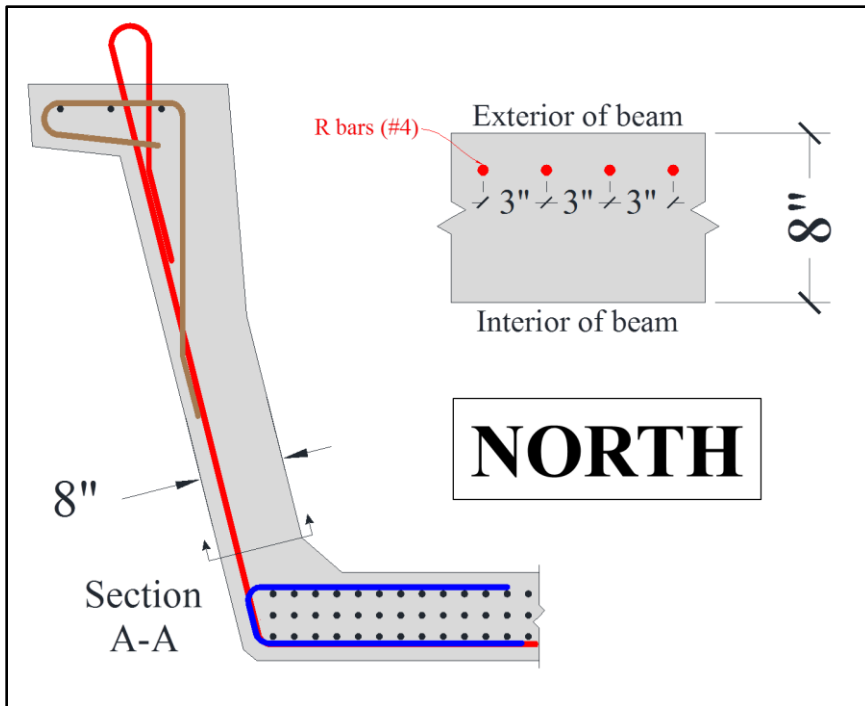


Figure 3-23: Beam 4 North reinforcement profile

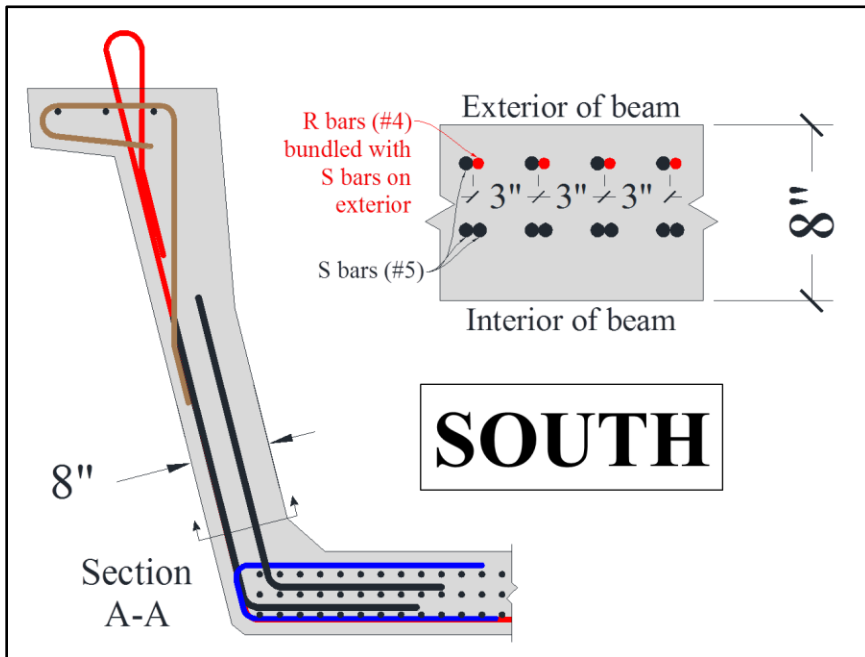


Figure 3-24: Beam 4 South reinforcement profile

3.2.6 Beam 5 Design

Beam 5 (shown in Figure 3-25) was fabricated offsite at a local precast yard. In order to match production beams being cast on the same line this beam contained 66 prestressing strands (layout shown in Figure 3-28). The purpose of Beam 5 was to test the feasibility of an alternative solution to the horizontal shear failures witnessed in Beams 1 through 3. In contrast to Beam 4, the design of Beam 5 maintained the standard five-inch-thick webs, but incorporated a 375% increase in shear reinforcement (detailed in Figure 3-26 and Figure 3-27). The Beam 5 alternative eliminated the need for a new interior void geometry and the requisite formwork. The increase in web-to-flange boundary reinforcement was accomplished by: (1) increasing the size of the R-bar from a No. 4 to a No. 5, (2) incorporating No. 6 S-bars on the interior face of the web, and (3) adding No. 4 C-bars to confine the prestressing strands.

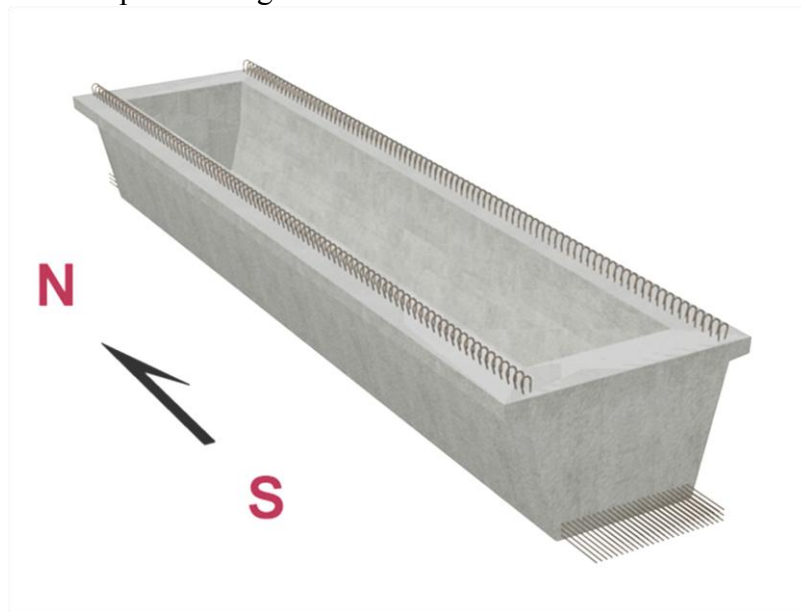


Figure 3-25: Rendering of Beam 5

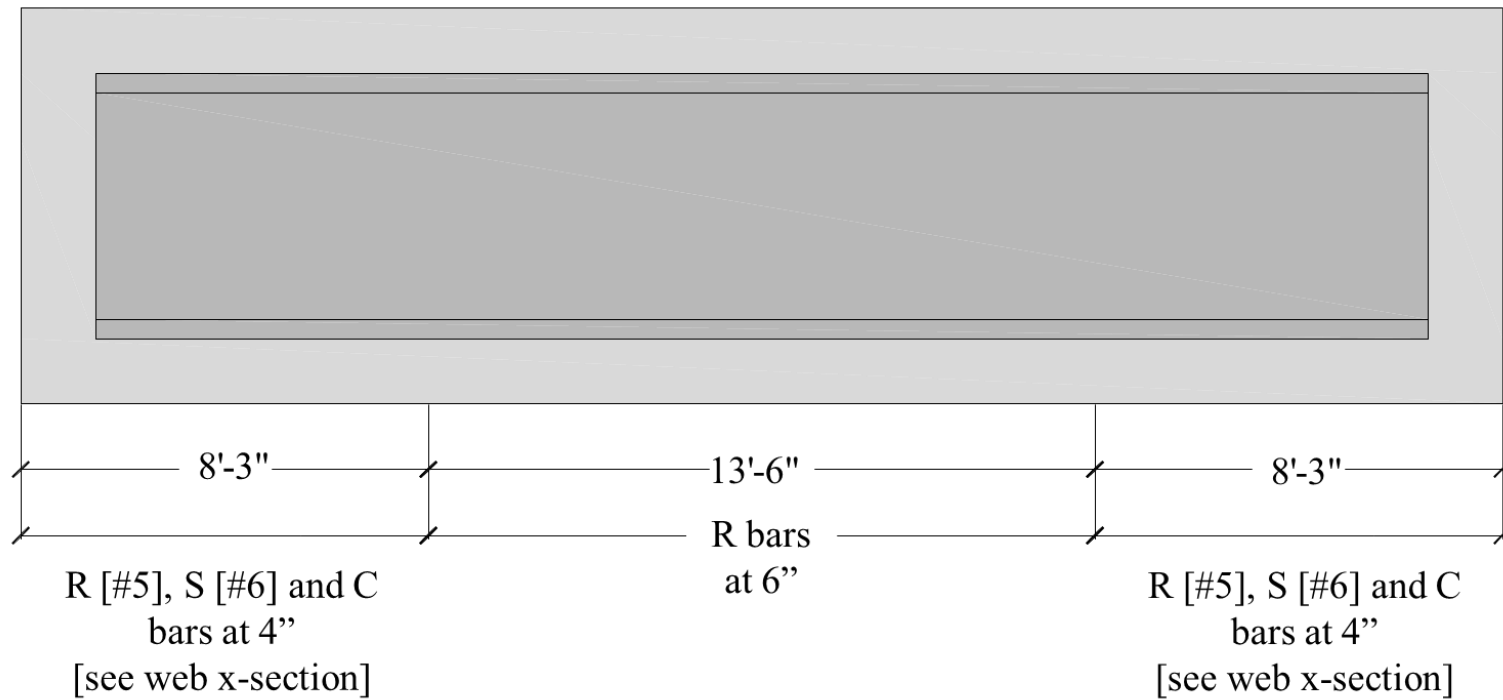


Figure 3-26: Beam 5 reinforcement layout

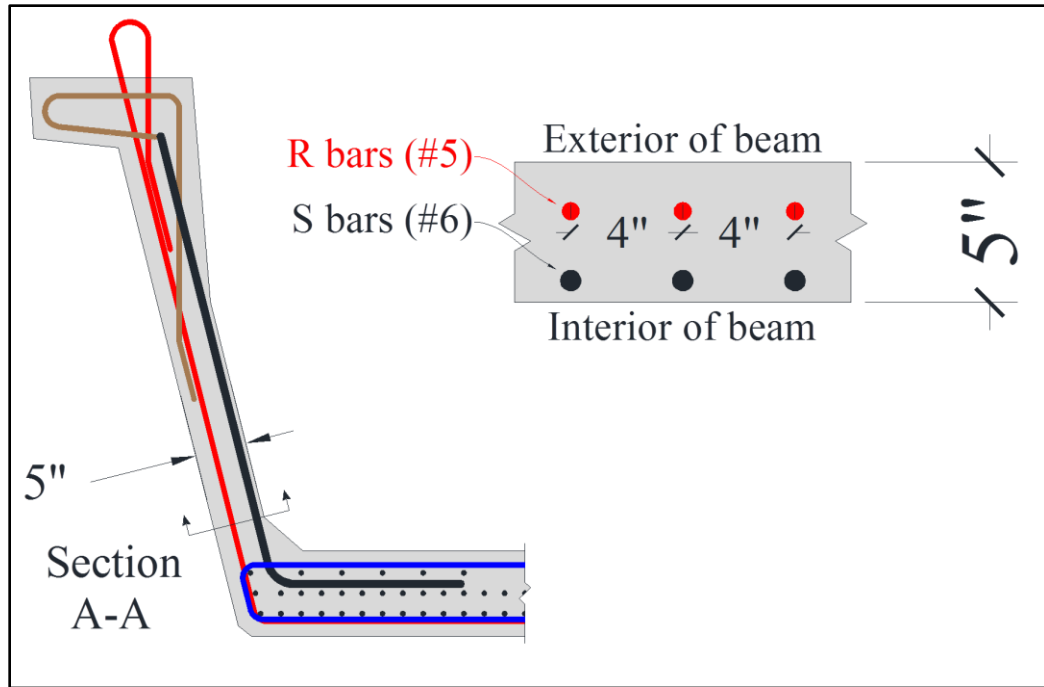


Figure 3-27: Beam 5 end region web cross section

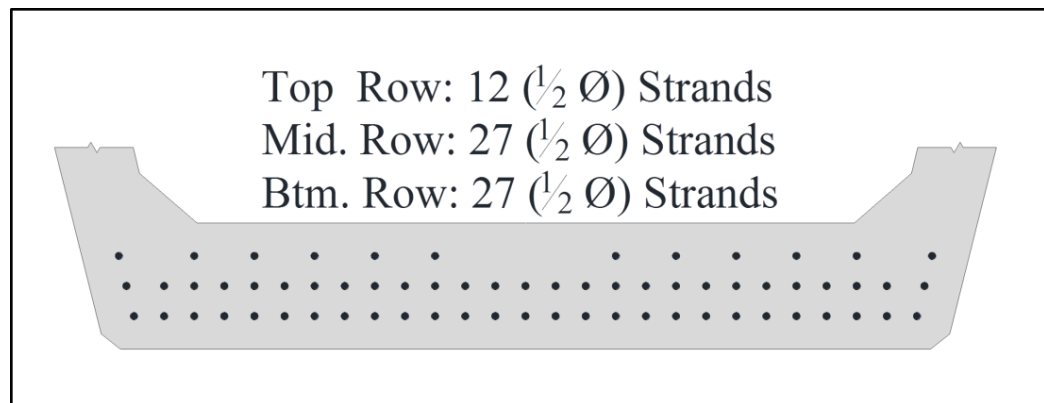


Figure 3-28: Beam 5 strand layout (66 total)

3.3 TEST SPECIMEN FABRICATION AT FERGUSON LABORATORY (BEAMS 1-4)

Beams 1 through 4 were fabricated in the 2.5-million-pound prestressing bed at Ferguson Structural Engineering Laboratory (pictured in Figure 3-1). Details regarding the design and construction of the self-reacting prestressing bed can be found in O’Callaghan (2007).



Figure 3-29: Ferguson Laboratory prestressing bed

In the interest of safety, the reinforcement cage was assembled and instrumented before the prestressing strands were fully stressed. All beams fabricated in-house required the installation of seventy-eight 0.5-inch diameter prestressing strands. Final gang stressing of the strands was completed after placement of the formwork and no more than one day prior to placement of the concrete. The following sections will cover the various stages of construction for a typical test specimen.

3.3.1 Reinforcement Cage Assembly

The reinforcement cage was assembled with the side forms in place for Beams 1 through 3. While the side forms provided support for the transverse reinforcement (see Figure 3-30), they ultimately interfered with assembly of the complex end blocks and debonding of strands.



Figure 3-30: Assembly of mild steel reinforcement with sideforms in-place

The construction scheme was therefore abandoned for the Beam 4 reinforcement cage in favor of techniques found at U-beam lines at local precast plants. Beam 4 included six top strands (three in each flange) and additional confinement steel (C-bars, Figure 3-7) around the bottom strands. To eliminate the construction conflicts and facilitate placement of the C-bars, temporary construction strands were used to support the transverse reinforcement (in lieu of the side forms). As shown in Figure 3-31, the temporary strands were positioned to engage the shear reinforcement protruding from the top of the beam.

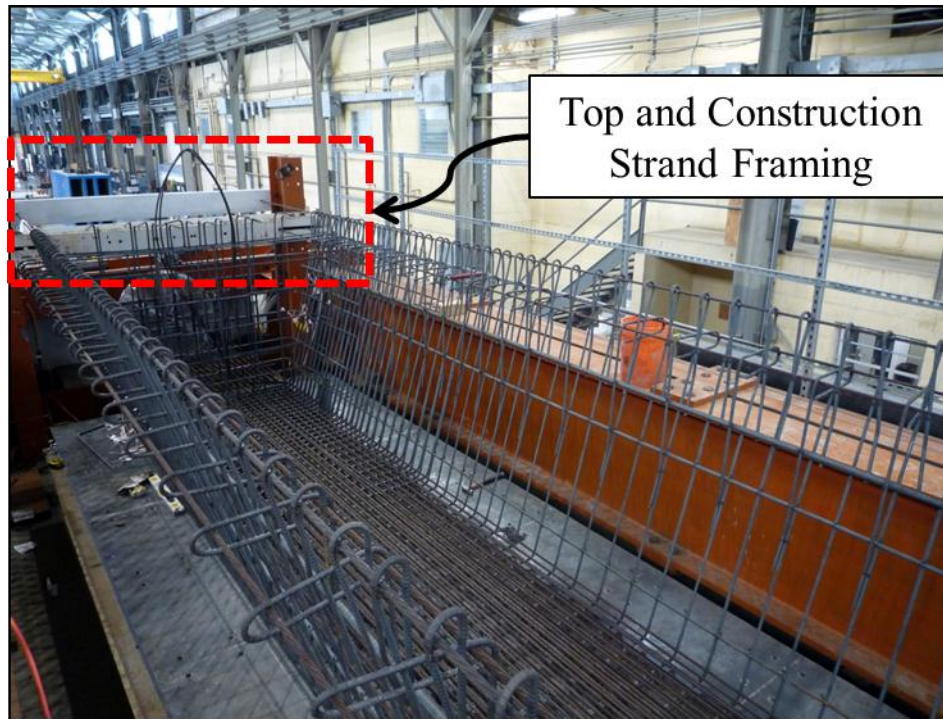


Figure 3-31: Beam 4 rebar cage assembly

3.3.2 Strand Pretensioning

The primary longitudinal reinforcement in the U-beams was 0.5-inch diameter low-relaxation prestressing strand (Grade 270). Stressing of the strands was completed in two stages. To begin, each strand was stressed to 1.5-kips with a monostrand jack. Monostrand stressing eliminated the slack in each strand and prevented over- or understressing during the final stage. Gang stressing was used to bring the strands to a final stress of 200-ksi. Four 800-kip rams reacted against the prestressing bed to advance the gang-stressing plate to its final position. The final stress values were confirmed by both ram pressure and the total elongation of the strands. Strand elongation was measured using linear potentiometers (shown in Figure 3-32) and mechanical dial gauges. To ensure accuracy of the stressing operations, movement of the dead-end anchorage plate was monitored and accounted for in the elongation measurements.

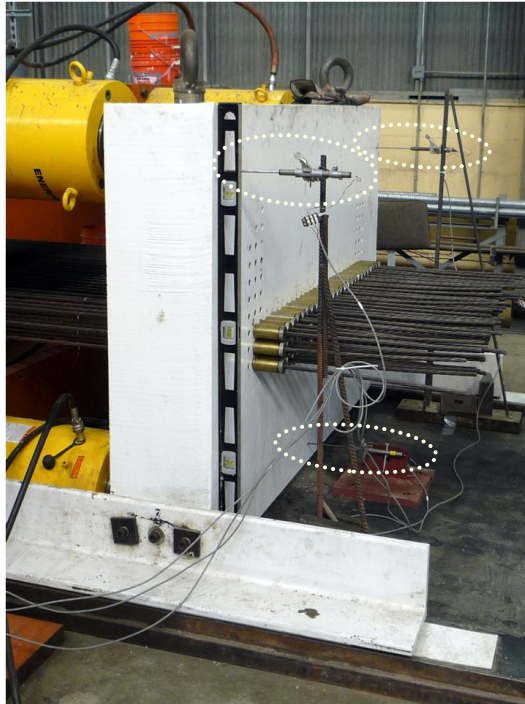


Figure 3-32: Gang-stressing plate being monitored during stressing

For Beam 4 the top strands were first stressed to 65-ksi or a load of 10-kips per strand. The stress in the top strands was then increased to 150-ksi, or 75% of the stress in the bottom strands, prior to concrete placement. These strands were not stressed to their full allowable capacity due to the strength limitations of the top strand framing (illustrated previously in Figure 3-31).

3.3.3 Formwork

The formwork for the standard U-beam geometry was manufactured by Hamilton Forms of Fort Worth, Texas. Working with the research team, Hamilton Forms was able to fabricate forms to accommodate the limited clearances of the FSEL prestressing bed. Industry-standard (free-standing) side forms were modified as shown in Figure 3-33 to

eliminate any interference with the prestressing bed. An interior void form, which could be configured for multiple end block geometries and skews, was also supplied by Hamilton Forms (see Figure 3-34).



Figure 3-33: Modified formwork from Hamilton Forms (Dunkman 2009)



Figure 3-34: Custom interior void from Hamilton Forms

To increase the web width of Beam 4, the construction of a new interior void form was necessary. The interior profile of the standard U-beam web was maintained, but

adjusted three inches inward as shown in Figure 3-35. Maintenance of the side form position therefore resulted in webs which were three inches wider.

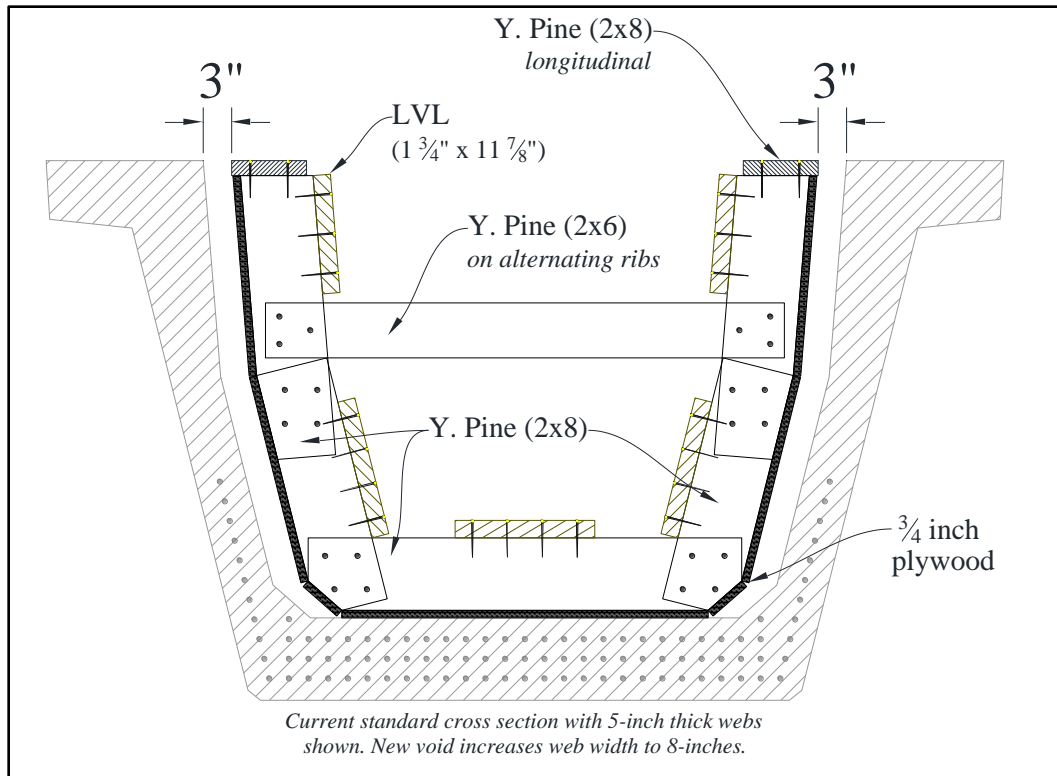


Figure 3-35: Design of wooden interior void for Beam 4

In an effort to reduce costs, the new interior void form was built onsite out of wood (Figure -3-36 and). Individual rib assemblies of the void form were constructed in a layout jig to maintain close tolerance to the final cross section. The rib assemblies were then fastened to multiple lengths of laminated veneer lumber (LVL). The LVL's served as the primary longitudinal structure of the void form. The completed frame was finally sheathed in plywood and sealed with acrylic caulk and polyurethane.

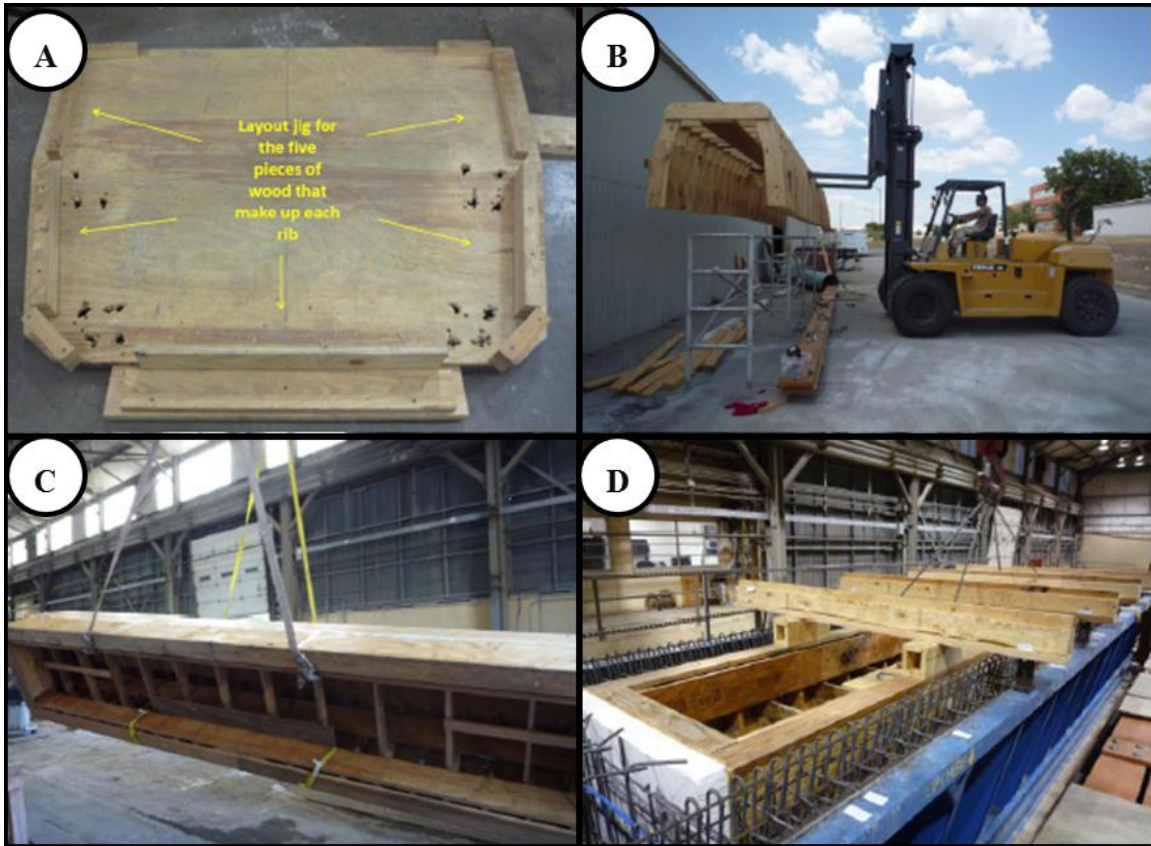


Figure -3-36: Construction of wooden interior void

(A)Layout jig for ribs of interior void, (B) initial layout of void, (C) & (D) finished void



Figure 37: Wooden interior void during construction prior to plywood skin installation

3.3.4 Concrete Placement

Each of the test specimens were cast monolithically in two stages (typical of U-beam construction at local precast plants): (1) bottom flange placement and (2) web and end block placement. At the beginning of the first stage, only the exterior formwork (i.e. side forms and bulkheads) was in position. Concrete was placed to achieve a bottom flange depth of approximately 8.25-inches (shown in Figure 3-38 (A)). The depth of the bottom flange was checked through the use of simple gauge (shown in Figure 3-38 (B)). Second stage concrete placement did not commence until the interior void form was secured in the final position. The void form was moved into place by overhead crane and

secured to the exterior formwork via rigid cross-pieces (as shown in Figure 3-38 (C & D)). The cross-pieces prevented the interior void from floating upward when the web and end block concrete was placed. After casting, the beam was covered with plastic in order to maintain a moist environment for optimal curing conditions.



Figure 3-38: U-beam casting procedure:
(A) Placement of bottom flange concrete
(B) Checking thickness of bottom flange
(C) Steel interior void (Beams 1, 2 & 3) installation
(D) Wooden interior void (Beam 4) installation

3.3.5 Temperature Monitoring

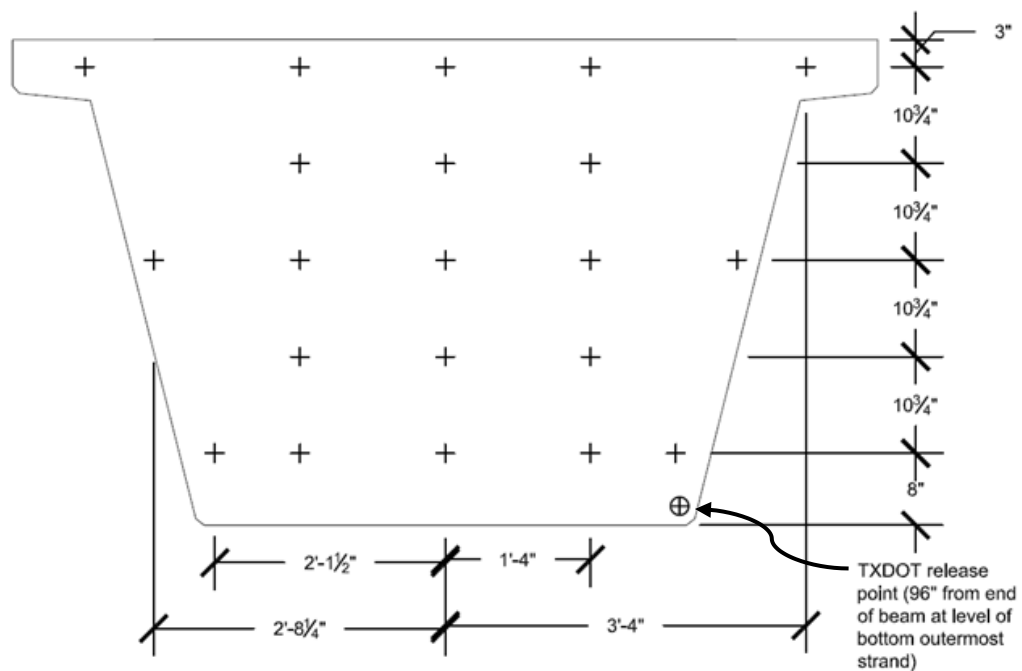
Thermocouples were used to monitor internal temperatures and match cure cylinders for all four U-beams fabricated at Ferguson Laboratory. Standard (4-inch by 8-inch) concrete test cylinders were match cured using the remote curing system shown in Figure 3-39. The system remotely monitored the internal concrete temperature at a location 8 feet from the end of the beam (as specified by TXDOT). Heated cylinder molds connected to the remote curing system were then programmed to match the measured beam temperature. Use of the remote curing system ensured that the concrete cylinders would be truly representative of the concrete placed within each of the beams (with regards to maturity and strength). Accurate evaluation of early concrete strength development facilitated precise timing of the prestress force transfer.



Figure 3-39: “Sure Cure” match curing system

In addition to the thermocouples utilized for match curing, an additional 21 thermocouples were placed within the end-block of each beam fabricated at the Ferguson Laboratory. Placement of the thermocouples is illustrated in Figure 3-40. Data gathered

from the supplementary thermocouple were used to evaluate the heat-generating potential of the different end block configurations. Of chief concern for the long-term performance of the end block were: (1) the absolute maximum temperature, (2) the maximum temperature differential, (3) the temperature profile at the time of release.



**Figure 3-40: Thermocouple locations
(not all locations utilized in each beam)**

3.3.6 Prestress Transfer

A key part of the construction of any prestressed concrete beam is the release of the prestressing force originally applied to the strands before casting. U-beam construction causes a slight complication to the typical release process in that it utilizes an interior void which must be removed before the prestressing force is released. Failure to include this step would cause the interior void to bind and could even cause some unwanted stresses on the beam itself. In the case of Beams 1 through 3 and 5 the interior void was constructed of steel and had been constructed such that it would flex inward when lifted from above. Therefore as illustrated in Figure 3-41 (A) the steel void was removed by simply lifting the void upward with an overhead crane. In the case of Beam 4 where the wooden interior void was used the removal was preceded by cutting all cross braces (constructed of 2x6 yellow pine). This allowed the void to flex inward, and the void was then removed in the same manner as the steel void.

After the removal of the interior void and the predetermined concrete compressive release strength had been reached, the prestressing strands were gradually released in unison by relieving the pressure on the hydraulic rams (shown in Figure 3-41 (A)). This allowed the gang stressing plate to slowly retract thus transferring the prestressing force to the cross section of the beam. The gradual introduction of the prestressing force to the section is of paramount importance since the dynamic introduction of such a large force could damage the beam.

Beam 4 contained six top strands which did not have a retractable plate for gang stressing. Therefore in order to gradually introduce the prestressing force an acetylene torch was used to gradually heat the strands (shown in Figure 3-41 (C)). This reduced their elastic modulus and caused the strands to gradually relax and transfer the

prestressing force to the top flanges of the cross section. After all six top strands had been released in this manner (for Beam 4) the gang stressing plate was used to release the 78 strands in the bottom flange.

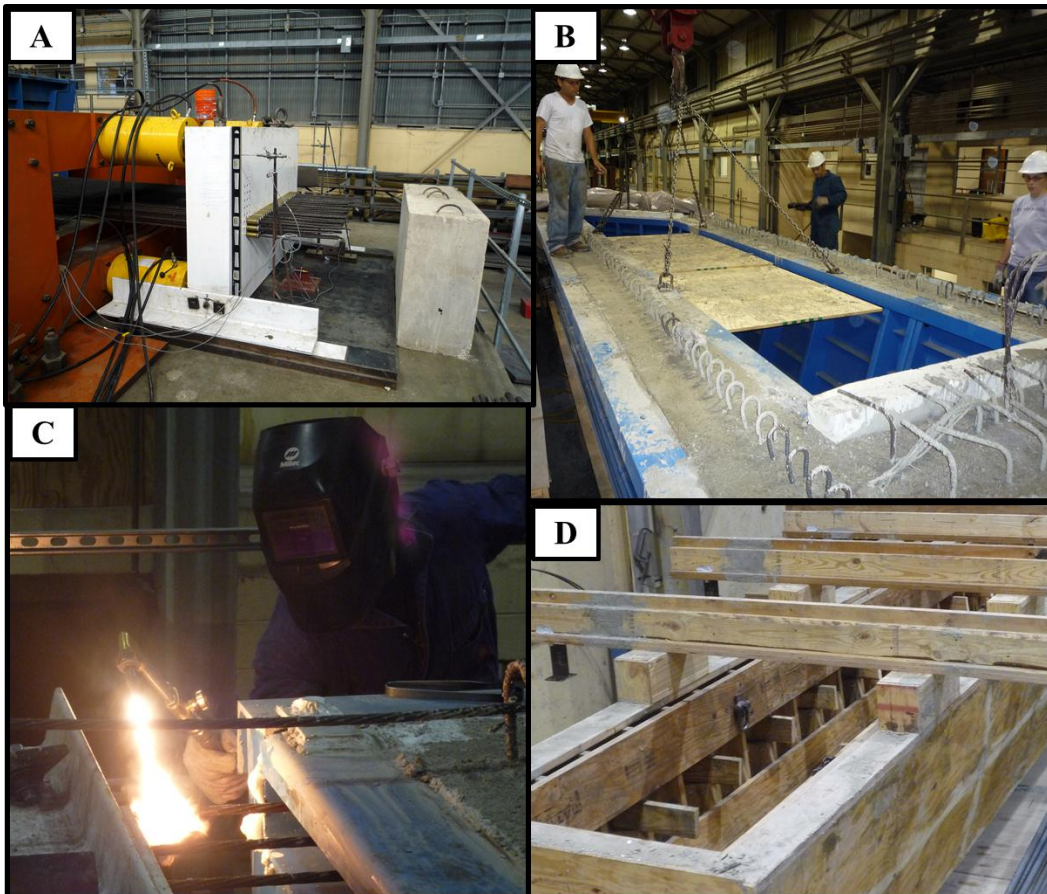


Figure 3-41: Prestress Transfer

***(A) Gang stressing plate allowed
for simultaneous release***

(B) Interior void removal prior to release

(C) Release of top strands in Beam 4

(D) Removed wooden interior void of Beam 4

3.4 TEST SPECIMEN FABRICATION AT PRECAST PLANT (BEAM 5)

Beam 5 was built at a precast plant in San Antonio, Texas. The decision to build the fifth beam at a local precast plant was made in the interest of saving time and staff effort; Beams 4 and 5 could then be constructed in a near simultaneous fashion. Due to the rapid line turnover in an active precast yard, no internal instrumentation was installed on this beam.

The reinforcement cage was assembled with the strands fully stressed and the side forms removed, as seen in Figure 3-42 – A. Once the reinforcement cage was completed, the side forms were installed and clamped across the bottom soffit of the form. The formwork was then ready to receive concrete for the bottom flange of the U-beam. Concrete was delivered from a central batching plant via a concrete hopper outfitted with a placing boom (Figure 3-42 – B). Concrete was first placed in the bottom flange, the interior void forms were then secured (Figure 3-42 – C) and placement of the U-beam webs proceeded. After concrete placement was complete, soaker hoses and burlap were laid across the top flange to ensure proper curing (shown in Figure 3-42 - D).



Figure 3-42: Construction sequence of Beam 5

(A) Assembly of reinforcement cage

(B) Placement of bottom flange concrete using mobile hopper

(C) Placing interior void

(D) Installed soaker pipe for curing

A match curing system was not available at the precast plant. The test cylinders were therefore placed in the interior void form in lieu of match curing. While proximity to the hydrating concrete was expected to facilitate strength gain, the cylinder maturity was not expected to match that of the beam. The cylinders likely yielded lower (relative to the beam) compressive strengths and therefore delayed the transfer of prestress to the U-beam; a conservative practice. Once these cylinders achieved the release strength the prestressing strands were released gradually through the use of hydraulic rams.

3.5 MATERIAL PROPERTIES

The engineering properties of the concrete, mild reinforcement and prestressing strand were established through standard ASTM testing protocols. Measured properties were used in all engineering calculations, including the evaluation of relevant code provisions. Testing methods and results for all construction materials are outlined below.

3.5.1 Concrete Properties

Three different concrete mixtures were utilized during the fabrication of the five test specimens. In the time period between the fabrication of Beams 2 and 3, the Texas Department of Transportation implemented a requirement for the use of at least 25% fly ash (by weight of total cementitious material) in all precast concrete mixtures. That specification change is reflected in the concrete mixture proportions listed in Table 3-2.

Table 3-2: Concrete mixture design

Material	Properties	Quantity			Units
		Beams 1 & 2	Beams 3 & 4	Beam 5	
Cementitious Material	Alamo Gray Type III	611	599	606	lb / yd ³ concrete
	Type F fly Ash	0	200	206	lb / yd ³ concrete
Coarse Aggregate	¾ in. Crushed Limestone	1,600	0	1,855	lb / yd ³ concrete
	½ in. Crushed Limestone	0	1,821	0	lb / yd ³ concrete
Fine Aggregate	River Sand	1,379	1,152	1,124	lb / yd ³ concrete
Water	--	202	252	167	lb / yd ³ concrete
Water/Cement Ratio	--	0.33	0.32	0.21	unit less
Water-Reducers	Sika Viscocrete 2100	13	7	0	oz/hundred weight cement
	Sikament 686	25	0	0	oz/hundred weight cement
	Sika 161	0	8	0	oz/hundred weight cement
	Superplasticizer	0	0	5	oz/hundred weight cement
Retarder	Sika Plastiment	5	4	4	oz/hundred weight cement
Desired Slump	--	9	9	6	inches

The compressive strength of the concrete was found by testing 4-inch by 8-inch test cylinders in accordance with ASTM C39. The compressive strength at the time of prestress transfer and shear testing is listed for each test specimen in Table 3-3.

Table 3-3: Concrete compressive strengths

Beam Strengths	Beam 1 N	Beam 1 S	Beam 2 N	Beam 2 S	Beam 3 N	Beam 3 S	Beam 4 N	Beam 4 S	Beam 5 N	Units
Release strength	6,300		6,400		6,300		6,400		6,100	psi
28-day strength	11,700		10,600		11,300		10,800		12,400	psi
Day of Test	11,900	11,900	11,500	11,500	11,400	12,100	11,400	11,400	13,200	psi
Deck Strength	Beam 1 N	Beam 1 S	Beam 2 N	Beam 2 S	Beam 3 N	Beam 3 S	Beam 4 N	Beam 4 S	Beam 5 N	Units
Day of Test	10,500	10,500	8,600	8,600	9,200	10,700	7,500	7,500	7,600	psi

3.5.2 Shear Reinforcement Properties

Standard reinforcing bars were used as transverse reinforcement in all but one test specimen; the north end of Beam 2 was reinforced with welded wire reinforcement (WWR). For each beam and reinforcement type, representative samples were taken to obtain the average yield and rupture stress in tension. All tests were conducted in accordance with ASTM A615. Results of the reinforcement tests are summarized in Table 3-4.

Table 3-4: Transverse reinforcing bar properties

Beam End	Classification - Type	Bar Size	f_{sy} (ksi)	f_{su} (ksi)
1	R - rebar	# 4	63	97
2	N R - WWR	# 4	86	108
	S R - rebar	# 4	65	97
3	R - rebar	# 4	65	103
4	R - rebar	# 4	63	101
	S - rebar	# 5	60	100
5	R - rebar	# 5	63	101
	S - rebar	# 6	60	100

3.5.3 Prestressing Strand Properties

At least three samples of prestressing strand were taken from each beam to determine the elastic modulus. An accurate assessment of the elastic modulus was needed to ensure proper pretensioning of the strand in the laboratory prestressing bed. Each strand sample was pulled in tension and elongation was measured with a 24-inch extensometer. The linear elastic modulus was then obtained using the stress-strain response of each strand. Linear elastic modulus values for each beam are summarized in Table 3-5.

Table 3-5: Helical and Linear Elastic Modulus' for Prestressing Strand

Beam	Helical Modulus	Linear Modulus
<i>units</i>	<i>ksi</i>	<i>ksi</i>
1	29,980	27,700
2	30,770	28,730
3	28,950	--
4	*	29,050
5	*	28,970
<i>* helical modulus not determined</i>		
<i>-- unreliable results therefore taken as 29,000 ksi</i>		

For strand samples taken from Beams 1, 2, and 3, the helical elastic modulus was also determined. In contrast to the linear elastic modulus, the helical elastic modulus is a characterization of the stress-strain behavior of a single wire within a seven-wire prestressing strand. During pretensioning operations, a single strain gauge was typically applied to each strand (Figure 3-43). Helical strain measured in this manner was converted to linear strain by multiplying by the ratio of the linear and helical moduli measured from the corresponding strand sample. Helical elastic modulus values for three of the beams are summarized in Table 3-5.

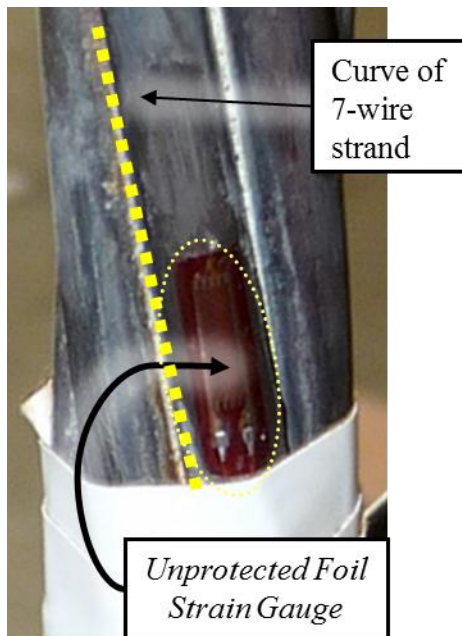


Figure 3-43: Unprotected foil strain gauge on strand

3.6 SHEAR TESTING

All U-beams discussed in this thesis were subjected to at least one shear loading to failure. In many cases post-tensioned stirrups were used to enable a second test on the same specimen. The sequence of testing involved: (1) transferring the beam to the load frame, (2) deck placement, (3) loading beam and rams moved into place, (4) electronic instrumentation connected and checked, (5) shear testing and recording of data both electronically and manually, (6) Cutting the beam into smaller sections for removal, and eventually, recycling. The following section will cover all these phases in detail.

3.6.1 Test Facility and Loading Configuration

The load frame was constructed in 2008 to allow large capacity shear testing of prestressed concrete members. The frame has a load capacity of 4,000-kips which is limited by the two 2,000-kip rams attached to the white spreader beam as shown in Figure 3-44. Six 3.5 inch diameter 95-ksi (grade B7) steel rods transfer the load from the spreader beam to the strong-floor. This strong floor has tunnels to allow for easy access to the nuts and washers holding the rods from below the slab as seen in Figure 3-44.

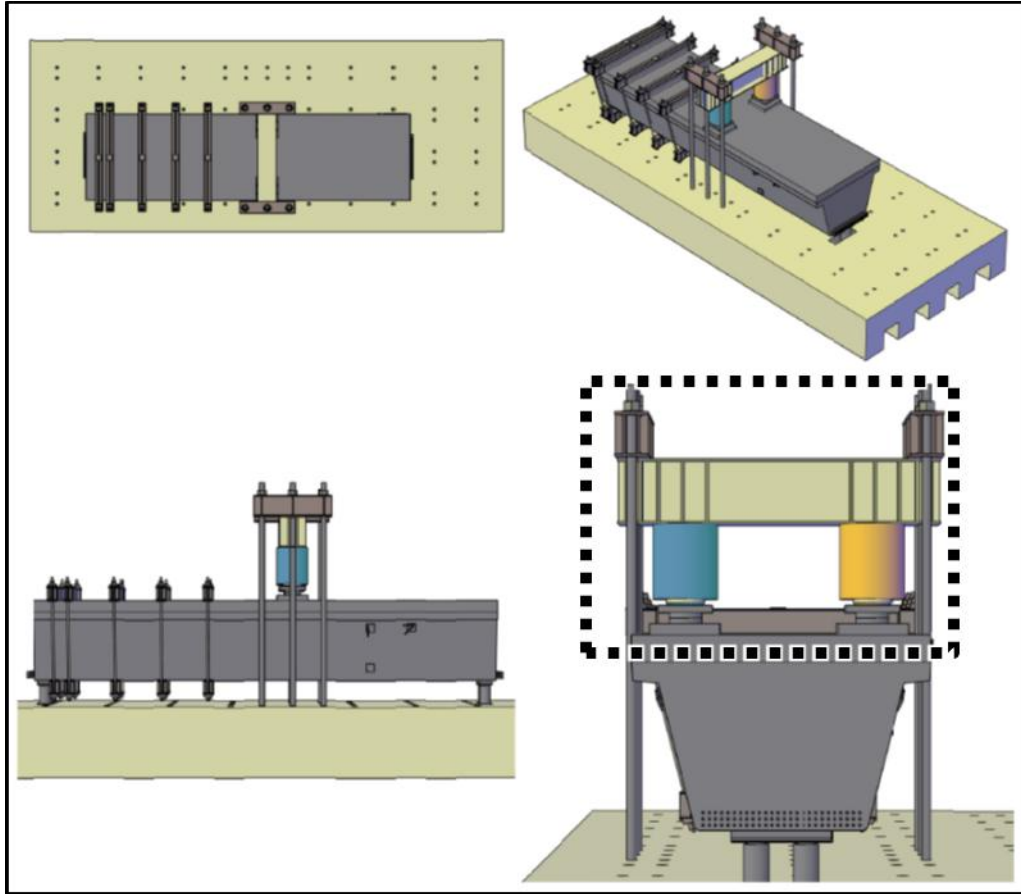


Figure 3-44: Shear test frame mounted on elevated strong floor at FSEL

A systematic loading procedure was followed to ensure that the load was evenly distributed both to the beam being tested and to each of the six rods supporting the load frame. First the white load beam (shown in Figure 3-44) was moved into place over the beam being tested. The hex nuts and washers for each of the rods were then installed and snugged against the load beam. At this point, the rams were still not in contact with the specimen, but were held level by temporary dunnage placed around the perimeter of the ram. The heads were then extended until they lifted the white loading beam *and* all six rods. At this point the dunnage was removed and the hex nuts underneath the slab were tightened. This procedure, although tedious, ensured the symmetric loading of the U-beam and prevented overloading to any single rod.

3.6.2 Selection of Span to Depth Ratio

Although sectional shear provisions of AASHTO LRFD Bridge Design Specifications apply to shear spans greater than twice the effective member depth ($a/d > 2$), in order to (i) provide a clear separation from this limit and (ii) be consistent with previous research on sectional shear, it was necessary to keep the shear span to depth ratio $[a/d]$ above 2.5. The weight restrictions of the gantry cranes at Ferguson Laboratory required that the test specimens be less than 30-feet in length, and therefore the a/d ratio was set by the shortest beams was 2.7 (beams 1 and 2 with the 45-degree end-block). This ratio was maintained in beams 3, 4 & 5 by offsetting the load point from the centerline thus resulting in a larger shear span on one end. The load configuration for all beams tested can be seen in Figure 3-45. In beams with skewed ends, the shear span was measured at the beam centerline when the beam specimen is viewed in plan (Beam 1 and 2 of Figure 3-45).

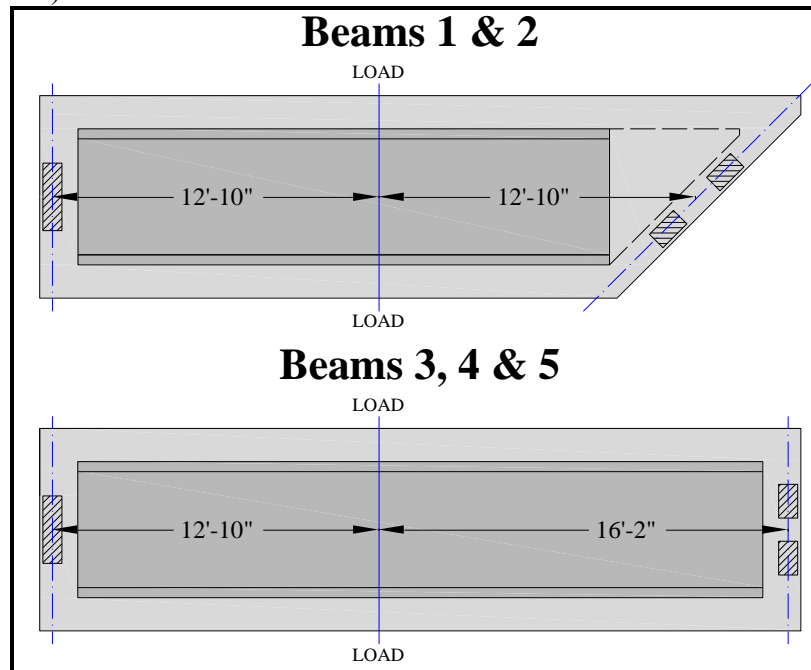


Figure 3-45: Loading configuration for all beams

3.6.3 Repair of Beam Prior to Second Test

In an effort to perform two shear tests on each beam five external stirrups, shown in Figure 3-46, were constructed to either prevent the failure of a test region during the first test or to repair a region in order to enable a second test on the same beam. These clamps are built-up members consisting of two C10X20 shapes joined by plates on the top and bottom flanges.

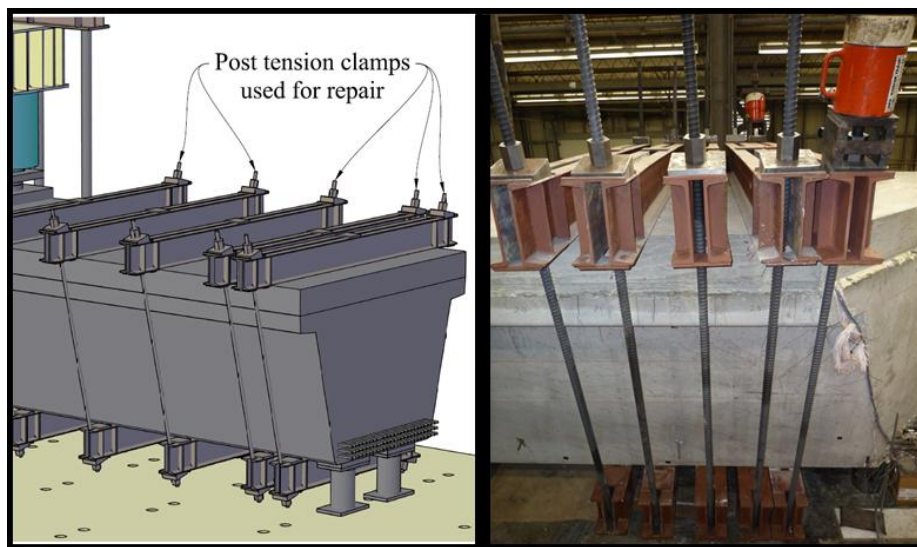


Figure 3-46: External post-tensioning stirrups

These members were placed on both the top and bottom of the specimen and post-tensioned together using 1.25-inch diameter DYWIDAG rods to a force of 100-kips per rod. This clamping force acts to distribute the shear across the portion of the beam not being tested but also is useful in repair to provide additional anchorage to the strands at the end of the beam. This method of repair was not always adequate to enable a second test especially in cases in which a compression failure in the web or anchorage failure in the end-region controlled, and therefore on beams 2, and 5 only one test was possible. Other repair methods were explored, but discounted because of cost and complexity.

3.6.4 Instrumentation

Many types of electronic and manual instrumentation were used during the shear testing of these specimens. Due to the volume of information being collected, two data acquisition systems were necessary to process and record the large amount of information being collected. Each of these instruments will be covered in detail in the following sections. They include: foil strain gauges, linear potentiometers, pressure transducers, and load cells (used during the shear testing as illustrated in Figure 3-47).

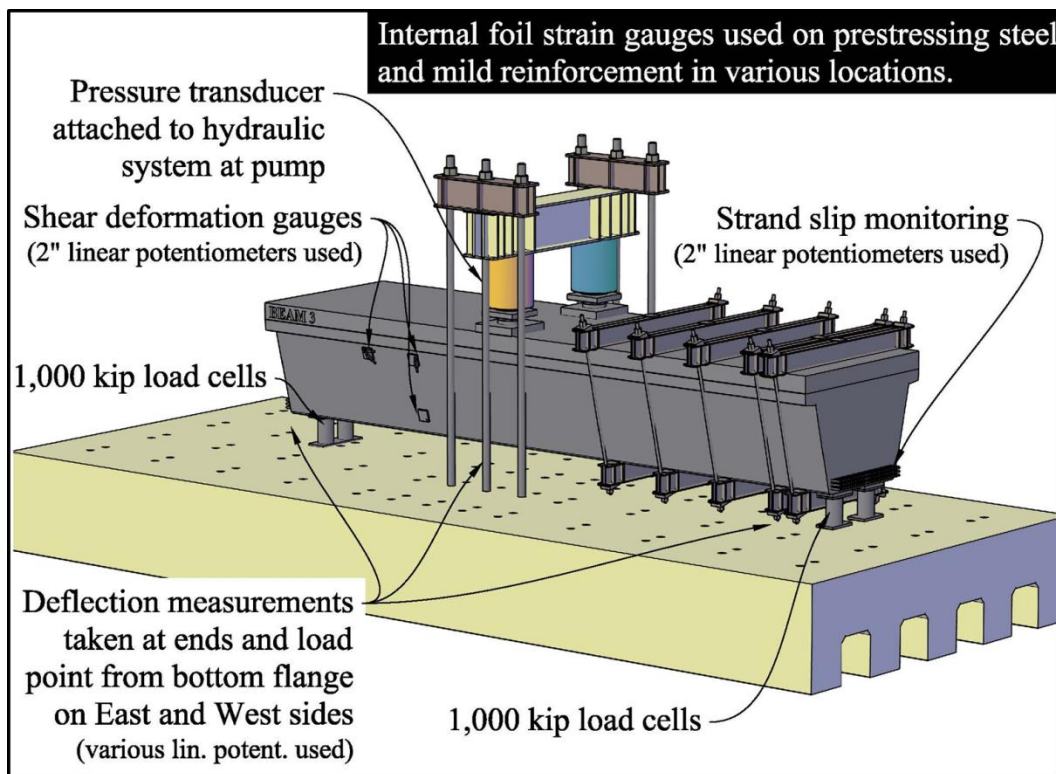


Figure 3-47: Locations and uses of instrumentation during shear testing (from Hovell, et al. 2010)

3.6.4.1 Internal Strain Gauges

Foil strain gauges, shown in Figure 3-48, were used to monitor the changes in strain of reinforcement and strand during release and shear testing. These gauges were attached directly to the rebar with Cyanoacrylate adhesive after the bar's deformations were removed, with care taken to not reduce the cross sectional area of the reinforcement. These gauges, although already waterproof by design were then covered with protective tape and the wires were protected against damage during casing. During release or shear testing these gauges were used to measure bar stresses.

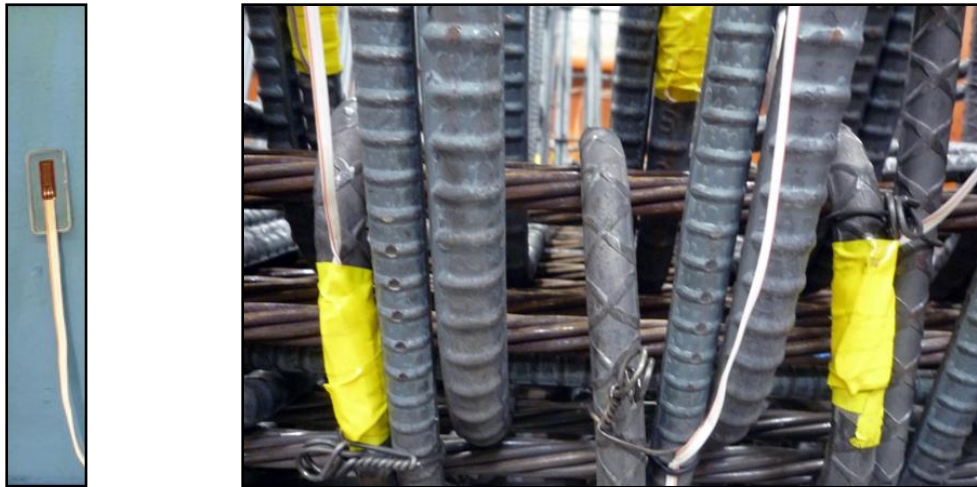


Figure 3-48: Encapsulated foil strain gauge for rebar and installed gauges

3.6.4.2 Linear Potentiometers

Linear Potentiometers of 2, 4 and 6-inch gauge lengths were used to measure linear displacements in a variety of applications. These instruments, shown in Figure 3-49, are designed to give a varied electrical resistance in linear proportion to the extension of the plunger highlighted below.

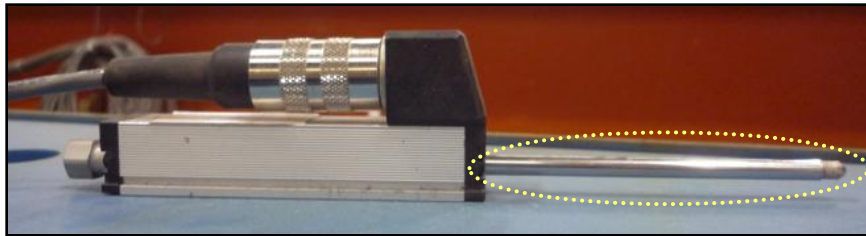


Figure 3-49: Two inch linear potentiometer

3.6.4.3 Deflection Monitoring

Linear potentiometers were used during shear testing to measure the load-point and end deflections of the beam. The actual deflection of the beam at the load point was determined by subtracting out the deflections of the bearing pads at the supports from the total deflection at midspan. As seen in Figure 3-50(A) the deflection was measured by epoxying a flat steel plate to the bottom of the beam prior to testing and reading the deflection of the top of the plate. The deflection reported herein is the deflection at the load point after accounting for the deflection at the supports (due to the compression of the bearing pad) as is demonstrated in Figure 3-50(B).

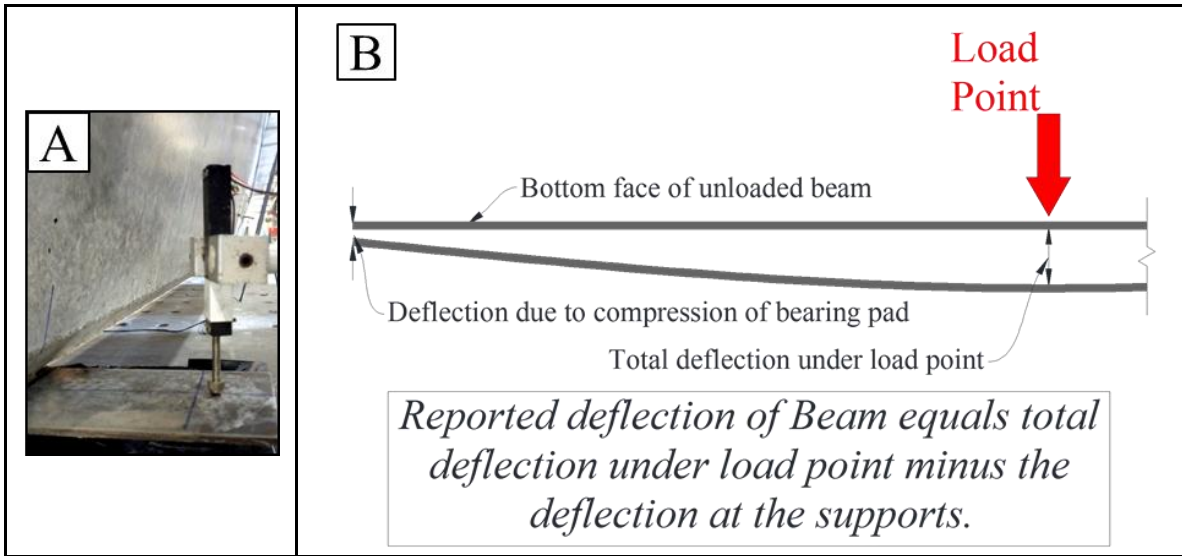


Figure 3-50: (A) Linear potentiometer measuring deflection during shear testing and (B) Correction of deflection readings for deflection at support

3.6.4.4 Strand Slip Monitoring

The same two inch linear potentiometer shown in Figure 3-49 was inserted into the frame shown in Figure 3-51 in order to measure strand slip. The plunger rested against the face of the beam and recorded any movement of the strand relative to the beam face.

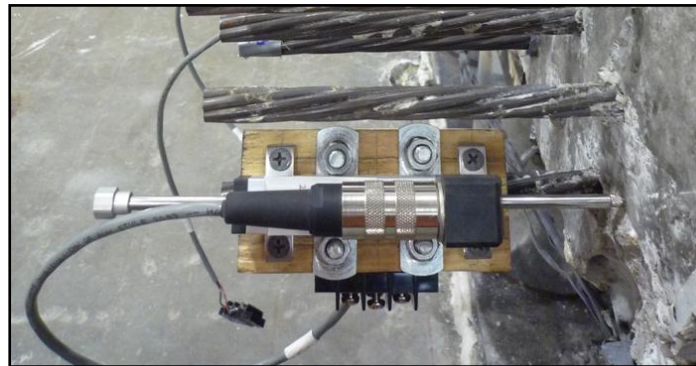


Figure 3-51: Strand slip gauge

3.6.4.5 Shear Deformation Monitoring

A system was set up to measure shear deformation in the web region. This system was comprised of three half-inch thick aluminum plates, three linear potentiometers, and steel piano wire as shown in Figure 3-52. The aluminum plates were attached to the beam by half-inch diameter rods that were epoxied into holes drilled into the sides of the beams on a 3-foot square grid. During the shear testing these holes were watched closely to confirm no cracks emanating from these areas. The original lengths between the points on these plates were measured prior to testing and then the deformation was converted to a strain by dividing by the original gauge length.



Figure 3-52: Shear deformation setup

3.6.5 Load Cells

Four 1,000-kip load cells, shown in Figure 3-53, were used at the three support points of the beam as the primary measurement for the load applied to the beam during shear testing. These readings were then confirmed by the pressure transducer attached to the loading rams.



Figure 3-53: 1,000-kip load cells

The shear values reported hereafter in this thesis were taken as the applied shear load (the applied load from the load frame) summed with the dead load of the beam and deck at one half the shear span (illustrated in Figure 3-54). In doing so the reported shear included the dead load of the beam.

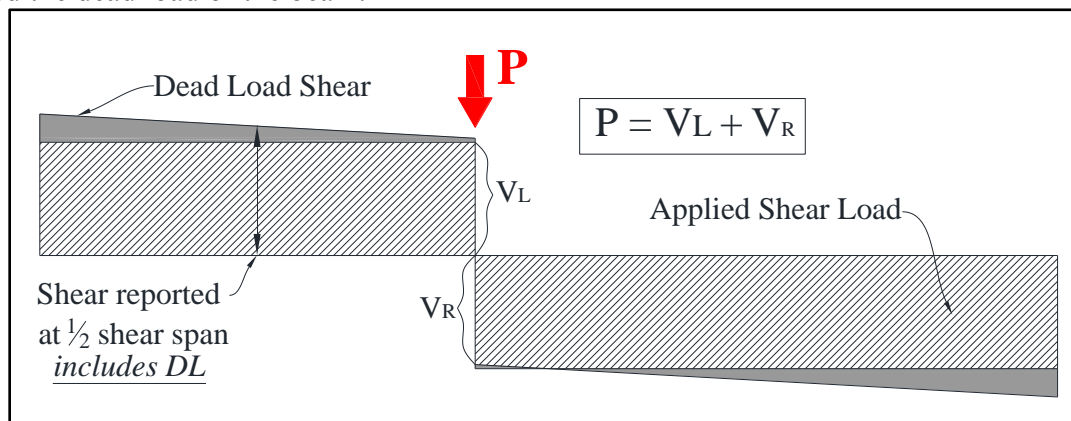


Figure 3-54: Description of reported shear values

3.7 SUMMARY

Five beams were constructed in an effort to gain an understanding of the structural behavior and structural adequacy of U-beams. Four of these beams were constructed at FSEL while one was constructed at a local precast plant. The primary variables of interest in each of these five beams were: (Beams 1 & 2) the influence of skewed end-block design on structural behavior, (Beam 3) influence of debonded strands on shear performance of U-beam, (Beam 4) effect of increased width and reinforcement area on the breakdown of the web-to-flange boundary, (Beam 5) influence of increasing the reinforcement area crossing the web-to-flange boundary while maintaining the original web thickness.

CHAPTER 4

Phase I Test Results

4.1 INTRODUCTION

The experimental program of TxDOT Project 0-5831 was originally aimed at improving the design and detailing of skewed end blocks in standard U-beams. End block geometry, as opposed to cross-sectional geometry, was the primary focus of the study. Phase I testing, described in Sections 3.2.2 through 3.2.4, is largely reflective of that original focus. Phase I specimens (Beams 1 through 3) were fabricated to meet the geometry and reinforcement details outlined by the Texas Department of Transportation (TxDOT) in the U-beam design standards (included in Appendix F).

Beams 1 and 2 featured the two skewed end block configurations currently allowed by TxDOT: a skewed beam end with (1) skewed interior void and (2) square interior void. As discussed in Section 0, the measured shear strength of Beams 1 and 2 did not meet the shear capacity as determined by the 2010 Interim of the AASHTO LRFD Bridge Design Specifications. Concerns regarding the effect of strand debonding on shear performance were subsequently raised. Beam 3 was constructed and tested to better understand the effects of strand debonding; 46% of the prestressing strands were debonded in both end-regions of the test specimen. The results of the five shear tests conducted during the first phase of experimental research are summarized in this chapter.

4.2 PHASE I TEST RESULTS

Shear and deformation data captured through a number of instruments (see Section 3.6.2 for descriptions and calculations of both shear and deformation values) were used to characterize the serviceability and strength of each U-beam specimen. The effects of void geometry and strand debonding on the performance of U-beams at both service and ultimate limit states are examined below.

4.2.1 Performance at Service Level Shear

Serviceability, as discussed in this document, refers to the structural performance of a member under routine loading (i.e. loads the structure would experience on a daily basis). Service level load is taken as the loading considering all dead loads and the AASHTO LRFD design truck and lane loads without any factors of safety.

A conservative estimate for the service shear experienced by a U-beam was obtained through simple summation of the structural dead weight and design truck loading (a single design truck load was used) for two extreme bridge configurations: (1) a 120-foot span with a 45-degree skew, and (2) a 140-foot span without skew. The calculations assumed a 12-foot centerline-to-centerline spacing of the girders, an 8-inch-thick, cast-in-place slab and a 2-inch sacrificial wearing surface. The service level shear at a distance of 80 inches from the centerline of the bearing pad was estimated to be 275kips. This estimate, although as realistic as possible, should only be treated as a convenient benchmark utilized for the purposes of evaluation of the test results.

The primary serviceability concern of prestressed concrete structures is the ingress of water into the cross section of the beam. Water infiltration leads to corrosion of both the primary and shear reinforcement resulting in loss of strength and durability.

Cracks in concrete members serve as a pathway for moisture seeping into the interior of the beam and are detrimental to the serviceability of a beam.

Therefore, in the case of prestressed concrete structures the discussion of adequate serviceability performance is often taken as synonymous with the cracking behavior of the structure at its service level load. Due to the importance of service level behavior, cracks locations and sizes were recorded during all U-beam shear tests at service level loads as defined in the preceding paragraph. These crack patterns were then compared to evaluate the effects of the void geometry and prestressing force on the serviceability of the beam.

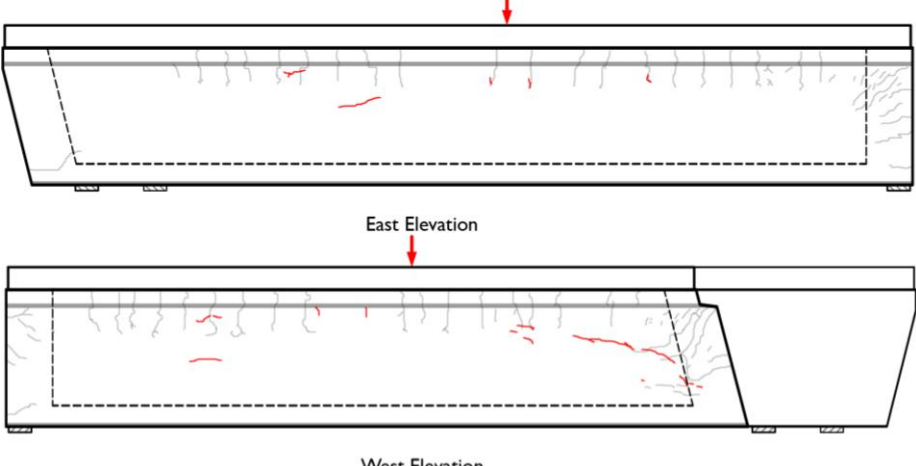
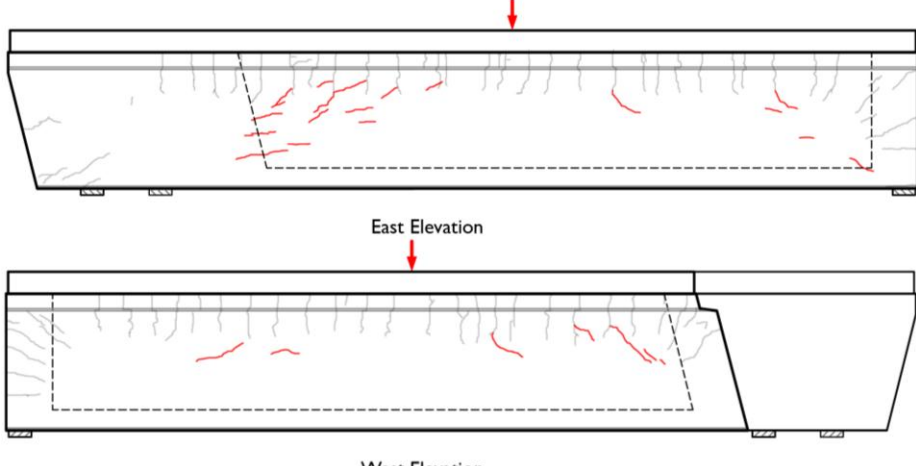
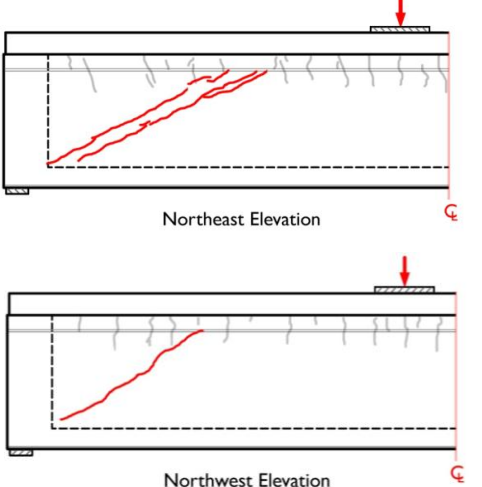
While the two bridge configurations were considered to be theoretical worst-case scenarios, the service level shears of two 145-foot U-beam bridges currently in service were calculated for reference purposes. Service shear levels calculated for these in-service structures were within 10% of the levels seen in the theoretical worst-case scenarios. Throughout this chapter a shear of 275 kips is therefore used for the evaluation of serviceability.

As expected, the severity of the service level cracking was directly related to the level of prestressing force present in the beam. End block geometry had little influence on service level performance. Beams 1 and 2 contained 78 fully bonded strands and exhibited minimal diagonal cracking under service level shear. In contrast, Beam 3 contained 47 fully bonded strands (46% debonding) and was therefore subject to a significantly smaller prestressing force. This caused an increase in the number and magnitude of the shear cracks observed under service level loading.

The cracking at service level shear is summarized for all three beams in Table 4-1. Cracking related to the transfer of prestress (i.e. bursting, spalling, and tension

cracks) are depicted in gray, while load-induced cracking is shown in red. All of the service level cracks in Beams 1 through 3 were less than 0.005 inches in width; typically referred to as hairline cracking. Due to the narrow width and scarcity of service level cracks in the Phase I test specimens; serviceability is not believed to be a concern in standard U-beams subjected to normal design loads (i.e. no overloads).

Table 4-1: Service level shear cracking observed in Beams 1 through

<p>BEAM 1 Shear = 285-kips</p>	 <p>East Elevation</p> <p>West Elevation</p>
<p>BEAM 2 Shear = 280-kips</p>	 <p>East Elevation</p> <p>West Elevation</p>
<p>BEAM 3 Shear = 275-kips</p>	 <p>Northeast Elevation</p> <p>Northwest Elevation</p> <p><i>Beam 3 South was clamped during test for cracking load. Therefore no service level cracking is shown.</i></p>

4.2.2 Performance at Maximum Applied Load

Modern design codes assume two possible methods of shear failure in prestressed concrete members: (1) the transverse reinforcement will reach its yield strength in tension or (2) the web of the beam will crush under compressive load. The results of the first phase of this project conclusively showed that neither of these failure mechanisms controlled the ultimate shear strength of the member. In all five shear tests conducted on Beams 1 through 3, load-carrying capacity was lost when the web-to-flange interface failed. This atypical failure mode prevented the test specimen from achieving the code-calculated shear capacity in each case.

The web-to-flange interface failure was characterized by the rapid growth of a horizontal crack from the bottom of the diagonal cracking to the outside edge of the bearing pad (as shown in Figure 4-1). Separation of the flange and webs was indicative of a loss of force transfer between the primary diagonal struts within the webs and the prestressed longitudinal reinforcement in the flange. Due to the loss of internal equilibrium, attempts to apply additional load only resulted in further deformation of the test specimens without any increase in applied load. The distortion of reinforcement and concrete spalling shown in Figure 4-2 indicated the large relative movement which occurred between the bottom flange and the webs at failure. Additional photographs of the horizontal shear failure mode can be found in Appendix C.

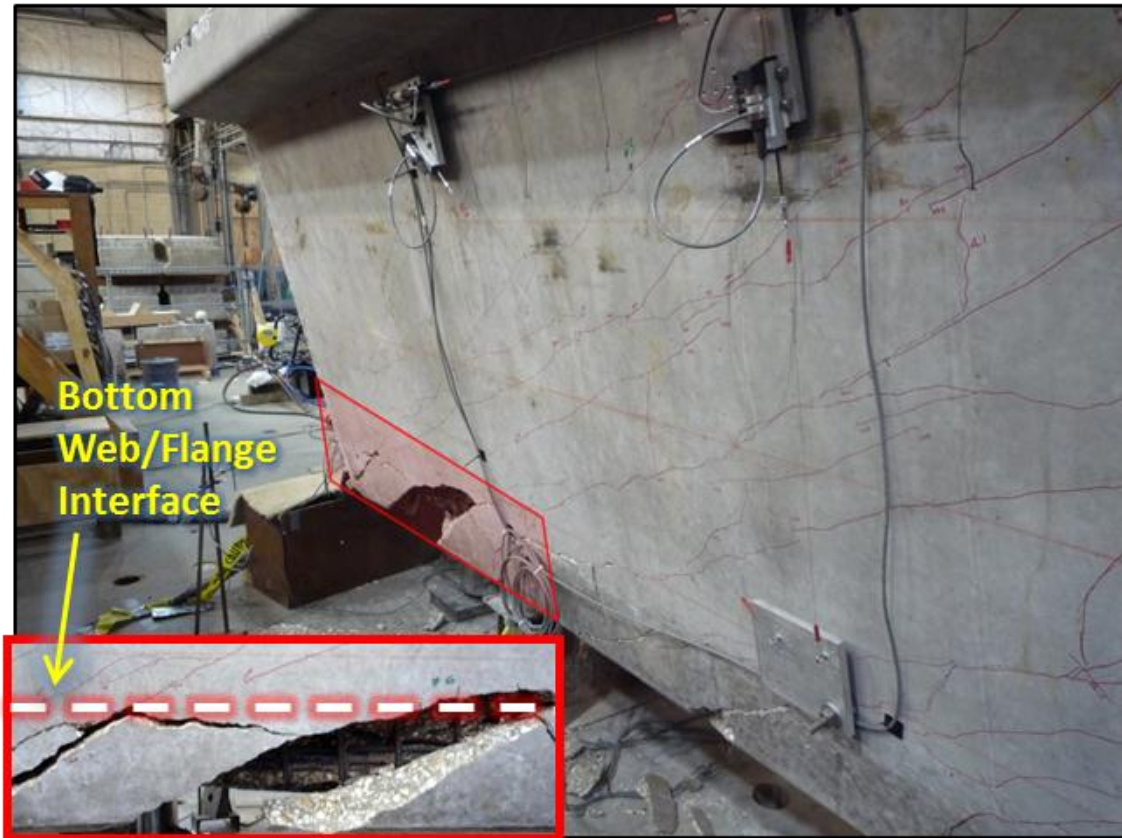
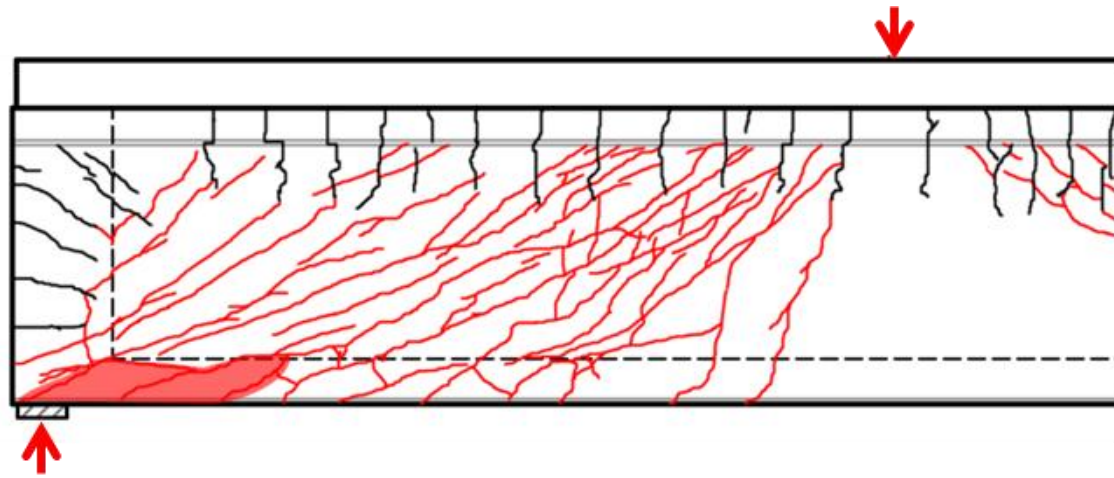


Figure 4-1: Beam 2 North, Web-to-Flange Interface Failure Crack

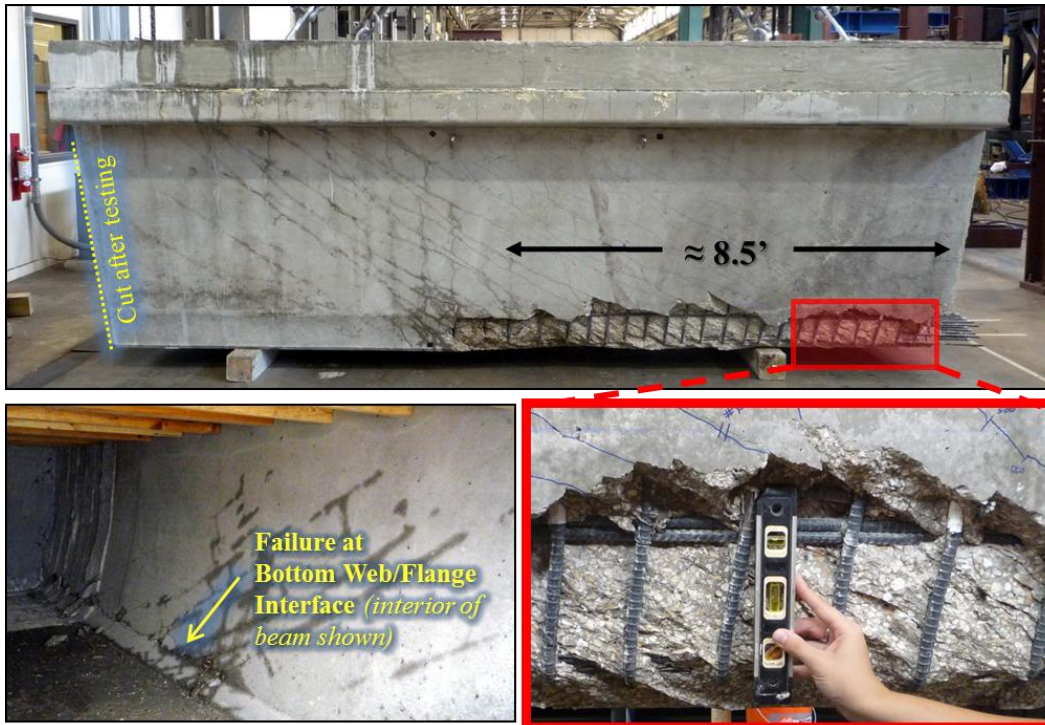


Figure 4-2: Beam 3 South, Web-to-Flange Interface Failure Crack

The diagrams shown in Figure 4-3 provide a comparison of the measured and code-calculated shear capacities for each of the Phase I shear tests. The solid line within each shear force diagram represents the applied shear (V_{test}) and includes the self-weight of the member. The dashed line represents the shear capacity ($V_{\text{calculated}}$) of the section based on the spacing of the transverse reinforcement and the provisions of the 2010 Interim AASHTO LRFD Bridge Design Specifications. A detailed explanation of the relevant AASHTO LRFD calculations for these beams can be found in Appendix A. It should be noted that the provisions of AASHTO LRFD Specifications are based on the assumption that shear failure will be governed by either the transverse steel yielding or

the web concrete crushing. As noted earlier, neither of these failure modes were observed in Beams 1 through 3. The ratio of the measured-to-calculated capacity for all three beams fell below a value of 1.0; indicating unconservative code estimates for shear capacity. While Beam 3 was quite close to meeting the code-calculated shear capacity ($V_{\text{test}}/V_{\text{calculated}} = 0.97$ on average), failure occurred in the region of the beam where the transverse reinforcement was spaced at 4 inches and therefore was theoretically the strongest.

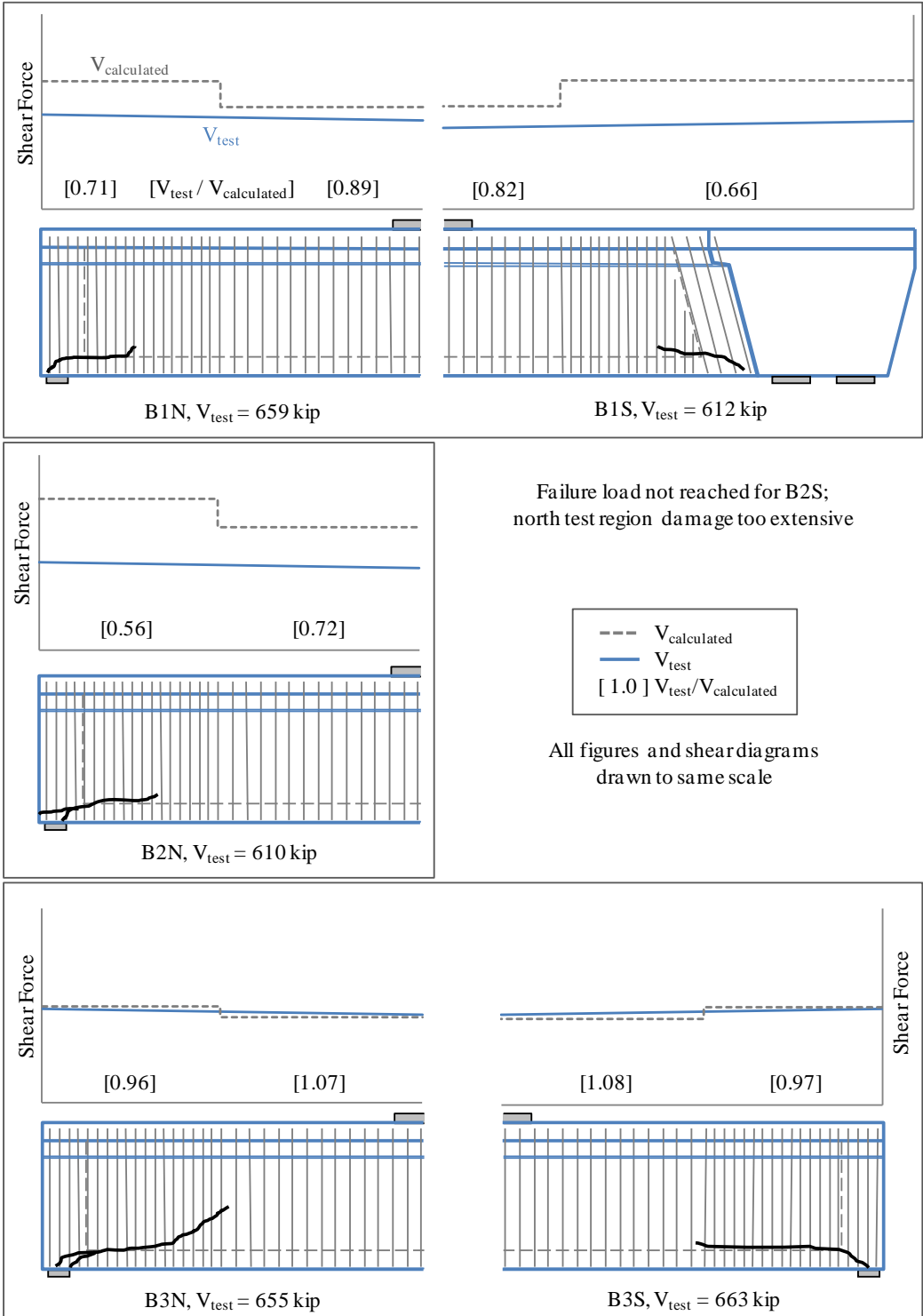


Figure 4-3: Summary of Phase I Shear Tests (Hovell, et al. 2010)

More generally, the maximum shear load recorded in each test was within 10 percent of the shear load recorded within any other test (to be clear this is V_{test} in kips), and there was no apparent correlation between the capacity and the end block configuration or the strand debonding scheme. Collectively, the test results suggested that an alternate failure mode (not accounted for in routine design procedures) was controlling the strength of the test specimens. This observation may have serious implications for in-service U-beam structures: premature failure via breakdown of the web-to-flange interface is a possibility under less predictable loading conditions which exist in the field.

4.3 CRITICAL EVALUATION OF PHASE I BEAM DESIGN

The two underlying assumption used in all prestressed concrete shear equations are that one of two failure methods will govern: either the shear reinforcement will yield or the web concrete will crush. As described in Chapter 3, the test region for all phase one beams contained a region with the transverse reinforcement spaced at 6-inches on center. Since the applied shear was constant it is assumed by the code equations that the beams would fail in this under-reinforced region due to yielding of the shear reinforcement. Because of the weak web-to-flange boundary this area never reached shear failure and instead the beam failed in an area which was assumed to be the strongest area of the beam (transverse reinforcement spaced at 4-inches).

Although horizontal shear failure has been reported in the literature, it has rarely resulted in an unconservative test result (relative to shear provisions within the applicable codes). The discrepancy between the results of the current study and those of other researcher's efforts is rooted in the unique geometry of the U-beam. In most single-webbed members, the supplementary reinforcement placed to resist the release stresses

also prevents the breakdown of the web-to-flange interface. In contrast, the large end-block of the double-webbed U-beam is used to control release stresses and therefore substantially less transverse reinforcement is needed in the webs. The disparity between the interface reinforcement found in a standard U-beam and an AASHTO Type IV (of equal height) girder is illustrated in Figure 4-4. The U-beam contains 1.2 square inches of reinforcement per linear foot of the two webs, while the AASHTO Type IV girder contains 9.6 square inches of reinforcement per linear foot of the single web (an 87.5% increase over the U-beam).

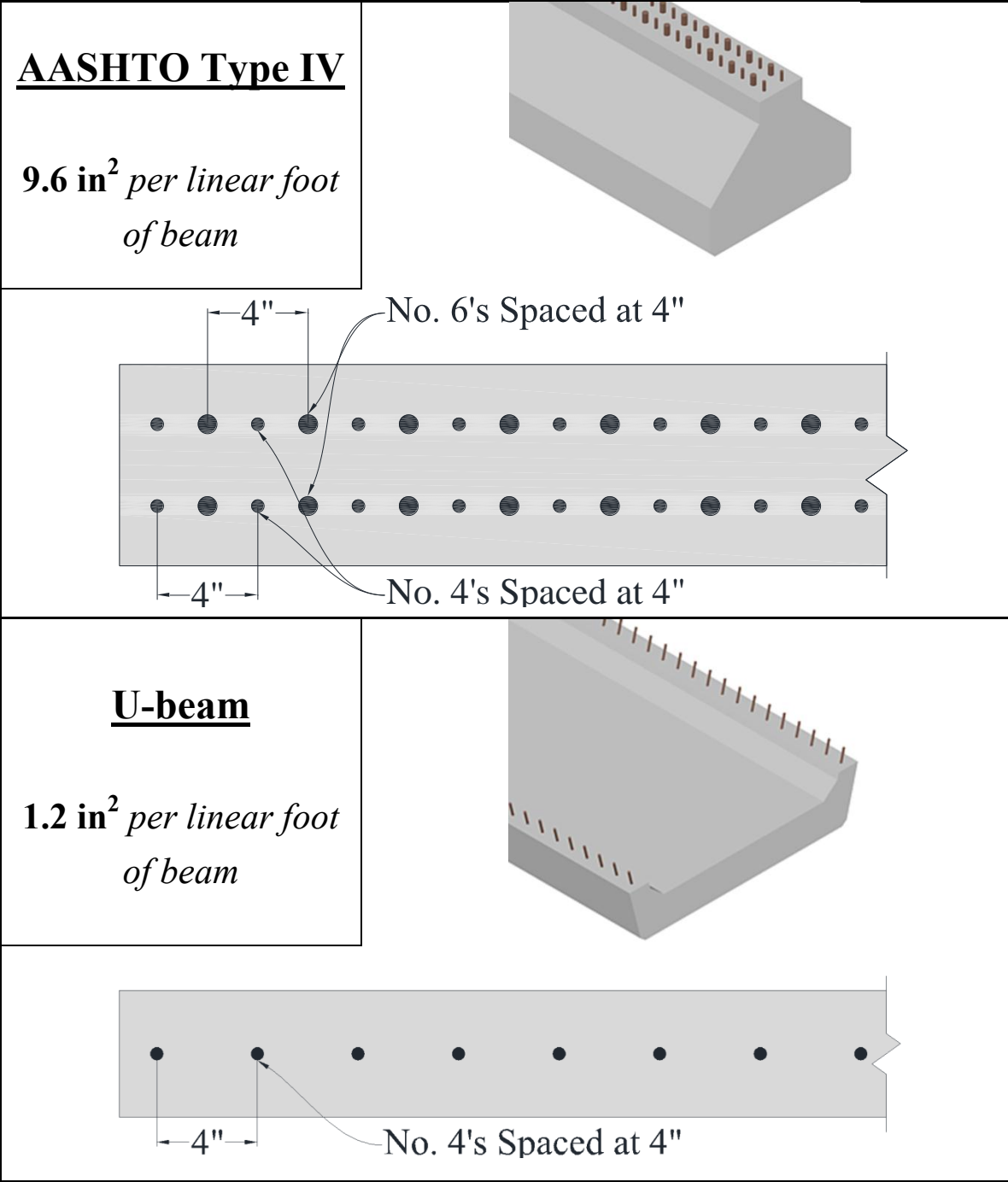


Figure 4-4: Transverse reinforcement crossing the web-to-flange interface comparison in AASHTO type IV and U-beam

The unique double-webbed geometry of the U-beam and the limiting web-to-flange interface failures poses an additional problem: assumed mobilization of both U-beam webs may not be possible as the beam is currently detailed. During the shear test of the south end of Beam 3, it became evident that one web of the beam reached failure before the other. The shear deformation was determined using the instrumentation shown in Figure 4-5. The southwest web of the beam exhibited deformations well above those found in the southeast web as shown in Figure 4-6. This is problematic due to the common design assumption that two webs will fail simultaneously which is an inherent assumption when the web width is taken as the sum of the two individual webs. Failure along one web-to-flange interface prevents gross yielding of the primary shear reinforcement and therefore inhibits plastic distribution of the load to the other web so that full load carrying capacity cannot be realized.

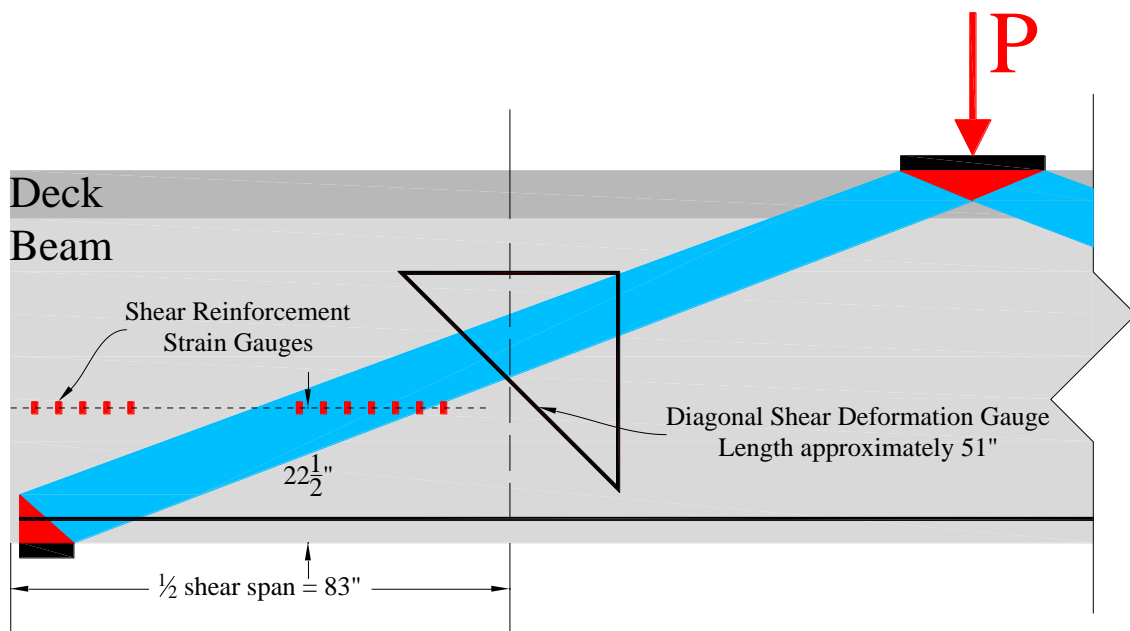


Figure 4-5: Location of Shear Deformation and Internal Strain Gauges

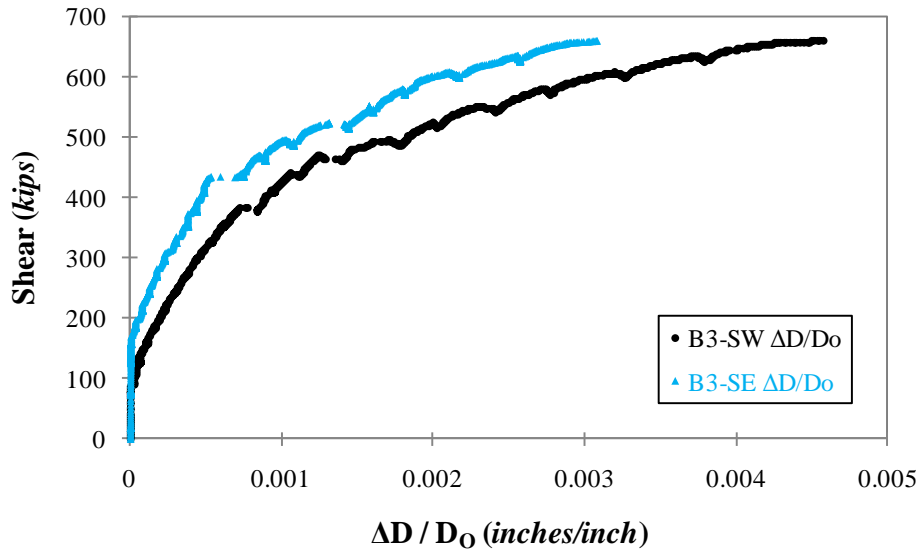


Figure 4-6: Graph of Diagonal Shear Deformation Gauge Beam 3 South

Although the multiple webs of the U-beam were the cause of this behavioral inconsistency (when compared to a beam with a single web) it still needed to maintain the cost effectiveness and quick design required by a standardized bridge girder section. Therefore, it was seen as necessary to redesign the end region details for future U-beams to prevent the premature breakdown of the web-to-flange interface.

4.4 SUMMARY

Phase one shear tests indicated that U-beams were not performing adequately under shear loading. The shear tests on Beam 3 indicated that the weakness of the web-to-flange interface was so great that it even precluded the beam from reaching the reduced shear strength expected from the introduction of debonded strands. Therefore, in phase two of this research a solution to the failure of the web-to-flange interface was developed by testing details which included thicker webs and an increased transverse reinforcement. The findings of these tests are discussed in detail in the following two chapters.

CHAPTER 5

Phase II Test Results and Discussion

5.1 INTRODUCTION

Phase I included five shear tests on three U-beams of standard cross-section. The measured shear strength of each specimen was less than the code-calculated shear capacities; irrespective of the strand debonding scheme, void or end block geometries. After thorough evaluation of the Phase I test results, it was noted that premature failure of the web-to-flange interface (not typically accounted for in design) precluded full development of the shear resistance within the twin webs of each U-beam. Elimination of the web-to-flange interface failure mechanism was therefore identified as the objective for Phase II testing.

In an effort to strengthen the web-to-flange interface, Phase II specimens featured revisions to both the cross-sectional geometry and reinforcement detailing of standard U-beams. Three new details were developed: (1) thickened webs with confining reinforcement, (2) thickened webs with confining and supplementary reinforcement, and (3) standard webs with confining and supplementary reinforcement. The new cross-sectional geometry and reinforcement details are described in Chapter 3, but are summarized in Figure 5-1 for convenience.

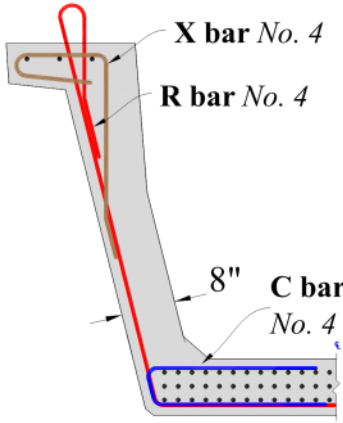
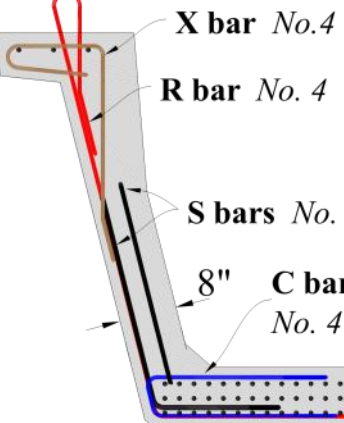
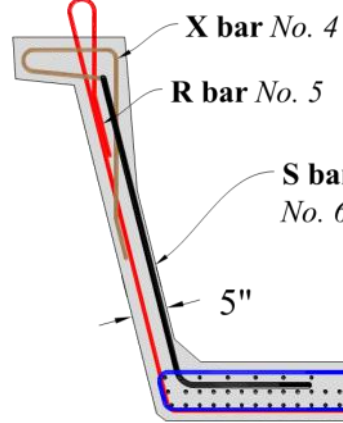
<p align="center"><u>Detail – A</u> <u>Beam 4 North</u></p>	<p align="center"><u>Detail – B</u> <u>Beam 4 South</u></p>	<p align="center"><u>Detail - C</u> <u>Beam 5</u></p>
 <p align="center"><i>Area of Steel Crossing web-to-flange interface: 0.6 in² per linear foot</i></p> <p align="center"><i>Small increase in Reinforcement Thickened webs</i></p>	 <p align="center"><i>Area of Steel Crossing web-to-flange interface: 3.28 in² per linear foot</i></p> <p align="center"><i>Large increase in Reinforcement Thickened webs</i></p>	 <p align="center"><i>Area of Steel Crossing web-to-flange interface: 2.25 in² per linear foot</i></p> <p align="center"><i>Large increase in Reinforcement Standard webs</i></p>

Figure 5-1: Description of beam designs tested in Phase II of Research

A total of three shear tests were conducted on the Phase II U-beams. As discussed below, two of the proposed details (Details B and C in Figure 5-1) were deemed to be viable solutions to the horizontal shear failure mechanism encountered in Phase I U-beams. Advantages and disadvantages of each detail are discussed at the end of this chapter.

5.2 PHASE II TEST RESULTS

The increases in both web thickness and reinforcement were anticipated to have significant impacts on the performance of the U-beams at service and ultimate limit states. The effectiveness of each new detail is examined below; other practical considerations, including those related to constructability, are discussed in Sections 1.3 and 1.4.

5.2.1 Performance at Service Level Shear

Since the Phase II beams were redesigns of the existing standard U-beam it is necessary to compare their behavior to that of the previous design (tested during Phase I). The service level behavior of the Phase I beams (discussed in Section 4.2.1) was favorable in that they showed few hairline cracks (cracks of less than 0.005-inches in width). Since the Phase II beams were meant as a redesign of the existing standard the same service level shear of 275-kips was used for comparison. This value was a result of considering the worst case scenario of two sample bridges: (1) a 120-foot bridge with a 45-degree skew and (2) a 140-foot bridge with no skew. A more detailed description of these calculations can be found in Section 4.2.1.

Beam 4, which featured thickened webs with and without additional reinforcement, showed no cracking at the assumed service level shear of 275 kips (shown in Figure 5-2, Detail - A). Notable diagonal cracking only began to form at high levels of shear corresponding to more than 80 percent of the maximum applied load of 973 kips. Beam 5 (shown in Figure 5-2, Detail – B), which featured standard webs with additional reinforcement, exhibited service level cracking similar to that observed during Phase I tests. The slight increase in cracking relative to Beams 1 and 2 can be attributed to the

lower prestressing force (12 fewer strands were utilized) in Beam 5. This behavior is consistent with the slight increase in cracking seen between Beams 1 and 2 when compared to Beam 3 (which contained debonded strands and therefore a lower prestressing force) in Phase I testing.

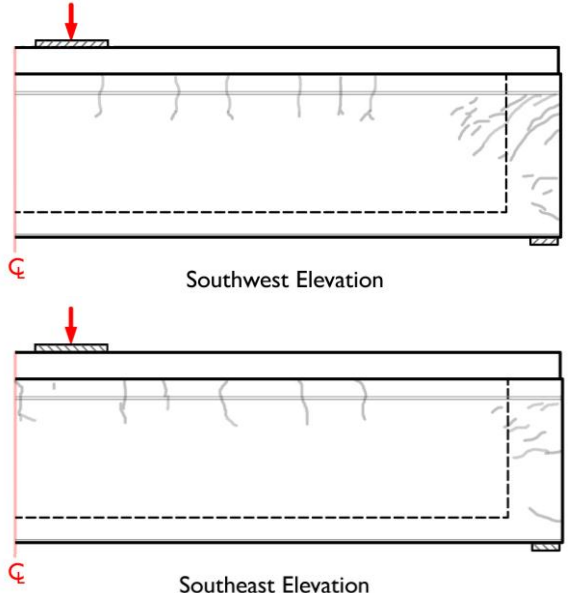
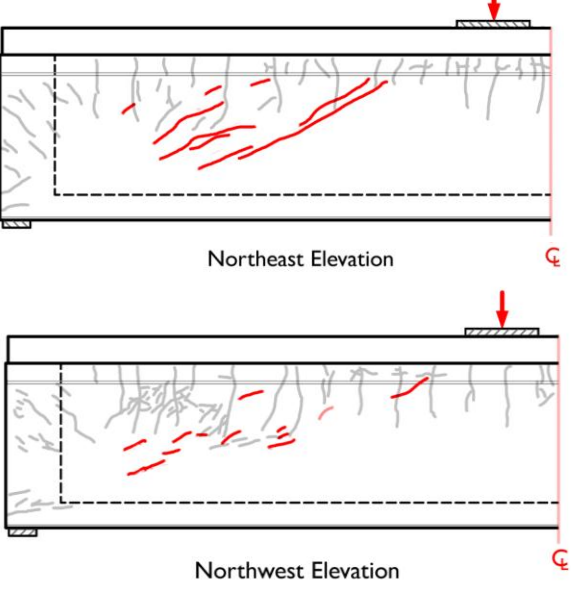
<p><u>Detail - A</u></p>	<p>BEAM 4 <i>at values less than 800-kips no shear cracking</i></p>	 <p>The Southwest Elevation (top) and Southeast Elevation (bottom) of Beam 4 show a beam under a central point load. The drawings illustrate the internal structure with strands and reinforcement. No shear cracks are present. A red arrow indicates the load, and a red 'f' symbol is at the bottom left of each elevation.</p>	<p><i>The North end of Beam 4 and the South end of Beam 5 were clamped during testing for service level shear (during the first shear test performed on the specimen). Therefore the service level cracking for those beams is not documented here.</i></p>
<p><u>Detail - B</u></p>	<p>BEAM 5 <i>Shear = 275-kips</i></p>	 <p>The Northeast Elevation (top) and Northwest Elevation (bottom) of Beam 5 show a beam under a central point load. Red dashed lines indicate diagonal shear cracks. A red arrow indicates the load, and a red 'f' symbol is at the bottom right of each elevation.</p>	

Figure 5-2: Phase II service level cracking behavior

The thickened web solution of Beam 4 virtually eliminated serviceability concerns related to diagonal cracking under service loads. This outcome can be attributed to the large concrete contribution (relative to the reinforcement contribution) to the shear capacity of Beam 4. The thick webs of the beam were able to resist the service level shear with little deformation and no apparent cracking. In contrast, the standard webs of Beam 5 cracked under the service level shear and deformed significantly as further demand was redistributed to the transverse reinforcement. While the service level cracking observed within the standard webs of Beam 5 was not severe in nature, it should be noted that a heavy reliance on the reinforcement contribution to shear capacity (as opposed to the concrete contribution) has been shown to result in reduced serviceability of prestressed concrete members (Avendaño, Shear Strength and Behavior of Prestressed Concrete Beams 2008).

5.2.2 Performance at Maximum Applied Load

Phase II revisions to the U-beam geometry and reinforcement detailing served two purposes: (1) experimental validation of solutions to the undesirable failure mode witnessed in Phase I, and (2) of the three configurations tested two exceeded the capacities predicted by the AASHTO LRFD (2009 Interim) code equations. The only specimen which did not reach its calculated capacity was Beam 4 North which contained thicker webs and a small increase in the transverse reinforcement. A description of each failure (and the behavior of Beam 4 South which was not loaded to failure) is given in the following sections.

5.2.2.1 *Beam 4 North*

The north end of beam 4 contained confining reinforcement and a small increase in the amount of shear reinforcement (R-bars spaced at 3-inches where current standard is 4-inches on center). The Beam 4 geometry was modified to include three extra inches of concrete in the webs thus making each web 8-inches thick (the current standard is 5-inches thick). This beam failed below its calculated capacity at a shear of 973-kips.

The failure initially appeared to have occurred due to localized anchorage loss directly over the bearing pad (figure shown in Appendix C), but when the beam was cut into shorter sections the interior was examined to reveal any failures of the web-to-flange interface. Extensive cracking was found along this interface (shown in Figure 5-3) similar to the cracking seen in Phase I testing. It was determined that the lack of steel crossing this boundary caused this failure mechanism to govern the strength of the member. Since this beam did not reach the AASHTO LRFD calculated shear capacity it was not considered an adequate solution for the problems experienced during Phase I testing.

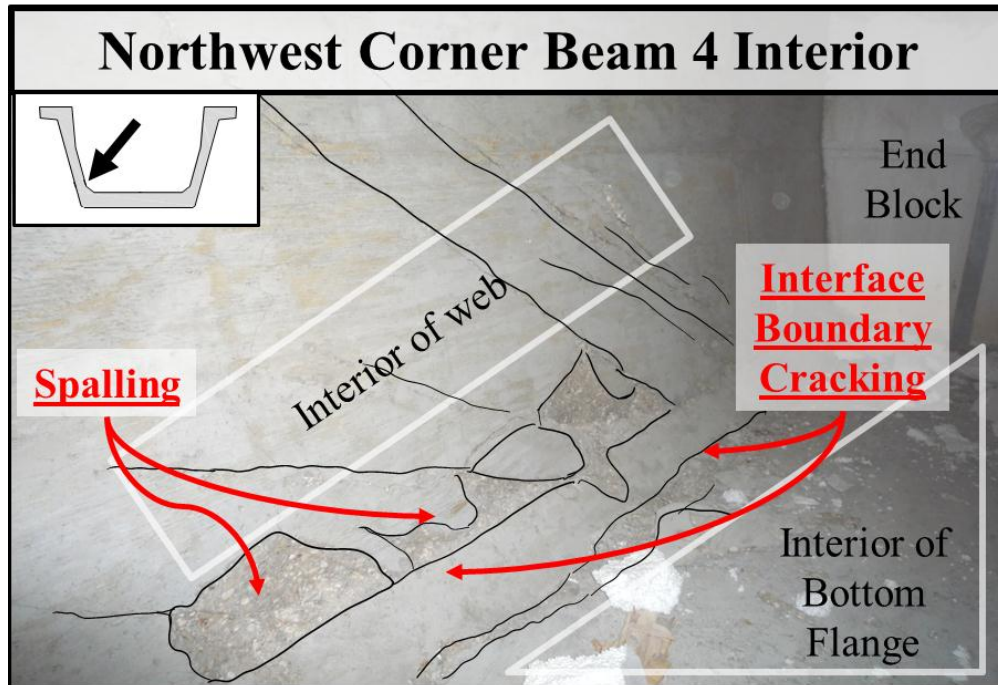


Figure 5-3: Interior of Beam 4 Showing Web-to-Flange Interface Failure

5.2.2.2 *Beam 4 South*

The south end of beam 4 included thickened webs and a large increase in transverse reinforcement. Because of the desire to prevent damage to the untested end of the beam the south end was not taken to failure but was instead loaded until it exceeded its calculated shear capacity. At this point the largest shear crack measured 0.016-inches; by comparison the cracks immediately prior to failure in previous beams ranged from 0.03 to 0.04-inches, also the strain gauge readings from the transverse reinforcement placed at a height of 22.5-inches from the bottom of the beam show strains of around half the yield strain as shown in Figure 5-6. Therefore it can be assumed with reasonable certainty that Beam 4 was not near failure at the time the testing was halted. This beam achieved its AASHTO LRFD calculated capacity and was considered an acceptable solution to the current problematic detail.

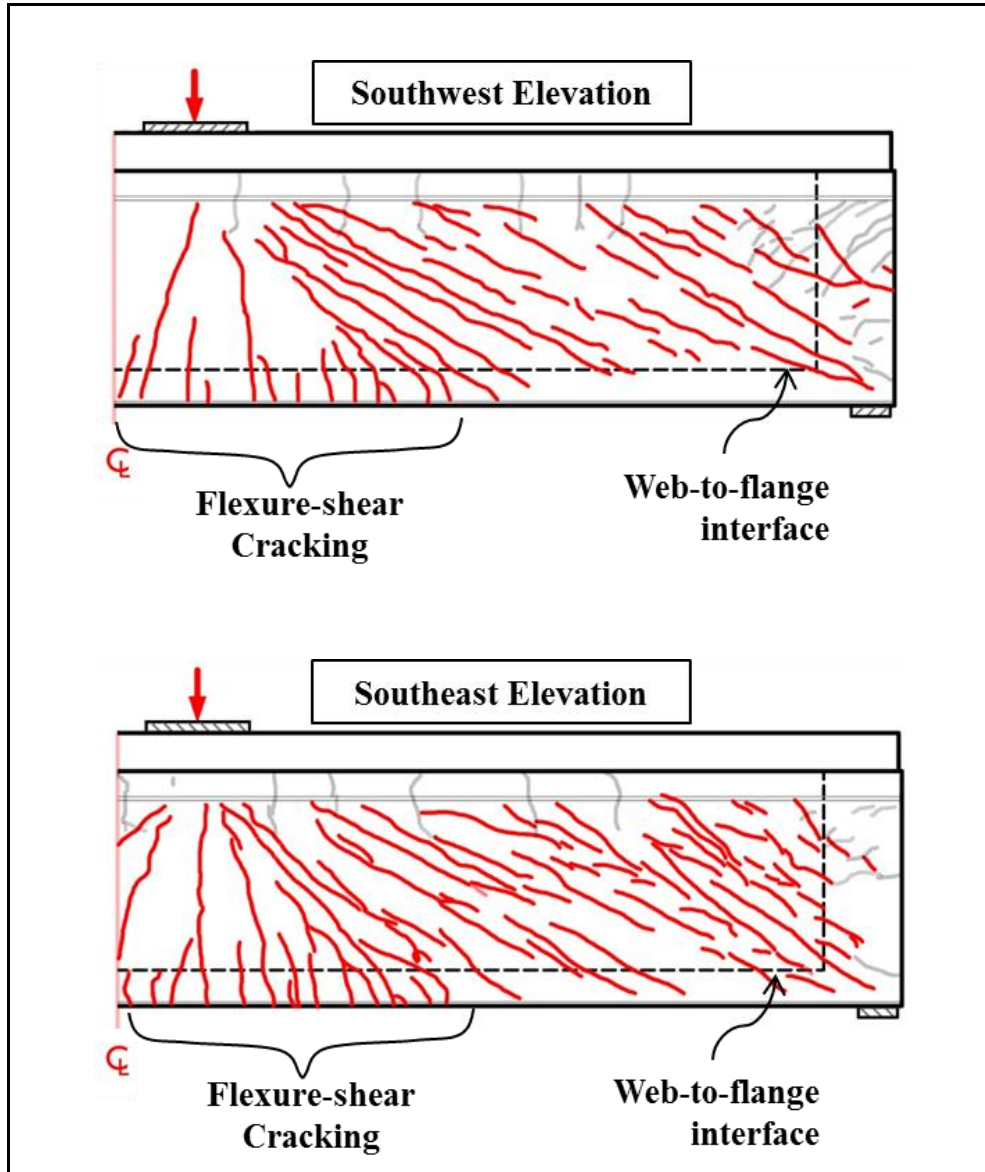


Figure 5-4: Beam 4 South Cracking at Maximum Applied Load

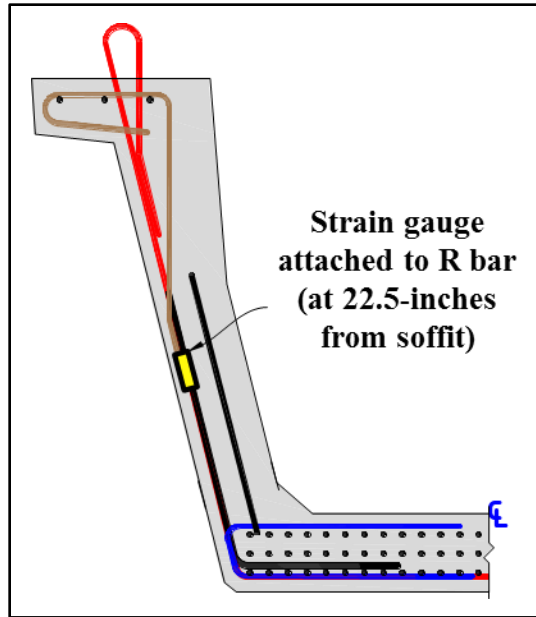


Figure 5-5: Strain gauge location in reference to Figure 5-6

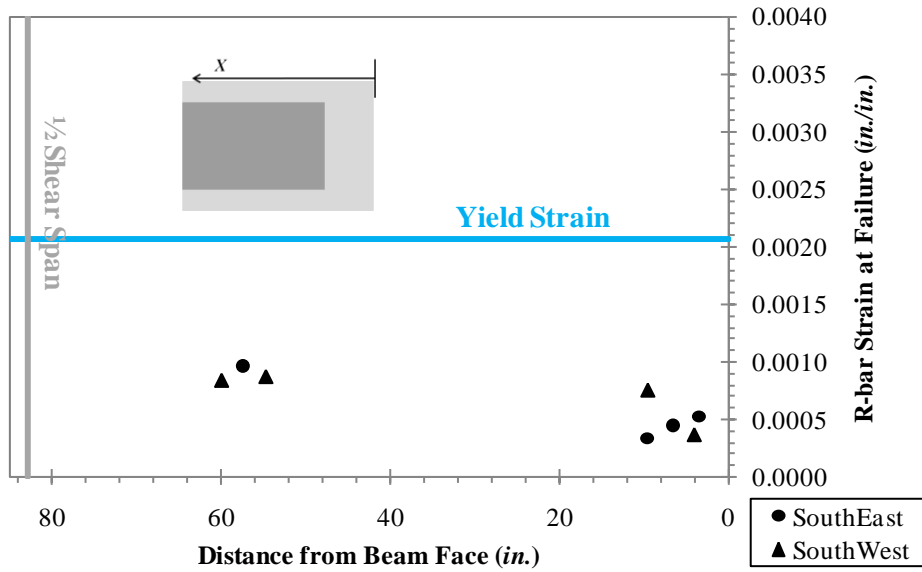


Figure 5-6: Beam 4 South Strain Gauge Data from Transverse Shear Reinforcement

5.2.2.3 *Beam 5 North*

Beam 5 maintained the original beam geometry (5-inch thick webs) while drastically increasing the amount of reinforcement crossing the web-to-flange interface. This increase in transverse reinforcement was terminated 8.25-feet from the end of the beam. As should be expected the failure was seen away from this heavily reinforced region and occurred in the region containing number 5 rebar spaced at 6-inches. This region of the beam experienced a large number of flexure-shear cracks which caused the failure shown in Figure 5-7 through Figure 5-9. As illustrated in Figure 5-8 this was indicative of flexure-shear failure in that it was sudden and violent. Figure 5-9 shows the large permanent displacement (7-inches) of the bottom flange at the point of failure.

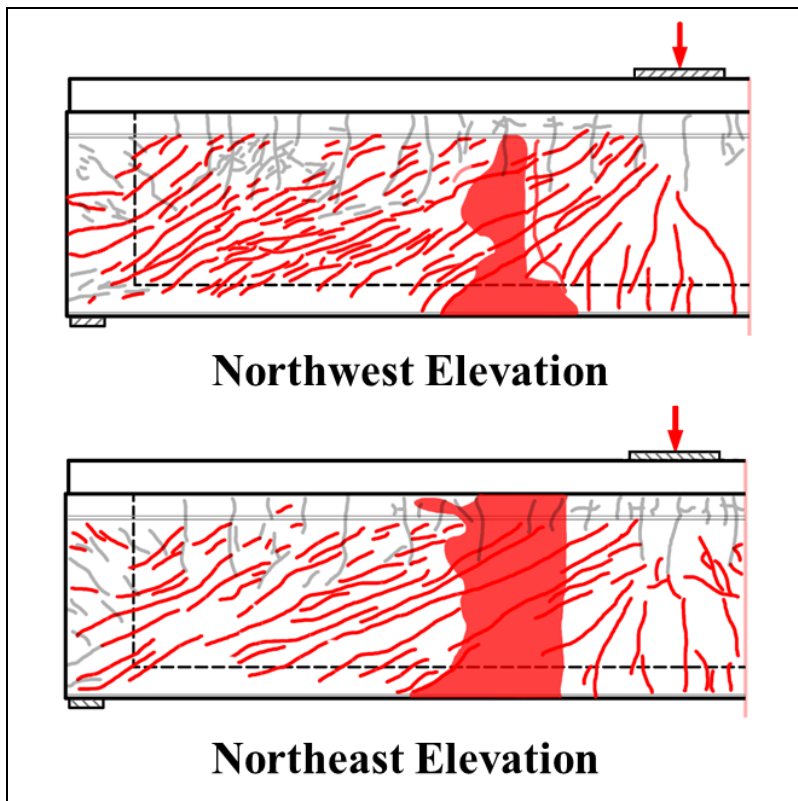


Figure 5-7: Beam 5 North cracking at failure



Figure 5-8: Beam 5 post-failure

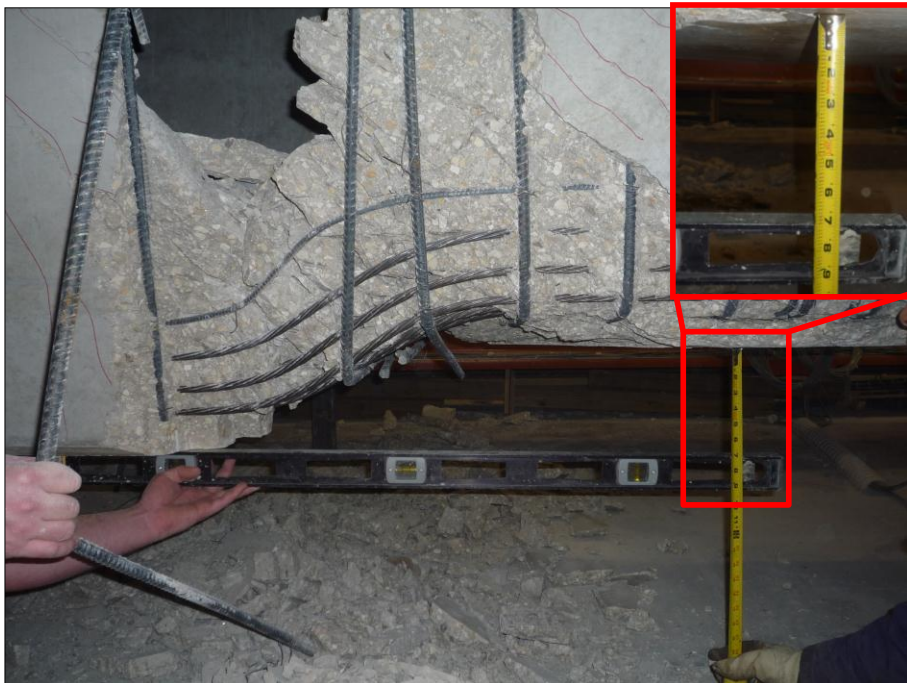


Figure 5-9: Beam 5 post-failure showing large permanent displacement

5.2.3 Comparison to AASHTO LRFD (2009 Interim) Calculated Capacities

The increase in transverse reinforcement crossing the web-to-flange boundary in Beam 4 South and Beam 5 North ensured that these beam's capacities were governed by a failure mechanism which the current code provisions predict. Therefore these beams performed well when they were compared to the provisions of AASHTO LRFD (2009 Interim). A summary of these predicted capacities and a comparison to their tested maximum loads is shown in Figure 5-10 while a more detailed description of the code equations and the capacity calculations are given in Appendix A.

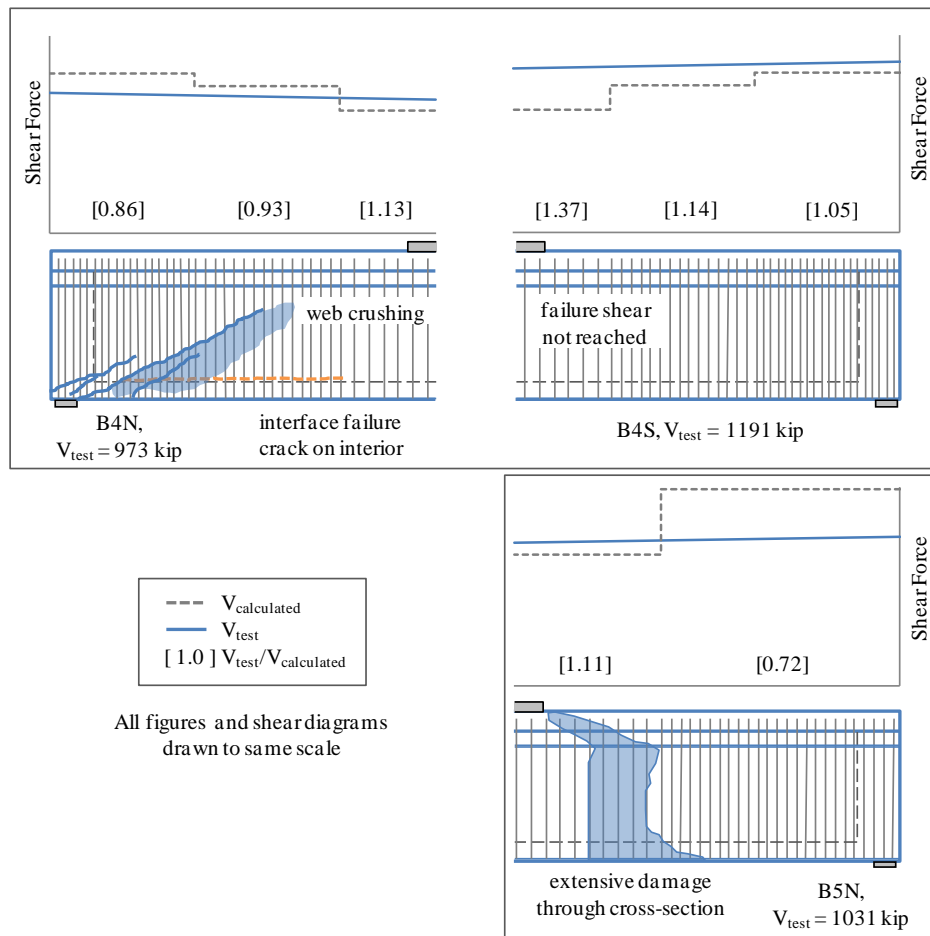


Figure 5-10: Tested versus Calculated Capacities, Phase II Beams (Hovell, et al. 2010)

5.3 UNDERSTANDING DIFFERENCES BETWEEN PHASE I AND PHASE II BEAMS

The difference between beams which reached their calculated capacities and those which failed prematurely along the web-to-flange interface was purely a matter of the amount of transverse reinforcement crossing the web-to-flange interface. In Beam 4 North and Beam 5 North there was a large amount of supplementary reinforcement crossing this boundary. The supplementary reinforcement prevented the primary shear reinforcement from being stressed to yield along the interface while still allowing the primary shear reinforcement to reach yield and behave as described by code equations.

The supplementary transverse reinforcement should not be seen as contributing to the shear strength of the member because it must be relied upon to prevent the failure of the web-to-flange interface, and to that end it may be terminated at its development length away from the web-to-flange interface. This early termination serves as a safeguard against a designer considering the supplementary reinforcement to be primary shear reinforcement and thus relying on the strength of these bars in shear capacity calculations.

5.4 FURTHER COMPARISON OF BEAMS 4 AND 5

Two design considerations which have not been discussed are the cracking at loads exceeding the service level shear and the constructability of the beam which is a concern due to the increase in reinforcement congestion in the end-region of the beam.

5.4.1 Cracking above Service Level Shear

A consideration in choosing the best design for future Texas U-Beams is the cracking behavior at loads beyond the service level shear. Beams may routinely

experience these loads when bridges are approved for heavy, permitted loads by the Texas Department of Transportation.

As was discussed in Section 5.2.1 the service level shear behavior of the beams is drastically different. Beam 4 did not show signs of first cracking until the shear was more than twice the service level. The discrepancy in cracking levels holds true for all load levels (as can be seen in Figure 5-11). At a $V_{\text{test}} / V_{\text{calculated}}$ of 1.14 Beam 5 failed while (although thoroughly cracked) Beam 4 South remained intact.

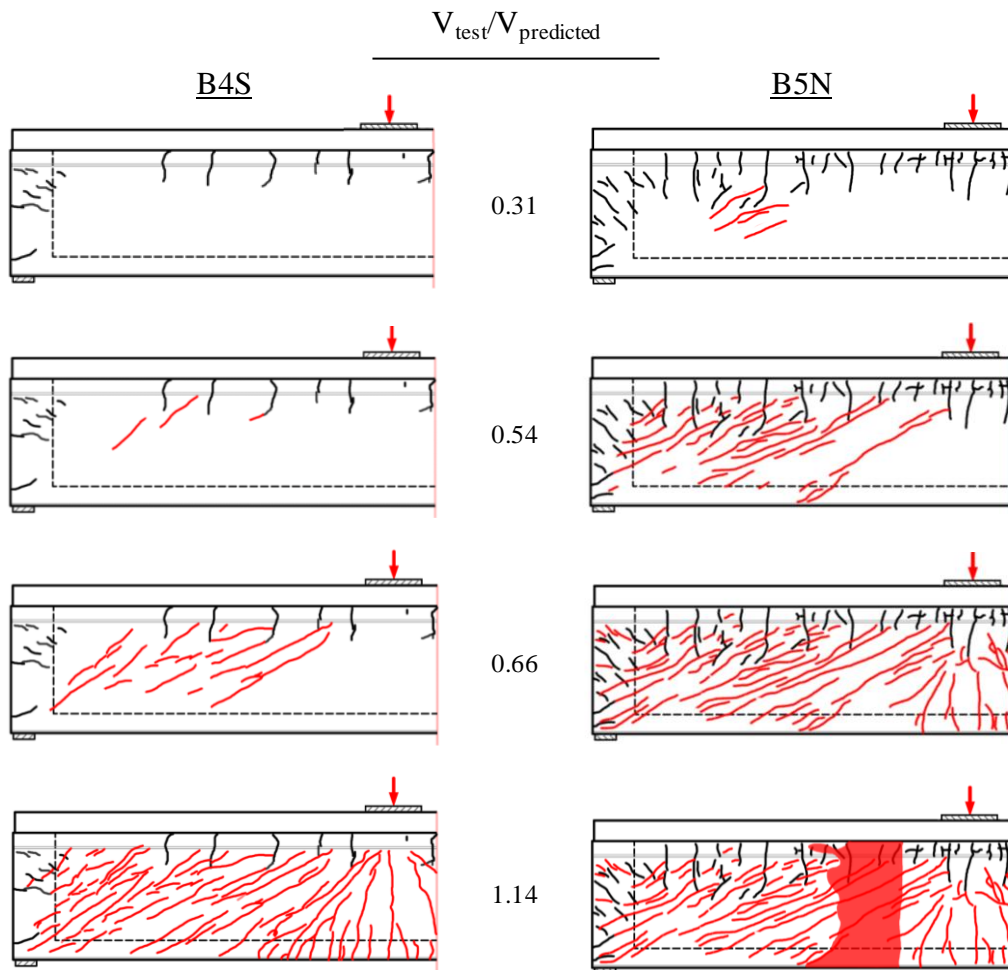


Figure 5-11: Cracking Comparison for Beam 4 South and Beam 5 (Hovell, et al. 2010)

5.4.2 Constructability

A non-structural consideration in beam design is constructability. This is a concern in Phase II beams because of the large increase in transverse reinforcement necessary to prevent the premature web-to-flange interface failure and the inclusion of confining reinforcement.



Figure 5-12: Bottom clear-cover in Beam 5

The current U-Beam standard (tested in Phase I) maintains a clear-cover of 1.5-inches on the bottom of the beam. This is the distance from the outermost steel reinforcement (the R-bar in this case) to the outer face of the beam. In Beam 5 the R-bars were increased from a number 4 to a number 5 bar. This increase would prevent the current cover requirements from being reached because of the location of the prestressing strand and therefore during the construction of Beam 5 1.5-inch rebar chairs were used to force the correct cover as illustrated in Figure 5-12. To install the chairs the strands were effectively “harped” by hand (Figure 5-13). This practice is problematic both because it induces a larger load into the prestressing strand after it has been brought to full stress and because it is a highly labor intensive procedure.



Figure 5-13: Manual Installation of Rebar Chairs for Beam 5

The increase in R-bar size also causes a reduction in clear-cover at the outer face of the webs. In Beam 5 this was solved by again prying back the reinforcement and inserting rebar chairs between the forms and the R-bars. The force on these chairs was enough in some cases to break the plastic chair and eventually in several places the rebar had to be held back with rebar tie wire as shown in Figure 5-14.

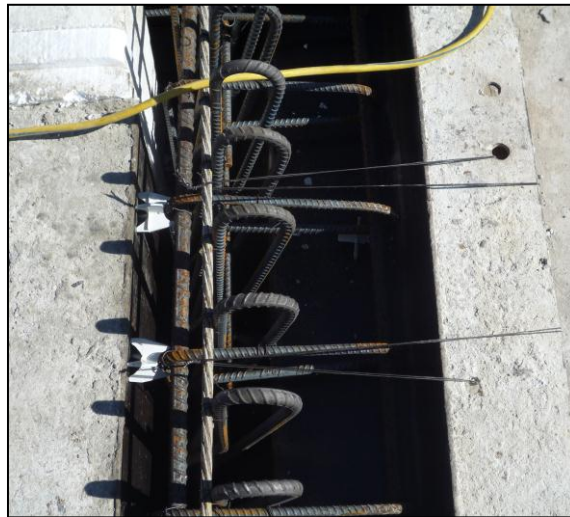


Figure 5-14: Rebar Tie Wire Holding Reinforcement for proper cover from Interior Void

5.5 GENERAL EXAMINATION OF WEB-TO-FLANGE INTERFACE FAILURE

Prior to the current study, failure of the web-to-flange interface had been reported by a number of researchers investigating the shear behavior of single-webbed prestressed concrete beams (such as Nagle and Kuchma (2007), Ma, Tadros, and Baishya (2000), Bruce, Russell, and Roller (2005) (Nagle and Kuchma 2007)). Despite positive identification of the unique failure mechanism, more detailed investigations were generally not warranted. Beams tested within the laboratory were failing at or above the shear capacity calculated through the use of applicable design equations. Comparisons between the code-calculated and measured shear capacities for Phase I (standard) U-beams did not prove to be as fortuitous. The results of the current experimental program have generally highlighted the need for further study of the horizontal shear failure mechanism in prestressed concrete members. Development of generalized design methodologies would eliminate the potential for premature web-to-flange interface failures for prestressed concrete members especially in cases involving atypical geometries. Following a brief description of the web-to-flange interface failure, the factors influencing the failure mechanism are identified and placed within the context of current and future research.

1.1.1 Description of Web-to-Flange Interface Failure

Within the context of the current study, web-to-flange interface failure is defined as a sudden transverse separation and large longitudinal displacement between the web and bottom flange of a monolithic, thin-webbed prestressed concrete member (shown in Figure 5-15).

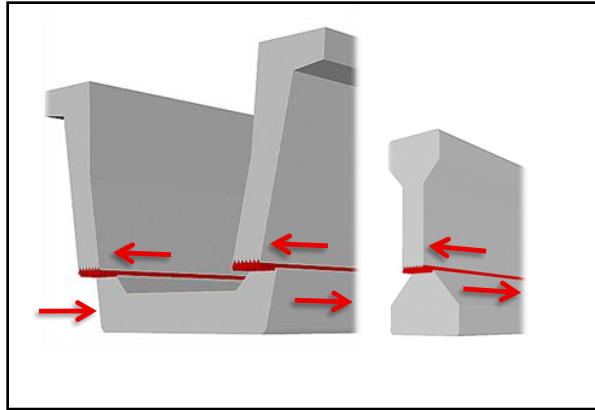


Figure 5-15: Web-to-Flange Interface Failure

Web-to-flange interface failure (sometimes referred to as horizontal shear failure) can occur in any concrete member, but is most prevalent in prestressed concrete girders due to the use of webs that are thin in comparison to the overall girder width. The transfer of external forces from the topside of a prestressed concrete girder to the support generates large horizontal shear stresses at the web-to-flange interface. The opposing forces at the interface are illustrated in Figure 5-15. The horizontal component of the diagonal compressive stress in each web is equilibrated by the longitudinal force applied by the prestressing tendons in the bottom flange. Breakdown of the interface between the web and flange leads to a loss of equilibrium and sudden failure.

1.1.2 Factors Influencing Web-to-Flange Interface Failure

Generalized treatment of the web-to-flange interface failure mechanism will be complicated by a number of factors. Examination of a typical prestressed beam end region (shown in Figure 5-16) clearly identifies the key parameters to be considered in future studies of web-to-flange interface failures.

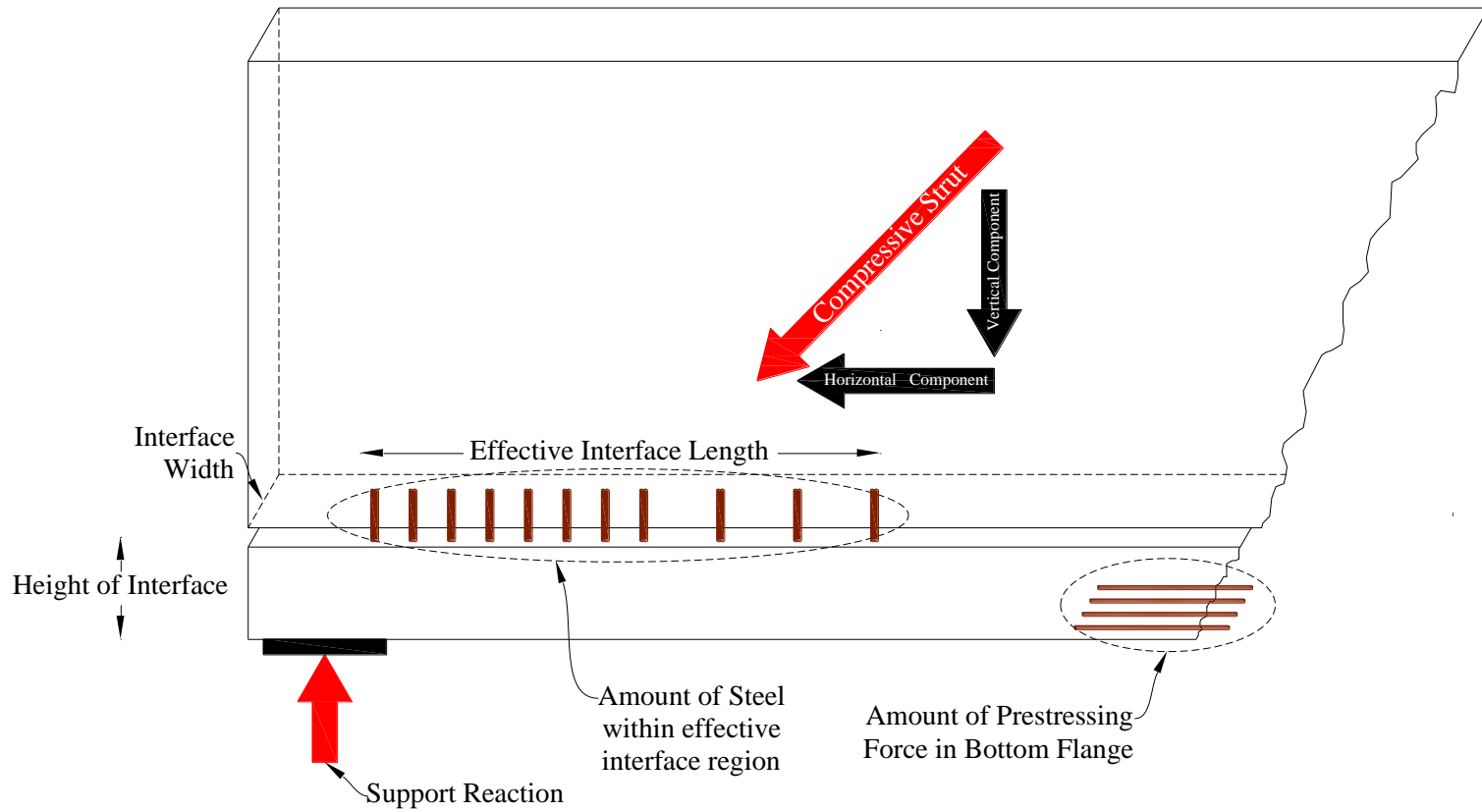


Figure 5-16: Variables affecting the susceptibility of prestressed concrete beams to failures at the web-to-flange interface

from Nagle and Kuchma (2007)

The factors included in the above figure are: (1) the amount of reinforcement crossing the interface, (2) the effective interface length, (3) the interface width, (4) the amount of prestressing force present in the bottom flange, (5) the magnitude and location of the externally applied load, (6) and the height of the web-to-flange interface region from the bottom of the beam. Although it is understood that all of these parameters contribute to the capacity of the web-to-flange boundary, little is known as to which ones are the primary contributors to strength.

Despite relatively few tests, the current experimental program was successful in revealing the importance of one aforementioned factor. The results of Phase II (refer to Table 5-1) clearly indicate that if sufficient reinforcement is placed across the web-to-flange interface shear failure along this boundary can be prevented.

Table 5-1: Summary of Phase II Shear Testing

Beam	Cross-sectional thickness at web-to-flange interface	Area of steel crossing web-to-flange interface	V_{test}/V_{calc}
Beam 4 North	16-inches	1.60 $in.^2/foot$	0.86
Beam 4 South	16-inches	5.23 $in.^2/foot$	greater than 1.05
Beam 5 N & S	10-inches	2.25 $in.^2/foot$	1.11

Alternatively, an increase in interface width did not yield significant strength gains unless there was a corresponding increase in reinforcement. It is nevertheless likely that a more optimal combination of interface width and reinforcement area exists for the U-beam. The aim of the project was to identify practical solutions to premature web-to-flange interface failures observed in Phase I testing. As stated earlier, a more generalized,

accurate approach to controlling web-to-flange interface failure will require a substantial amount of testing and analysis of the parameters identified above.

1.1.3 Applicable Research

The examination of web-to-flange interface failures shares a number of similarities with the study of shear friction in monolithic concrete members and horizontal shear in composite concrete members. Study of the literature regarding these mechanisms may provide valuable insight into the future treatment of web-to-flange interface failures.

The horizontal shear provisions in both ACI 318-08 and the AASHTO LRFD Specifications describe the transfer of shear across a joint. These provisions were never intended for use in the area of the web-flange interface at the support, but instead for the interface between the deck and the girders and at the web / flange interface away from the support (well into the B-region).

These equations assume that there is a normal force across the joint as a result of the joint opening and therefore straining the reinforcement. This effect is referred to in the literature as the “clamping force” (Birkeland and Birkeland 1966) and is illustrated in Figure 5-17.

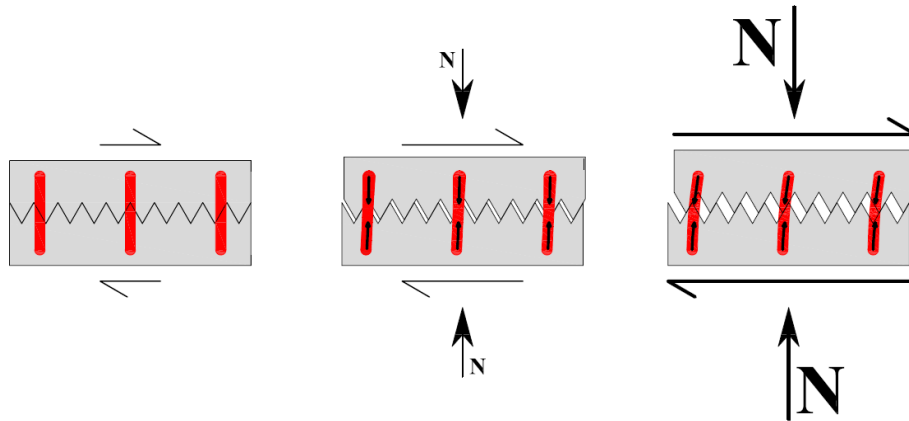


Figure 5-17: Clamping force illustration (Birkeland and Birkeland 1966)

A report by Nagle (2007) was the first to specifically address the breakdown occurring at the web-to-flange boundary. In his report Nagle offered an easy, hand calculation to check the adequacy of the web-to-flange interface. The equations used existing horizontal shear provisions found in both the ACI code and the AASHTO specifications with a few small modifications. Using these equations paired with a simplified strut and tie model provided an easy way for checking and preventing this failure mechanism in I-beams, the most typical type of prestressed concrete beams in use today.

5.6 SUMMARY

Two of the three designs developed in Phase II of testing provided acceptable alternatives to the current design of the Texas U-Beam. The benefits of each design are evident in that one allows the use of existing formwork and the other ensures a higher failure load, minimizes cracking, and ensures cover requirements. The benefits of ensuring that future U-Beams fail in a manner which can be predicted by code equations outweigh the costs of these modifications, but future testing and optimization of these

solutions is advised in order to assure that all of the concerns identified in this study have been addressed.

More research is necessary in order to fully understand the mechanisms which cause failure of the web-to-flange interface. Generalized treatment of web-to-flange interface failure will ultimately require the consideration of multiple variables and resolution of very complex boundary conditions. Current code provisions which address shear friction in monolithic concrete could provide a logical starting point for the treatment of web-to-flange interface failure.

CHAPTER 6

Summary, Conclusions and Recommendations

6.1 SUMMARY

The findings presented in this thesis are the product of Texas Department of Transportation (TxDOT) Project 0-5831, “Bursting and Shear Behavior of Prestressed Concrete Beams with End Blocks.” The purpose of this study was to investigate the bursting and shear behavior of TxDOT standardized U-beams and box beams with multiple end block configurations. The scope of this thesis is limited to the preliminary evaluation of the shear behavior of standard and modified U-beams.

The testing program involved two main stages: (Phase I) involved the testing of the current standard design for U-beams and (Phase II) covered the redesign of the U-beam in order to address the concerns raised during the Phase I testing.

During Phase I of the research program three beams were tested in shear. The two main variables under consideration were: (1) the configuration of the interior void as it related to an external skewed end block (2) and the number of debonded strands in the bottom flange (and therefore the level of the prestressing force). Upon evaluating the results of Phase I it was discovered that the beams were failing below their code-calculated shear capacities. During Phase I it became clear that the failure mechanism causing the low shear capacity was failure of the web-to-flange interface. Therefore, the Phase II the research program focused on redesign of the end region of the U-beam in an effort to prevent premature failure of the web-to-flange interface.

Phase II of this research program focused on preventing the failure of the web-to-flange interface. Three variables were addressed during this phase in an effort to both

understand and prevent this failure mechanism: (1) increase of the web thickness without an increase in the transverse reinforcement, (2) increase in web thickness with an increase in the transverse reinforcement crossing the interface, (3) and maintaining the current web width while increasing the transverse reinforcement crossing the interface.

Phase II resulted in two viable redesigns of the beam end-regions. Both designs incorporated an increase in the transverse reinforcement crossing the interface, but one called for an increase in the web width while the other did not. Although more research is required to fully understand the web-to-flange interface failure; In Phase II, it was found that the primary variable influencing the breakdown of the web-to-flange boundary was the transverse reinforcement crossing that boundary.

6.2 CONCLUSIONS AND RECOMMENDATIONS

Full-scale testing of multiple specimens provided a realistic evaluation of the shear behavior of TxDOT standardized U-beams. Observations and data gathered over the course of two experimental phases provide a clear picture of the modifications necessary for serviceability and strength of TxDOT standardized U-beams. Conclusions relating to the performance of standard and modified (as discussed above) U-beams are summarized below.

- The results of **Phase I testing indicate that the standard 54-inch U-beam is incapable of achieving the code-calculated shear capacity (AASHTO LRFD Bridge Design Specifications, Interim 2010) due to a failure of the web-to-flange interface.** Failure of the web-to-flange interface has been tied to a lack of transverse reinforcement across the boundary. The transverse reinforcement present at the web-to-flange

interface of a standard U-beam is 88 percent less than that crossing the interface of two 54-inch AASHTO I-Beams; which together have a moment capacity comparable to a single 54-inch U-Beam.

- **At least an eighty eight percentage increase in transverse reinforcement at the web-to-flange interface is necessary to: (1) prevent premature interface failure, and (2) ensure that standard U-beams are capable of achieving the code-calculated shear capacity.**

The supplementary reinforcement at the web-to-flange boundary must not be relied upon as primary shear reinforcement. Such a design implies dual demand on the transverse reinforcement which could inadvertently result in an undesirable failure mechanism. It is recommended that the supplementary interface reinforcement be terminated at a location well below the top flange of the beam while still allowing for development of the bars above the web-to-flange interface. This detailing consideration will prevent designers from relying on the strength of the supplementary reinforcement in shear calculations.

- **An increase in the thickness of the standard U-beam webs is not necessary to eliminate premature web-to-flange interface failure. However, increased web thickness does provide benefits with regards to the constructability and serviceability of U-beams.** Thickened webs easily accommodated the reinforcement necessary to preclude web-to-flange interface failure. Concrete placement and maintenance of code-specified cover was greatly facilitated by the thickened webs. The thickened webs were also capable of supporting a much greater shear

demand (well in excess of service level shear) prior to exhibiting distress through diagonal cracking.

Recommendations will be formalized in October of 2012 (following the completion of all experimental activities) through the development and submittal of new construction drawings for the TxDOT standard U-beam. Research into the shear behavior the TxDOT standardized U-Beam is continuing in an effort to optimize cross-section and reinforcement details with regards to constructability, serviceability and ultimate strength.

6.3 FUTURE WORK

The results of the current experimental program have generally highlighted the need for further study of the web-to-flange failure mechanism in prestressed concrete members. Development of generalized design methodologies would eliminate the potential for premature horizontal shear failure in future concepts for (atypical) prestressed concrete members. Specifically, additional research should be conducted to: (1) ascertain the effects of load and support conditions on the stress distribution at the web-to-flange interface, and (2) evaluate the applicability of traditional shear friction models to the assessment of interface strength

APPENDIX A

AASHTO LRFD (2009 Interim) Calculations

A.1 OVERVIEW

Section A.2 of this appendix will describe in detail the process for calculating the shear capacities of members using the AASHTO LRFD 2009 Interim Specifications as well as discuss several previous versions of the code equations which may still be in use in some design offices. In Section A.3 the calculations will be performed for each beam tested in this research program including calculations for all spacing of transverse reinforcement.

A.2 AASHTO LRFD GENERAL PROCEDURE

The equations that make up the AASHTO LRFD (2009 Interim) general procedure for shear design were developed out of the relationships and equations proposed in the Modified Compression Field Theory (MCFT). Due to the basis in MCFT the general procedure is a model of the post shear-cracking behavior of concrete. Many assumptions have been made in incorporating this theory into a simplified design procedure (Hawkins, et al. 2005). They are:

- Plane sections remain plane.
- Shear stress is assumed to be linearly distributed over the depth of the member. Therefore it is assumed the strain can be computed at the section's mid-depth as one-half of the strain at the centroid of the tensile zone.

- The direction of the compressive stress resultant is constant over the depth of the member.
- The average crack spacing is taken as 12-inches for members containing minimum transverse reinforcement. Otherwise the crack spacing is calculated and is directly related to the depth of the member (which incorporates a size effect for members not containing the minimum amount of transverse steel).
- The stirrups yield prior to the concrete crushing. This is a common assumption in most design equations which is typically ensured by a limit on the maximum shear stress of a section (discussed in the last paragraph of this section.)

When these design equations were first introduced the procedure for calculating the ultimate shear capacity of concrete sections was iterative and not easily performed using hand calculations. Unfortunately in the first edition these provisions difficult to automate due to the β variable which needed to be pulled from graphs published in the specifications (shown in Figure A-1.)

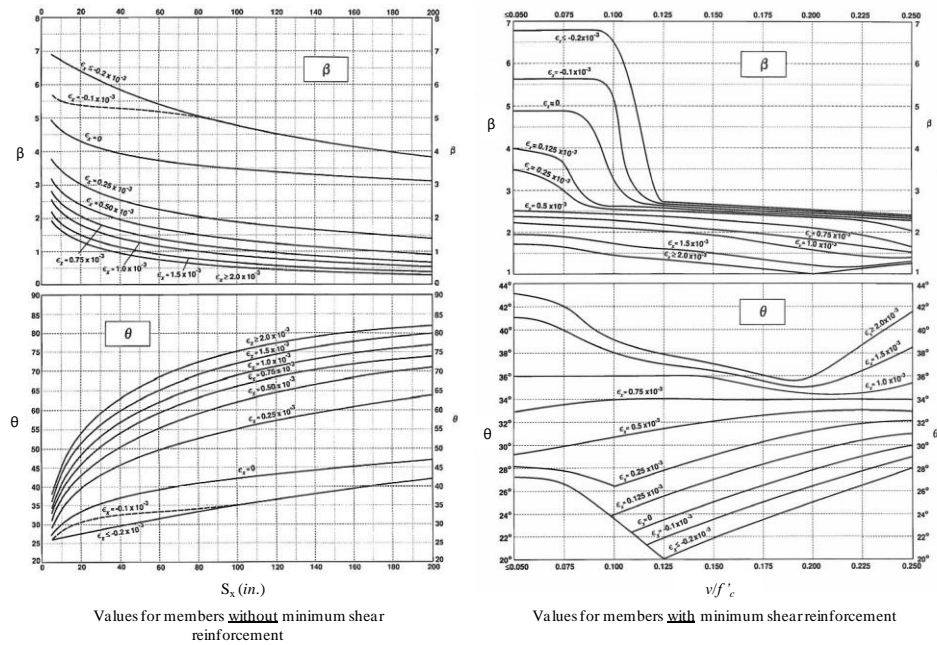


Figure A-1: Graphs to find values of β (AASHTO 1994)

This was partially solved when the tables (shown in Table A-1 and Table A-2) were adopted into the specifications in future interim revisions. This allowed for computer programming to be more readily developed which could interpolate between values of β using the strain at mid-depth and the iterative values of θ .

Table A-1: Interpolative tables for finding values of β for members without minimum shear reinforcement (AASHTO 2007)

S_{xe} (in.)	$\epsilon_s \times 1000$										
	≤ -0.20	≤ -0.10	≤ -0.05	≤ 0	≤ 0.125	≤ 0.25	≤ 0.50	≤ 0.75	≤ 1.00	≤ 1.50	≤ 2.00
≤ 5	25.4	25.5	25.9	26.4	27.7	28.9	30.9	32.4	33.7	35.6	37.2
	6.36	6.06	5.56	5.15	4.41	3.91	3.26	2.86	2.58	2.21	1.96
≤ 10	27.6	27.6	28.3	29.3	31.6	33.5	36.3	38.4	40.1	42.7	44.7
	5.78	5.78	5.38	4.89	4.05	3.52	2.88	2.50	2.23	1.88	1.65
≤ 15	29.5	29.5	29.7	31.1	34.1	36.5	39.9	42.4	44.4	47.4	49.7
	5.34	5.34	5.27	4.73	3.82	3.28	2.64	2.26	2.01	1.68	1.46
≤ 20	31.2	31.2	31.2	32.3	36.0	38.8	42.7	45.5	47.6	50.9	53.4
	4.99	4.99	4.99	4.61	3.65	3.09	2.46	2.09	1.85	1.52	1.31
≤ 30	34.1	34.1	34.1	34.2	38.9	42.3	46.9	50.1	52.6	56.3	59.0
	4.46	4.46	4.46	4.43	3.39	2.82	2.19	1.84	1.60	1.30	1.10
≤ 40	36.6	36.6	36.6	36.6	41.2	45.0	50.2	53.7	56.3	60.2	63.0
	4.06	4.06	4.06	4.06	3.20	2.62	2.00	1.66	1.43	1.14	0.95
≤ 60	40.8	40.8	40.8	40.8	44.5	49.2	55.1	58.9	61.8	65.8	68.6
	3.50	3.50	3.50	3.50	2.92	2.32	1.72	1.40	1.18	0.92	0.75
≤ 80	44.3	44.3	44.3	44.3	47.1	52.3	58.7	62.8	65.7	69.7	72.4
	3.10	3.10	3.10	3.10	2.71	2.11	1.52	1.21	1.01	0.76	0.62

Table A-2: Interpolative tables for finding values of β for members with at least minimum shear reinforcement (AASHTO 2007)

$\frac{V_u}{f'_c}$	$\epsilon_x \times 1,000$								
	≤ -0.20	≤ -0.10	≤ -0.05	≤ 0	≤ 0.125	≤ 0.25	≤ 0.50	≤ 0.75	≤ 1.00
≤ 0.075	22.3 6.32	20.4 4.75	21.0 4.10	21.8 3.75	24.3 3.24	26.6 2.94	30.5 2.59	33.7 2.38	36.4 2.23
≤ 0.100	18.1 3.79	20.4 3.38	21.4 3.24	22.5 3.14	24.9 2.91	27.1 2.75	30.8 2.50	34.0 2.32	36.7 2.18
≤ 0.125	19.9 3.18	21.9 2.99	22.8 2.94	23.7 2.87	25.9 2.74	27.9 2.62	31.4 2.42	34.4 2.26	37.0 2.13
≤ 0.150	21.6 2.88	23.3 2.79	24.2 2.78	25.0 2.72	26.9 2.60	28.8 2.52	32.1 2.36	34.9 2.21	37.3 2.08
≤ 0.175	23.2 2.73	24.7 2.66	25.5 2.65	26.2 2.60	28.0 2.52	29.7 2.44	32.7 2.28	35.2 2.14	36.8 1.96
≤ 0.200	24.7 2.63	26.1 2.59	26.7 2.52	27.4 2.51	29.0 2.43	30.6 2.37	32.8 2.14	34.5 1.94	36.1 1.79
≤ 0.225	26.1 2.53	27.3 2.45	27.9 2.42	28.5 2.40	30.0 2.34	30.8 2.14	32.3 1.86	34.0 1.73	35.7 1.64
≤ 0.250	27.5 2.39	28.6 2.39	29.1 2.33	29.7 2.33	30.6 2.12	31.3 1.93	32.8 1.70	34.3 1.58	35.8 1.50

The final simplification was adopted into the 2008 Interim Specifications. In this edition linear equations were developed to calculate β , ϵ_s , and θ . These equations eliminated the need for interpolation between the values of β and perhaps more importantly eliminated the need for iterations to find the angle of the compressive diagonal (θ) which could now be calculated directly. The equations for the three variables are shown in Equation A-1 through Equation A-5.

For sections containing at least the minimum amount of shear reinforcement.

$$\beta = \frac{4.8}{(1 + 750\epsilon_s)} \quad \text{Equation A-1}$$

For sections containing less than the minimum amount of shear reinforcement.

$$\beta = \frac{4.8}{(1 + 750\epsilon_s)} \frac{51}{(39 + s_{xe})} \quad \text{Equation A-2}$$

Where:

$$s_{xe} = 12in. \leq s_x \frac{1.38}{a_g + 0.63} \leq 80in. \quad \text{Equation A-3}$$

For all cases:

$$\theta = 29 + 3500\varepsilon_s$$

Equation A-4

Where:

$$\varepsilon_s = \frac{\left(\frac{|M_u|}{d_v} + 0.5N_u + |V_u - V_p| - A_{ps}f_{po} \right)}{E_s A_s + E_p A_{ps}}$$

Equation A-5

Where:

- A_{ps} Area of prestressing steel on the tension side of member (in^2)
- A_s Area of mild steel on the flexural tension side of member (in^2)
- a_g Maximum aggregate size in the web concrete (*inches*)
- f_{po} $\Delta\varepsilon_p * E_p$ (*psi*)
- $\Delta\varepsilon_p$ Strain differential between prestressing strand and concrete (*in./in.*)
- E_p Modulus of elasticity of prestressing strand (*psi*)
- N_u Factored axial force in member (taken as positive if tensile) (*pounds*)
- M_u Factored moment in member, but not to be taken as less than $(V_u - V_p)d_v$ (*lb.-in.*)
- s_x The lesser of either d_v or the maximum distance between layers of longitudinal crack control reinforcement, where the area of the reinforcement in each layer is not less than $0.003b_v s_x$ (*in*)
- V_u Factored shear force in member (*pounds*)
- V_p Vertical component of the prestressing force resisting shear (*pounds*)

The general equation for the shear strength of concrete members is found in Equation A-6. The concrete and steel components of this equation are found by using Equation A-7 and Equation A-8 with the three variables found using Equation A-1 through Equation A-5. Note that all equations have been converted to psi units for easier cross-comparison.

The nominal shear capacity of a concrete member shall be taken as:

$$V_n = V_c + V_s + V_p \leq 0.25f'_c b_v d_v \quad \text{Equation A-6}$$

See note in the following paragraphs on 0.25 limit.

The concrete contribution to the shear strength of the member shall be taken as:

$$V_c = \beta \sqrt{f'_c} b_v d_v \quad \text{Equation A-7}$$

The steel contribution to the shear strength of the member shall be taken as:

$$V_s = \frac{A_v f_y d_v (\cot \theta + \cot \alpha) \sin \alpha}{s} \quad \text{Equation A-8}$$

Where:

- β Variable relating the concrete's resistance to slip across a crack
- f'_c 28-day compressive strength of concrete (*psi*)
- b_v Minimum web width inside depth of d_v (*inches*)
- d_v Effective shear depth measured perpendicular to the neutral axis between the compressive and tensile resultants due to flexure, but not to be taken as less than the greater of 0.9*(transformed steel area's depth) or 0.72*h*. (*inches*)

A_v	Area of shear reinforcement within a distance s . (in^2)
f_y	Yield strength of transverse steel. (psi)
θ	Angle of inclination of diagonal compressive stresses. ($degrees$)
α	Angle of inclination of transverse reinforcement to the longitudinal axis. ($degrees$)
s	Transverse reinforcement longitudinal spacing. ($inches$)

Another important difference between the MCFT based procedure and those used in the ACI code is the requirement for longitudinal steel. In the ACI code the requirement is implicit in that it requires all longitudinal steel be continued for a distance past what is needed for moment capacity. Though the stated purpose of this is continuity is to allow for moment redistribution (ACI 318 2008) it has the added benefit of providing the longitudinal ties needed for shear capacity (Hawkins, et al. 2005). In the AAHSTO LRFD code the requirement for longitudinal steel as related to the shear capacity of a member is explicitly laid out in the form of Equation A-9:

“...the tensile capacity of the longitudinal reinforcement on the flexural tension side of the member shall be proportioned to satisfy:” (AASHTO 2009 Interim) §5.8.3.5

$$A_{ps}f_{ps} + A_s f_y \geq \frac{|M_u|}{d_v \phi_f} + 0.5 \frac{N_u}{\phi_c} + \left(\left| \frac{V_u}{\phi_v} - V_p \right| - 0.5V_s \right) \cot \theta \quad \text{Equation A-9}$$

f_{ps}	Stress in prestressing steel at nominal flexural strength (psi)
ϕ_f	Strength reduction factor for flexure equal to 0.9
ϕ_c	Strength reduction factor for compression equal to 0.7

ϕ_v Strength reduction factor for shear equal to 0.9

The final important difference between the ACI 318-08 shear provisions and those of the AASHTO LRFD (2009 Interim) are the limits imposed on the vertical shear stress of the members. The purpose of these limits is to prevent the concrete from crushing before the shear steel yields. This both prevents a brittle failure and maintains the assumption present in code equations that the steel will yield before the concrete crushes. In ACI 318-08 the limit is imposed only on the concrete contribution to shear strength, but in the AASHTO LRFD Specifications the limit is imposed on the overall shear stress of the member as shown in Equation A-6.

This limit has a restriction that it must only be used for members which are built integrally with the supports. For members in which the ends are free to rotate (such as simply supported members as well as other members not built integrally with the supports) the allowable shear stress was reduced to $0.18f'_c$, unless the end region is designed using strut and tie modeling. This provision is an attempt to account for the funneling action at the support which causes a force discontinuity in the bottom flange and can lead to premature failures. This maximum stress reduction (to $0.18f'_c$) was recommended in NCHRP Report 579, but Avendaño (2008) calls for a further reduction (to $0.16f'_c$) of this limit to account for the same type of behavior.

A.3 AASHTO LRFD (2009 INTERIM EDITION) SHEAR STRENGTH CALCULATIONS

The remainder of this Appendix is devoted to shear strength calculations using the AASHTO LRFD Bridge Design Specifications equations for the general procedure. The calculations are set out in the following order:

- Beam 1 North
 - 4-inch spacing of transverse reinforcement
 - 6-inch spacing of transverse reinforcement
- Beam 1 South
 - 4-inch spacing of transverse reinforcement
 - 6-inch spacing of transverse reinforcement
- Beam 2 North
 - 4-inch spacing of transverse reinforcement
 - 6-inch spacing of transverse reinforcement
- Beam 3 South
 - 4-inch spacing of transverse reinforcement
 - 6-inch spacing of transverse reinforcement
- Beam 4 North and South
 - 3-inch spacing of transverse reinforcement
 - 4-inch spacing of transverse reinforcement
 - 6-inch spacing of transverse reinforcement
- Beam 5 North
 - 4-inch spacing of transverse reinforcement
 - 6-inch spacing of transverse reinforcement

Beam 1N (s = 4") Geometry and Concrete Properties				Calculated Constants for MCFT from AASHTO LRFD 2009					
Beam		Deck		Constant	Value	Units	Description	Equ. #	
h_{beam}	54	<i>inch</i>	h_{deck}	8	<i>inch</i>	A_{ps}	11.934	in^2	area of prestressing steel on member's flexural tension side
f'_c beam	11.96	<i>ksi</i>	f'_c deck	10.5	<i>ksi</i>	$h_{composite}$	62.75	<i>inch</i>	height of deck and girder
b_v	10	<i>inch</i>	$b_{effective\ deck}$	96	<i>in</i>	d_p	58.75	<i>inch</i>	dist. from extreme ten. to extreme comp
E_c	6234	<i>ksi</i>				d_c	50	<i>inch</i> **	** not the same d_c reported in shear section
A_{ct}	717.5	in^2				c	5.63	<i>inch</i>	distance from extreme comp fiber to neutral axis
Steel Properties						k	0.28	<i>unitless</i>	
						β_1	0.65	<i>unitless</i>	
Prestressing Steel Properties		Mild Steel Properties				a	3.66	<i>inch</i>	
Total # Strands	78	<i>unitless</i>	Compression Steel in Deck			f_{ps}	262.8	<i>ksi</i>	
Area of Each Strand	0.153	$in^2 / strand$	A'_s	0	in^2	M_n	178485	<i>kip * inch</i>	
f_{pu}	270	<i>ksi</i>	f'_s	60	<i>ksi</i>	M_U limit	43114	<i>kip * inch</i>	used in calculating ϵ
\bar{y}_p	4	<i>inch</i>	Tension Steel in Beam (if added then need mod.s)			θ	28.69	<i>degrees</i>	A.4
V_p	0	<i>kips</i>	A_s	0	in^2	d_c	52.88	<i>inch</i>	Here using 0.9 due to non-linear analysis results
f_{po}	202.5	<i>ksi</i>	f_y	60	<i>ksi</i>	<i>critical section</i>	57.4	<i>inch</i>	
Type of Strand	low lax	<i>text</i>	E_s	29300	<i>ksi</i>	ϵ_s	-0.00008919	<i>in / in</i>	A.5
E_p	28500	<i>ksi</i>	Transverse Steel in Beam			β	5.144	<i>unitless</i>	A.1, A.2
			Minimum Shear Steel?	YES	<i>yes or no</i>	V_C	297	<i>kips</i>	A.7
			α	90	<i>degrees</i>	V_S	609	<i>kips</i>	A.8
			A_v	0.4	in^2	Limited 0.25?	NO	0.143	Adjacent cell shows value of potential limit
			$f_{y\ v}$	63	<i>ksi</i>	V_n	906	<i>kips</i>	A.6
			s	4	<i>inch</i>	V_n unlimited	906	<i>kips</i>	A.6
Miscellaneous Properties						ϕ	0.9	<i>unitless</i>	
						ϕV_n	815	<i>kips</i>	
Load Properties		Other Properties				<i>critical section</i>	57.4	<i>inch</i>	<i>critical section for iteration</i>
M_u	61969.854	<i>kip * inch</i>	Shear Span	152	<i>inches</i>	difference in V	-6.460E-06	<i>kips</i>	difference between the calculated and assumed shear
N_u	0	<i>kips</i>	Width of Bearing Pad	9	<i>inches</i>	$V_U = V_n * \phi$	815	<i>kips</i>	
V_u	815	<i>kips</i>				Roots	10.5	<i>unitless</i>	this is the roots value of Vs when units are in psi

Beam 1N (s = 6") Geometry and Concrete Properties					Calculated Constants for MCFT from AASHTO LRFD 2009					
Beam			Deck		Constant	Value	Units	Description	Equ. #	
h_{beam}	54	inch	h_{deck}	8	inch	A_{ps}	11.934	in ²	area of prestressing steel on member's flexural tension side	
f'_c beam	11.96	ksi	f'_c deck	10.5	ksi	$h_{composite}$	62.75	inch	height of deck and girder	
b_v	10	inch	$b_{effective\ deck}$	96	in	d_p	58.75	inch	dist. from extreme ten. to extreme comp	
E_c	6234	ksi				d_c	50	inch **	** not the same d_c reported in shear section	
A_{ct}	717.5	in ²				c	5.63	inch	distance from extreme comp fiber to neutral axis	
Steel Properties					k	0.28	unitless			
					β_1	0.65	unitless			
Prestressing Steel Properties			Mild Steel Properties		a	3.66	inch			
Total # Strands	78	unitless	Compression Steel in Deck		f_{ps}	262.8	ksi			
Area of Each Strand	0.153	in ² / strand	A'_s	0	in ²	M_n	178485	kip * inch		
f_{pu}	270	ksi	f'_s	60	ksi	M_U limit	34670	kip * inch	used in calculating ϵ	
\bar{y}_p	4	inch	Tension Steel in Beam (if added then need mod.s)		θ	28.40	degrees		A.4	
V_p	0	kips	A_s	0	in ²	d_v	52.88	inch	Here using 0.9 due to non-linear analysis results	
f_{po}	202.5	ksi	f_y	60	ksi	critical section	57.4	inch		
Type of Strand	low lax	text	E_s	29300	ksi	ϵ_s	-0.00017007	in / in		A.5
E_p	28500	ksi	Transverse Steel in Beam		β	5.502	unitless		A.1, A.2	
			Minimum Shear Steel?	YES	yes or no	V_c	318	kips		A.7
			α	90	degrees	V_s	411	kips		A.8
			A_v	0.4	in ²	Limited 0.25?	NO	0.115	Adjacent cell shows value of potential limit	A.6
			$f_{y\ v}$	63	ksi	V_n	729	kips		A.6
			s	6	inch	V_n unlimited	729	kips		A.6
Miscellaneous Properties					ϕ	0.9	unitless			
Load Properties					Other Properties		ϕV_n	656	kips	
					critical section	57.4	inch	critical section for iteration		
M_u	49832.602	kip * inch	Shear Span	152	inches	difference in V	-4.137E-08	kips	difference between the calculated and assumed shear	
N_u	0	kips	Width of Bearing Pad	9	inches	$V_U = V_n * \phi$	656	kips		
V_u	656	kips				Roots	7.1	unitless	this is the roots value of Vs when units are in psi	

Beam 1S (s = 4") Geometry and Concrete Properties					Calculated Constants for MCFT from AASHTO LRFD 2009						
Beam			Deck			Constant	Value	Units	Description	Equ. #	
h_{beam}	54	inch	h_{deck}	8	inch	A_{ps}	11.934	in ²	area of prestressing steel on member's flexural tension side		
f'_c_{beam}	11.96	ksi	f'_c_{deck}	10.5	ksi	$h_{composite}$	62.75	inch	height of deck and girder		
b_v	10	inch	$b_{effective\ deck}$	96	in	d_p	58.75	inch	dist. from extreme ten. to extreme comp		
E_c	6234	ksi				d_c	50	inch **	** not the same d_c reported in shear section		
A_{ct}	717.5	in ²				c	5.63	inch	distance from extreme comp fiber to neutral axis		
Steel Properties					k	0.28	unitless				
					β_1	0.65	unitless				
Prestressing Steel Properties			Mild Steel Properties			a	3.66	inch			
Total # Strands	78	unitless	Compression Steel in Deck			f_{ps}	262.8	ksi			
Area of Each Strand	0.153	in ² / strand	A'_s	0	in ²	M_n	178485	kip * inch			
f_{pu}	270	ksi	f'_s	60	ksi	M_U limit	43071	kip * inch	used in calculating ϵ		
\bar{y}_p	4	inch	Tension Steel in Beam (if added then need mod.s)			θ	28.70	degrees		A.4	
V_p	0	kips	A_s	0	in ²	d_v	52.88	inch	Here using 0.9 due to non-linear analysis results		
f_{po}	202.5	ksi	f_y	60	ksi	critical section	57.4	inch			
Type of Strand	low lax	text	E_s	29000	ksi	ϵ_s	-0.00008640	in / in		A.5	
E_p	28500	ksi	Transverse Steel in Beam			β	5.133	unitless		A.1, A.2	
			Minimum Shear Steel?	YES	yes or no	V_c	297	kips		A.7	
			α	90	degrees	V_s	609	kips		A.8	
			A_v	0.4	in ²	Limited 0.25?	NO	0.143	Adjacent cell shows value of potential limit	A.6	
			f_{yv}	63	ksi	V_n	905	kips		A.6	
			s	4	inch	V_n unlimited	905	kips		A.6	
Miscellaneous Properties					ϕ	0.9	unitless				
Load Properties					Other Properties			ϕV_n	815	kips	
					critical section	57.4	inch	critical section for iteration			
M_u	62722.175	kip * inch	Shear Span	154	inches	difference in V	-6.555E-06	kips	difference between the calculated and assumed shear		
N_u	0	kips	Width of Bearing Pad	9	inches	$V_U = V_n * \phi$	815	kips			
V_u	815	kips				Roots	10.5	unitless	this is the roots value of Vs when units are in psi		

Beam 1S (s = 6") Geometry and Concrete Properties					Calculated Constants for MCFT from AASHTO LRFD 2009					
Beam			Deck		Constant	Value	Units	Description	Equ. #	
h_{beam}	54	inch	h_{deck}	8	inch	A_{ps}	11.934	in ²	area of prestressing steel on member's flexural tension side	
f'_c beam	11.96	ksi	f'_c deck	10.5	ksi	$h_{composite}$	62.75	inch	height of deck and girder	
b_v	10	inch	$b_{effective\ deck}$	96	in	d_p	58.75	inch	dist. from extreme ten. to extreme comp	
E_c	6234	ksi				d_c	50	inch **	** not the same d_c reported in shear section	
A_{ct}	717.5	in ²				c	5.63	inch	distance from extreme comp fiber to neutral axis	
Steel Properties					k	0.28	unitless			
					β_1	0.65	unitless			
Prestressing Steel Properties			Mild Steel Properties		a	3.66	inch			
Total # Strands	78	unitless	Compression Steel in Deck		f_{ps}	262.8	ksi			
Area of Each Strand	0.153	in ² / strand	A'_s	0	in ²	M_n	178485	kip * inch		
f_{pu}	270	ksi	f'_s	60	ksi	M_U limit	34634	kip * inch	used in calculating ϵ	
\bar{y}_p	4	inch	Tension Steel in Beam (if added then need mod.s)		θ	28.41	degrees		A.4	
V_p	0	kips	A_s	0	in ²	d_c	52.88	inch	Here using 0.9 due to non-linear analysis results	
f_{po}	202.5	ksi	f_y	60	ksi	critical section	57.4	inch		
Type of Strand	low lax	text	E_s	29000	ksi	ϵ_s	-0.00016783	in / in		A.5
E_p	28500	ksi	Transverse Steel in Beam		β	5.491	unitless		A.1, A.2	
			Minimum Shear Steel?	YES	yes or no	V_C	317	kips		A.7
			α	90	degrees	V_S	411	kips		A.8
			A_v	0.4	in ²	Limited 0.25?	NO	0.115	Adjacent cell shows value of potential limit	A.6
			$f_{y\ v}$	63	ksi	V_n	728	kips		A.6
			s	6	inch	V_n unlimited	728	kips		A.6
Miscellaneous Properties					ϕ	0.9	unitless			
Load Properties					Other Properties		ϕV_n	655	kips	
					critical section	57.4	inch	critical section for iteration		
M_u	50436.761	kip * inch	Shear Span	154	inches	difference in V	-4.273E-08	kips	difference between the calculated and assumed shear	
N_u	0	kips	Width of Bearing Pad	9	inches	$V_U = V_n * \phi$	655	kips		
V_u	655	kips				Roots	7.1	unitless	this is the roots value of Vs when units are in psi	

Beam 2N (s = 4") Geometry and Concrete Properties					Calculated Constants for MCFT from AASHTO LRFD 2009					
Beam			Deck		Constant	Value	Units	Description	Equ. #	
h_{beam}	54	inch	h_{deck}	8	inch	A_{ps}	11.934	in ²	area of prestressing steel on member's flexural tension side	
f'_c beam	11.48	ksi	f'_c deck	8.61	ksi	$h_{composite}$	62.75	inch	height of deck and girder	
b_v	10	inch	$b_{effective\ deck}$	96	in	d_p	58.75	inch	dist. from extreme ten. to extreme comp	
E_c	6107	ksi				d_c	50	inch **	** not the same d_c reported in shear section	
A_{ct}	717.5	in ²				c	6.83	inch	distance from extreme comp fiber to neutral axis	
Steel Properties					k	0.28	unitless			
					β_1	0.65	unitless			
Prestressing Steel Properties			Mild Steel Properties		a	4.44	inch			
Total # Strands	78	unitless	Compression Steel in Deck		f_{ps}	261.2	ksi			
Area of Each Strand	0.153	in ² / strand	A'_s	0	in ²	M_n	176229	kip * inch		
f_{pu}	270	ksi	f'_s	60	ksi	M_U limit	51713	kip * inch	used in calculating ϵ	
\bar{y}_p	4	inch	Tension Steel in Beam (if added then need mod.s)		θ	28.98	degrees			A.4
V_p	0	kips	A_s	0	in ²	d_v	52.88	inch	Here using 0.9 due to non-linear analysis results	
f_{po}	202.5	ksi	f_y	60	ksi	critical section	57.4	inch		
Type of Strand	low lax	text	E_s	29000	ksi	ϵ_s	-0.00000696	in / in		A.5
E_p	28500	ksi	Transverse Steel in Beam		β	4.825	unitless			A.1, A.2
			Minimum Shear Steel?	YES	yes or no	V_C	273	kips		A.7
			α	90	degrees	V_S	814	kips		A.8
			A_v	0.4	in ²	Limited 0.25?	NO	0.179	Adjacent cell shows value of potential limit	A.6
			$f_{y\ v}$	85.2	ksi	V_n	1087	kips		A.6
			s	4	inch	V_n unlimited	1087	kips		A.6
Miscellaneous Properties					ϕ	0.9	unitless			
					ϕV_n	978	kips			
Load Properties			Other Properties		critical section	57.4	inch	critical section for iteration		
M_u	74329.785	kip * inch	Shear Span	152	inches	difference in V	-4.972E-04	kips	difference between the calculated and assumed shear	
N_u	0	kips	Width of Bearing Pad	9	inches	$V_U = V_n * \phi$	978	kips		
V_u	978	kips				Roots	14.4	unitless	this is the roots value of Vs when units are in psi	

Beam 2N (s = 6") Geometry and Concrete Properties					Calculated Constants for MCFT from AASHTO LRFD 2009					
Beam			Deck			Constant	Value	Units	Description	Equ. #
h_{beam}	54	inch	h_{deck}	8	inch	A_{ps}	11.934	in ²	area of prestressing steel on member's flexural tension side	
f'_c beam	11.48	ksi	f'_c deck	8.61	ksi	$h_{composite}$	62.75	inch	height of deck and girder	
b_v	10	inch	$b_{effective\ deck}$	96	in	d_p	58.75	inch	dist. from extreme ten. to extreme comp	
E_c	6107	ksi				d_c	50	inch **	** not the same d_c reported in shear section	
A_{ct}	717.5	in ²				c	6.83	inch	distance from extreme comp fiber to neutral axis	
Steel Properties					k	0.28	unitless			
					β_1	0.65	unitless			
Prestressing Steel Properties			Mild Steel Properties			a	4.44	inch		
Total # Strands	78	unitless	Compression Steel in Deck			f_{ps}	261.2	ksi		
Area of Each Strand	0.153	in ² / strand	A'_s	0	in ²	M_n	176229	kip * inch		
f_{pu}	270	ksi	f'_s	60	ksi	M_U limit	40404	kip * inch	used in calculating ϵ	
\bar{y}_p	4	inch	Tension Steel in Beam (if added then need mod.s)			θ	28.59	degrees		A.4
V_p	0	kips	A_s	0	in ²	d_v	52.88	inch	Here using 0.9 due to non-linear analysis results	
f_{po}	202.5	ksi	f_y	60	ksi	critical section	57.4	inch		
Type of Strand	low lax	text	E_s	29000	ksi	ϵ_s	-0.00011735	in / in		A.5
E_p	28500	ksi	Transverse Steel in Beam			β	5.263	unitless		A.1, A.2
			Minimum Shear Steel?	YES	yes or no	V_C	298	kips		A.7
			α	90	degrees	V_S	551	kips		A.8
			A_v	0.4	in ²	Limited 0.25?	NO	0.140	Adjacent cell shows value of potential limit	A.6
			$f_{y\ v}$	85.2	ksi	V_n	849	kips		A.6
			s	6	inch	V_n unlimited	849	kips		A.6
Miscellaneous Properties					ϕ	0.9	unitless			
					ϕV_n	764	kips			
Load Properties			Other Properties			critical section	57.4	inch	critical section for iteration	
M_u	58075.149	kip * inch	Shear Span	152	inches	difference in V	-1.646E-07	kips	difference between the calculated and assumed shear	
N_u	0	kips	Width of Bearing Pad	9	inches	$V_U = V_n * \phi$	764	kips		
V_u	764	kips				Roots	9.7	unitless	this is the roots value of Vs when units are in psi	

Beam 3N (s = 4") Geometry and Concrete Properties					Calculated Constants for MCFT from AASHTO LRFD 2009					
Beam			Deck			Constant	Value	Units	Description	Equ. #
h_{beam}	54	inch	h_{deck}	8	inch	A_{ps}	6.426	in ²	area of prestressing steel on member's flexural tension side	
$f'_{\text{c beam}}$	11.39	ksi	$f'_{\text{c deck}}$	9.21	ksi	$h_{\text{composite}}$	62.75	inch	height of deck and girder	
b_v	10	inch	$b_{\text{effective deck}}$	96	in	d_p	58.55	inch	dist. from extreme ten. to extreme comp	
E_c	6083	ksi				d_c	49.8	inch **	** not the same d_c reported in shear section	
A_{ct}	717.5	in ²				c	3.49	inch	distance from extreme comp fiber to neutral axis	
Steel Properties					k	0.28	unitless			
					β_1	0.65	unitless			
Prestressing Steel Properties			Mild Steel Properties			a	2.27	inch		
Total # Strands	42	unitless	Compression Steel in Deck			f_{ps}	265.5	ksi		
Area of Each Strand	0.153	in ² / strand	A'_{s}	0	in ²	M_n	97952	kip * inch		
f_{pu}	270	ksi	f'_{s}	60	ksi	M_U limit	32208	kip * inch	used in calculating ϵ	
\bar{y}_p	4.2	inch	Tension Steel in Beam (if added then need mod.s)			θ	32.88	degrees		A.4
V_p	0	kips	A_s	0	in ²	d_v	52.70	inch	Here using 0.9 due to non-linear analysis results	
f_{po}	202.5	ksi	f_y	60	ksi	critical section	57.2	inch		
Type of Strand	low lax	text	E_s	29000	ksi	ϵ_s	0.00110895	in / in		A.5
E_p	28500	ksi	Transverse Steel in Beam			β	2.620	unitless		A.1, A.2
			Minimum Shear Steel?	YES	yes or no	V_c	147	kips		A.7
			α	90	degrees	V_s	532	kips		A.8
			A_v	0.4	in ²	Limited 0.25?	NO	0.113	Adjacent cell shows value of potential limit	A.6
			$f_{y v}$	65.25	ksi	V_n	679	kips		A.6
			s	4	inch	V_n unlimited	679	kips		A.6
Miscellaneous Properties					ϕ	0.9	unitless			
Load Properties			Other Properties			ϕV_n	611	kips		
			critical section	57.2	inch	critical section	57.2	inch	critical section for iteration	
M_u	47063.961	kip * inch	Shear Span	154	inches	difference in V	7.464E-05	kips	difference between the calculated and assumed shear	
N_u	0	kips	Width of Bearing Pad	9	inches	$V_U = V_n * \phi$	611	kips		
V_u	611	kips				Roots	9.5	unitless	this is the roots value of Vs when units are in psi	

Beam 3N (s = 6") Geometry and Concrete Properties					Calculated Constants for MCFT from AASHTO LRFD 2009					
Beam			Deck			Constant	Value	Units	Description	Equ. #
h_{beam}	54	inch	h_{deck}	8	inch	A_{ps}	6.426	in ²	area of prestressing steel on member's flexural tension side	
f'_c beam	11.39	ksi	f'_c deck	9.21	ksi	$h_{composite}$	62.75	inch	height of deck and girder	
b_v	10	inch	$b_{effective\ deck}$	96	in	d_p	58.55	inch	dist. from extreme ten. to extreme comp	
E_c	6083	ksi				d_c	49.8	inch **	** not the same d_c reported in shear section	
A_{ct}	717.5	in ²				c	3.49	inch	distance from extreme comp fiber to neutral axis	
Steel Properties					k	0.28	unitless			
					β_1	0.65	unitless			
Prestressing Steel Properties			Mild Steel Properties			a	2.27	inch		
Total # Strands	42	unitless	Compression Steel in Deck			f_{ps}	265.5	ksi		
Area of Each Strand	0.153	in ² / strand	A'_s	0	in ²	M_n	97952	kip * inch		
f_{pu}	270	ksi	f'_s	60	ksi	M_U limit	29097	kip * inch	used in calculating ϵ	
\bar{y}_p	4.2	inch	Tension Steel in Beam (if added then need mod.s)			θ	30.10	degrees		A.4
V_p	0	kips	A_s	0	in ²	d_v	52.70	inch	Here using 0.9 due to non-linear analysis results	
f_{po}	202.5	ksi	f_y	60	ksi	critical section	57.2	inch		
Type of Strand	low lax	text	E_s	29000	ksi	ϵ_s	0.00031537	in / in		A.5
E_p	28500	ksi	Transverse Steel in Beam			β	3.882	unitless		A.1, A.2
			Minimum Shear Steel?	YES	yes or no	V_C	218	kips		A.7
			α	90	degrees	V_S	395	kips		A.8
			A_v	0.4	in ²	Limited 0.25?	NO	0.102	Adjacent cell shows value of potential limit	A.6
			$f_{y\ v}$	65.25	ksi	V_n	614	kips		A.6
			s	6	inch	V_n unlimited	614	kips		A.6
Miscellaneous Properties					ϕ	0.9	unitless			
Load Properties			Other Properties			ϕV_n	552	kips		
M_u	42517.054	kip * inch	Shear Span	154	inches	critical section	57.2	inch	critical section for iteration	
N_u	0	kips	Width of Bearing Pad	9	inches	difference in V	-3.307E-07	kips	difference between the calculated and assumed shear	
V_u	552	kips				$V_U = V_n * \phi$	552	kips		
						Roots	7.0	unitless	this is the roots value of Vs when units are in psi	

Beam 3S (s = 4") Geometry and Concrete Properties					Calculated Constants for MCFT from AASHTO LRFD 2009					
Beam			Deck			Constant	Value	Units	Description	Equ. #
h_{beam}	54	inch	h_{deck}	8	inch	A_{ps}	6.426	in ²	area of prestressing steel on member's flexural tension side	
f'_c beam	12.1	ksi	f'_c deck	10.5	ksi	$h_{composite}$	62.75	inch	height of deck and girder	
b_v	10	inch	$b_{effective\ deck}$	96	in	d_p	58.55	inch	dist. from extreme ten. to extreme comp	
E_c	6270	ksi				d_c	49.8	inch **	** not the same d_c reported in shear section	
A_{ct}	717.5	in ²				c	3.07	inch	distance from extreme comp fiber to neutral axis	
Steel Properties					k	0.28	unitless			
					β_1	0.65	unitless			
Prestressing Steel Properties			Mild Steel Properties			a	2.00	inch		
Total # Strands	42	unitless	Compression Steel in Deck			f_{ps}	266.0	ksi		
Area of Each Strand	0.153	in ² / strand	A'_s	0	in ²	M_n	98389	kip * inch		
f_{pu}	270	ksi	f'_s	60	ksi	M_U limit	32253	kip * inch	used in calculating ϵ	
\bar{y}_p	4.2	inch	Tension Steel in Beam (if added then need mod.s)			θ	32.92	degrees		A.4
V_p	0	kips	A_s	0	in ²	d_v	52.70	inch	Here using 0.9 due to non-linear analysis results	
f_{po}	202.5	ksi	f_y	60	ksi	critical section	57.2	inch		
Type of Strand	low lax	text	E_s	29300	ksi	ϵ_s	0.00112047	in / in		A.5
E_p	28500	ksi	Transverse Steel in Beam			β	2.608	unitless		A.1, A.2
			Minimum Shear Steel?	YES	yes or no	V_C	151	kips		A.7
			α	90	degrees	V_S	529	kips		A.8
			A_v	0.4	in ²	Limited 0.25?	NO	0.107	Adjacent cell shows value of potential limit	A.6
			$f_{y\ v}$	65	ksi	V_n	680	kips		A.6
			s	4	inch	V_n unlimited	680	kips		A.6
Miscellaneous Properties					ϕ	0.9	unitless			
					ϕV_n	612	kips			
Load Properties			Other Properties			critical section	57.2	inch	critical section for iteration	
M_u	47129.989	kip * inch	Shear Span	154	inches	difference in V	5.774E-07	kips	difference between the calculated and assumed shear	
N_u	0	kips	Width of Bearing Pad	9	inches	$V_U = V_n * \phi$	612	kips		
V_u	612	kips				Roots	9.1	unitless	this is the roots value of Vs when units are in psi	

Beam 3S (s = 6") Geometry and Concrete Properties					Calculated Constants for MCFT from AASHTO LRFD 2009					
Beam			Deck			Constant	Value	Units	Description	Equ. #
h_{beam}	54	inch	h_{deck}	8	inch	A_{ps}	6.426	in ²	area of prestressing steel on member's flexural tension side	
f'_c beam	12.1	ksi	f'_c deck	10.5	ksi	$h_{composite}$	62.75	inch	height of deck and girder	
b_v	10	inch	$b_{effective\ deck}$	96	in	d_p	58.55	inch	dist. from extreme ten. to extreme comp	
E_c	6270	ksi				d_c	49.8	inch **	** not the same d_c reported in shear section	
A_{ct}	717.5	in ²				c	3.07	inch	distance from extreme comp fiber to neutral axis	
Steel Properties					k	0.28	unitless			
					β_1	0.65	unitless			
Prestressing Steel Properties			Mild Steel Properties			a	2.00	inch		
Total # Strands	42	unitless	Compression Steel in Deck			f_{ps}	266.0	ksi		
Area of Each Strand	0.153	in ² / strand	A'_s	0	in ²	M_n	98389	kip * inch		
f_{pu}	270	ksi	f'_s	60	ksi	M_U limit	29171	kip * inch	used in calculating ϵ	
\bar{y}_p	4.2	inch	Tension Steel in Beam (if added then need mod.s)			θ	30.17	degrees		A.4
V_p	0	kips	A_s	0	in ²	d_c	52.70	inch	Here using 0.9 due to non-linear analysis results	
f_{po}	202.5	ksi	f_y	60	ksi	critical section	57.2	inch		
Type of Strand	low lax	text	E_s	29300	ksi	ϵ_s	0.00033436	in / in		A.5
E_p	28500	ksi	Transverse Steel in Beam			β	3.838	unitless		A.1, A.2
			Minimum Shear Steel?	YES	yes or no	V_C	222	kips		A.7
			α	90	degrees	V_S	393	kips		A.8
			A_v	0.4	in ²	Limited 0.25?	NO	0.096	Adjacent cell shows value of potential limit	A.6
			$f_{y\ v}$	65	ksi	V_n	615	kips		A.6
			s	6	inch	V_n unlimited	615	kips		A.6
Miscellaneous Properties					ϕ	0.9	unitless			
					ϕV_n	554	kips			
Load Properties			Other Properties			critical section	57.2	inch	critical section for iteration	
M_u	42625.867	kip * inch	Shear Span	154	inches	difference in V	-4.584E-07	kips	difference between the calculated and assumed shear	
N_u	0	kips	Width of Bearing Pad	9	inches	$V_U = V_n * \phi$	554	kips		
V_u	554	kips				Roots	6.8	unitless	this is the roots value of Vs when units are in psi	

Beam 4N&S (s = 3") Geometry and Concrete Properties					Calculated Constants for MCFT from AASHTO LRFD 2009					
Beam			Deck		Constant	Value	Units	Description	Equ. #	
h_{beam}	54	inch	h_{deck}	8	inch	A_{ps}	11.934	in ²	area of prestressing steel on member's flexural tension side	
$f'_{\text{c beam}}$	11.44	ksi	$f'_{\text{c deck}}$	7.5	ksi	$h_{\text{composite}}$	62.75	inch	height of deck and girder	
b_v	16	inch	$b_{\text{effective deck}}$	96	in	d_p	58.75	inch	dist. from extreme ten. to extreme comp	
E_c	6097	ksi				d_c	50	inch **	** not the same d_c reported in shear section	
A_{ct}	856	in ²				c	7.52	inch	distance from extreme comp fiber to neutral axis	
Steel Properties					k	0.28	unitless			
					β_1	0.68	unitless			
Prestressing Steel Properties			Mild Steel Properties		a	5.08	inch			
Total # Strands	78	unitless	Compression Steel in Deck		f_{ps}	260.3	ksi			
Area of Each Strand	0.153	in ² / strand	A'_s	0	in ²	M_n	174633	kip * inch		
f_{pu}	270	ksi	f'_s	60	ksi	M_U limit	54001	kip * inch	used in calculating ϵ	
\bar{y}_p	4	inch	Tension Steel in Beam (if added then need mod.s)		θ	29.93	degrees		A.4	
V_p	0	kips	A_s	0	in ²	d_v	52.90	inch	Here using 0.9 due to non-linear analysis results	
f_{po}	202.5	ksi	f_y	60	ksi	critical section	57.4	inch		
Type of Strand	low lax	text	E_s	29300	ksi	ϵ_s	0.00026473	in / in		A.5
E_p	28500	ksi	Transverse Steel in Beam		β	4.005	unitless		A.1, A.2	
			Minimum Shear Steel?	YES	yes or no	V_c	362	kips		A.7
			α	90	degrees	V_s	772	kips		A.8
			A_v	0.4	in ²	Limited 0.25?	NO	0.117	Adjacent cell shows value of potential limit	A.6
			$f_{y v}$	63	ksi	V_n	1134	kips		A.6
			s	3	inch	V_n unlimited	1134	kips		A.6
Miscellaneous Properties					ϕ	0.9	unitless			
Load Properties					ϕV_n	1021	kips			
					Other Properties					critical section
M_u	78602.291	kip * inch	Shear Span	154	inches	difference in V	2.077E-07	kips	difference between the calculated and assumed shear	
N_u	0	kips	Width of Bearing Pad	9	inches	$V_U = V_n * \phi$	1021	kips		
V_u	1021	kips				Roots	8.5	unitless	this is the roots value of Vs when units are in psi	

Beam 4N&S (s = 4") Geometry and Concrete Properties					Calculated Constants for MCFT from AASHTO LRFD 2009					
Beam			Deck		Constant	Value	Units	Description	Equ. #	
h_{beam}	54	inch	h_{deck}	8	inch	A_{ps}	11.934	in ²	area of prestressing steel on member's flexural tension side	
$f'_{\text{c beam}}$	11.44	ksi	$f'_{\text{c deck}}$	7.5	ksi	$h_{\text{composite}}$	62.75	inch	height of deck and girder	
b_v	16	inch	$b_{\text{effective deck}}$	96	in	d_p	58.75	inch	dist. from extreme ten. to extreme comp	
E_c	6097	ksi				d_c	50	inch **	** not the same d_c reported in shear section	
A_{ct}	856	in ²				c	7.52	inch	distance from extreme comp fiber to neutral axis	
Steel Properties					k	0.28	unitless			
					β_1	0.68	unitless			
Prestressing Steel Properties			Mild Steel Properties		a	5.08	inch			
Total # Strands	78	unitless	Compression Steel in Deck		f_{ps}	260.3	ksi			
Area of Each Strand	0.153	in ² / strand	A'_{s}	0	in ²	M_n	174633	kip * inch		
f_{pu}	270	ksi	f'_{s}	60	ksi	M_U limit	49692	kip * inch	used in calculating ϵ	
\bar{y}_p	4	inch	Tension Steel in Beam (if added then need mod.s)		θ	28.93	degrees			A.4
V_p	0	kips	A_s	0	in ²	d_v	52.90	inch	Here using 0.9 due to non-linear analysis results	
f_{po}	202.5	ksi	f_y	60	ksi	critical section	57.4	inch		
Type of Strand	low lax	text	E_s	29300	ksi	ϵ_s	-0.00001979	in / in		A.5
E_p	28500	ksi	Transverse Steel in Beam		β	4.872	unitless			A.1, A.2
			Minimum Shear Steel?	YES	yes or no	V_C	441	kips		A.7
			α	90	degrees	V_S	603	kips		A.8
			A_v	0.4	in ²	Limited 0.25?	NO	0.108	Adjacent cell shows value of potential limit	A.6
			$f_{y v}$	63	ksi	V_n	1044	kips		A.6
			s	4	inch	V_n unlimited	1044	kips		A.6
Miscellaneous Properties					ϕ	0.9	unitless			
Load Properties			Other Properties		ϕV_n	939	kips			
			critical section			57.4	inch	critical section for iteration		
M_u	72329.911	kip * inch	Shear Span	154	inches	difference in V	-8.157E-04	kips	difference between the calculated and assumed shear	
N_u	0	kips	Width of Bearing Pad	9	inches	$V_U = V_n * \phi$	939	kips		
V_u	939	kips				Roots	6.7	unitless	this is the roots value of Vs when units are in psi	

B4N&S (s = 6") Geometry and Concrete Properties					Calculated Constants for MCFT from AASHTO LRFD 2009					
Beam			Deck		Constant	Value	Units	Description	Equ. #	
h_{beam}	54	inch	h_{deck}	8	inch	A_{ps}	11.934	in^2	area of prestressing steel on member's flexural tension side	
$f'_{\text{c beam}}$	11.44	ksi	$f'_{\text{c deck}}$	7.5	ksi	$h_{\text{composite}}$	62.75	inch	height of deck and girder	
b_v	16	inch	$b_{\text{effective deck}}$	96	in	d_p	58.75	inch	dist. from extreme ten. to extreme comp	
E_c	6097	ksi				d_c	50	inch **	** not the same d_c reported in shear section	
A_{ct}	856	in^2				c	7.52	inch	distance from extreme comp fiber to neutral axis	
Steel Properties					k	0.28	unitless			
					β_1	0.68	unitless			
Prestressing Steel Properties			Mild Steel Properties		a	5.08	inch			
Total # Strands	78	unitless	Compression Steel in Deck		f_{ps}	260.3	ksi			
Area of Each Strand	0.153	$\text{in}^2 / \text{strand}$	A'_s	0	in^2	M_n	174633	kip * inch		
f_{pu}	270	ksi	f'_s	60	ksi	M_U limit	41471	kip * inch	used in calculating ϵ	
\bar{y}_p	4	inch	Tension Steel in Beam (if added then need mod.s)		θ	28.69	degrees		A.4	
V_p	0	kips	A_s	0	in^2	d_v	52.90	inch	Here using 0.9 due to non-linear analysis results	
f_{po}	202.5	ksi	f_y	60	ksi	critical section	57.4	inch		
Type of Strand	low lax	text	E_s	29300	ksi	ϵ_s	-0.00008843	in / in		A.5
E_p	28500	ksi	Transverse Steel in Beam		β	5.141	unitless		A.1, A.2	
			Minimum Shear Steel?	YES	yes or no	V_C	465	kips		A.7
			α	90	degrees	V_S	406	kips		A.8
			A_v	0.4	in^2	Limited 0.25?	NO	0.090	Adjacent cell shows value of potential limit	A.6
			$f_{y v}$	63	ksi	V_n	871	kips		A.6
			s	6	inch	V_n unlimited	871	kips		A.6
Miscellaneous Properties					ϕ	0.9	unitless			
Load Properties					Other Properties		ϕV_n	784	kips	
					critical section	57.4	inch	critical section for iteration		
M_u	60364.083	kip * inch	Shear Span	154	inches	difference in V	-9.097E-04	kips	difference between the calculated and assumed shear	
N_u	0	kips	Width of Bearing Pad	9	inches	$V_U = V_n * \phi$	784	kips		
V_u	784	kips				Roots	4.5	unitless	this is the roots value of Vs when units are in psi	

Beam 5N (s = 4") Geometry and Concrete Properties					Calculated Constants for MCFT from AASHTO LRFD 2009					
Beam			Deck			Constant	Value	Units	Description	Equ. #
h_{beam}	54	inch	h_{deck}	8	inch	A_{ps}	10.098	in ²	area of prestressing steel on member's flexural tension side	
f'_c beam	13.23	ksi	f'_c deck	7.6	ksi	$h_{composite}$	62.75	inch	height of deck and girder	
b_v	10	inch	$b_{effective\ deck}$	96	in	d_p	59.06	inch	dist. from extreme ten. to extreme comp	
E_c	6556	ksi				d_c	50.31	inch **	** not the same d_c reported in shear section	
A_{ct}	717.5	in ²				c	6.36	inch	distance from extreme comp fiber to neutral axis	
Steel Properties					k	0.28	unitless			
					β_1	0.67	unitless			
Prestressing Steel Properties			Mild Steel Properties			a	4.26	inch		
Total # Strands	66	unitless	Compression Steel in Deck			f_{ps}	261.9	ksi		
Area of Each Strand	0.153	in ² / strand	A'_s	0	in ²	M_n	150529	kip * inch		
f_{pu}	270	ksi	f'_s	60	ksi	M_U limit	70775	kip * inch	used in calculating ϵ	
\bar{y}_p	3.69	inch	Tension Steel in Beam (if added then need mod.s)			θ	43.78	degrees		A.4
V_p	0	kips	A_s	0	in ²	d_v	53.15	inch	Here using 0.9 due to non-linear analysis results	
f_{po}	202.5	ksi	f_y	60	ksi	critical section	57.7	inch		
Type of Strand	low lax	text	E_s	29300	ksi	ϵ_s	0.00422358	in / in		A.5
E_p	28500	ksi	Transverse Steel in Beam			β	1.152	unitless		A.1, A.2
			Minimum Shear Steel?	YES	yes or no	V_C	70	kips		A.7
			α	90	degrees	V_S	1409	kips		A.8
			A_v	1.5	in ²	Limited 0.25?	NO	0.210	Adjacent cell shows value of potential limit	A.6
			$f_{y\ v}$	67.75	ksi	V_n	1479	kips		A.6
			s	4	inch	V_n unlimited	1479	kips		A.6
Miscellaneous Properties					ϕ	0.9	unitless			
					ϕV_n	1332	kips			
Load Properties			Other Properties			critical section	57.7	inch	critical section for iteration	
M_u	102526.176	kip * inch	Shear Span	154	inches	difference in V	7.648E-05	kips	difference between the calculated and assumed shear	
N_u	0	kips	Width of Bearing Pad	9	inches	$V_U = V_n * \phi$	1332	kips		
V_u	1332	kips				Roots	23.0	unitless	this is the roots value of Vs when units are in psi	

Beam 5N (s = 6") Geometry and Concrete Properties					Calculated Constants for MCFT from AASHTO LRFD 2009					
Beam			Deck			Constant	Value	Units	Description	Equ. #
h_{beam}	54	inch	h_{deck}	8	inch	A_{ps}	10.098	in ²	area of prestressing steel on member's flexural tension side	
$f'_{\text{c beam}}$	13.23	ksi	$f'_{\text{c deck}}$	7.6	ksi	$h_{\text{composite}}$	62.75	inch	height of deck and girder	
b_v	10	inch	$b_{\text{effective deck}}$	96	in	d_p	59.06	inch	dist. from extreme ten. to extreme comp	
E_c	6556	ksi				d_c	50.31	inch **	** not the same d_c reported in shear section	
A_{ct}	717.5	in ²				c	6.36	inch	distance from extreme comp fiber to neutral axis	
Steel Properties					k	0.28	unitless			
					β_1	0.67	unitless			
Prestressing Steel Properties			Mild Steel Properties			a	4.26	inch		
Total # Strands	66	unitless	Compression Steel in Deck			f_{ps}	261.9	ksi		
Area of Each Strand	0.153	in ² / strand	A'_s	0	in ²	M_n	150529	kip * inch		
f_{pu}	270	ksi	f'_s	60	ksi	M_U limit	44265	kip * inch	used in calculating ϵ	
\bar{y}_p	3.69	inch	Tension Steel in Beam (if added then need mod.s)			θ	29.00	degrees		A.4
V_p	0	kips	A_s	0	in ²	d_v	53.15	inch	Here using 0.9 due to non-linear analysis results	
f_{po}	202.5	ksi	f_y	60	ksi	critical section	57.7	inch		
Type of Strand	low lax	text	E_s	29300	ksi	ϵ_s	-0.00000114	in / in		A.5
E_p	28500	ksi	Transverse Steel in Beam			β	4.804	unitless		A.1, A.2
			Minimum Shear Steel?	YES	yes or no	V_c	294	kips		A.7
			α	90	degrees	V_s	632	kips		A.8
			A_v	0.62	in ²	Limited 0.25?	NO	0.132	Adjacent cell shows value of potential limit	A.6
			$f_{y v}$	63.75	ksi	V_n	925	kips		A.6
			s	6	inch	V_n unlimited	925	kips		A.6
Miscellaneous Properties					ϕ	0.9	unitless			
					ϕV_n	833	kips			
Load Properties			Other Properties			critical section	57.7	inch	critical section for iteration	
M_u	64123.335	kip * inch	Shear Span	154	inches	difference in V	2.071E-05	kips	difference between the calculated and assumed shear	
N_u	0	kips	Width of Bearing Pad	9	inches	$V_U = V_n * \phi$	833	kips		
V_u	833	kips				Roots	10.3	unitless	this is the roots value of Vs when units are in psi	

APPENDIX B

Concrete and Reinforcement Properties

This appendix provides all the concrete mix designs and concrete and reinforcement strengths and properties which were tested in this program. All tests were run in accordance with the applicable ASTM standard specification.

Contents

B.1 Concrete Mix Designs.....	133
B.2 Concrete Compressive Strengths	134
B.3 Transverse Reinforcement Properties	134
B.4 Prestressing Strand Properties.....	136

B.1 CONCRETE MIX DESIGNS

Table B-1: U-Beam Girder Concrete Mix Design

Material	Properties	Quantity			Units
		Beams 1 & 2	Beams 3 & 4	Beam 5	
Cementitious Material	Alamo Gray Type III	611	599	606	lb / yd ³ concrete
	Type F Fly Ash	0	200	206	lb / yd ³ concrete
Coarse Aggregate	¾ in. Crushed Limestone	1,600	0	1,855	lb / yd ³ concrete
	½ in. Crushed Limestone	0	1,821	0	lb / yd ³ concrete
Fine Aggregate	River Sand	1,379	1,152	1,124	lb / yd ³ concrete
Water	--	202	252	167	lb / yd ³ concrete
Water/Cement Ratio	--	0.33	0.32	0.21	unit less
Water-Reducers	Sika Viscocrete 2100	13	7	0	oz/hundred weight cement
	Sikament 686	25	0	0	oz/hundred weight cement
	Sika 161	0	8	0	oz/hundred weight cement
	Superplasticizer	0	0	5	oz/hundred weight cement
Retarder	Sika Plastiment	5	4	4	oz/hundred weight cement
Desired Slump	--	9	9	6	inches

Table B-2: Deck Concrete Mix Design

Material	Properties	Quantity			Units
		Beams 0	Beams 1 - 4	Beam 5	
Cementitious Material	Type I cement	0	525	604	lb / yd ³ concrete
	Type III cement	611	0	0	lb / yd ³ concrete
	Type F Fly Ash	0	175	203	lb / yd ³ concrete
Coarse Aggregate	¾ in. Crushed Limestone	1,600	0	0	lb / yd ³ concrete
	1 in. River Rock	0	1,795	0	lb / yd ³ concrete
	1 in. Dolomite	0	0	1,728	lb / yd ³ concrete
Fine Aggregate	River Sand	1,379	1,295	1,728	lb / yd ³ concrete
Water	--	202	145	131	lb / yd ³ concrete
Water/Cement Ratio	--	0.33	0.21	0.16	unit less
Water-Reducers	Sika Viscocrete 2100	13	0	0	oz/hundred weight cement
	Sikament 686	25	0	0	oz/hundred weight cement
	Superplasticizer	0	55	69	oz/hundred weight cement
Retarder	Sika Plastiment	5	0	0	oz/hundred weight cement
Desired Slump	--	9	8	8	inches

B.2 CONCRETE COMPRESSIVE STRENGTHS

Table B-3: U-Beam Girder and Deck Concrete Compressive Strengths

Beam Strengths	Beam 1 N	Beam 1 S	Beam 2 N	Beam 2 S	Beam 3 N	Beam 3 S	Beam 4 N	Beam 4 S	Beam 5 N	Units
Release strength	6,300		6,400		6,300		6,400		6,100	psi
28-day strength	11,700		10,600		11,300		10,800		12,400	psi
Strength at time of Testing	11,900	11,900	11,500	11,500	11,400	12,100	11,400	11,400	13,200	psi
Deck Strength	Beam 1 N	Beam 1 S	Beam 2 N	Beam 2 S	Beam 3 N	Beam 3 S	Beam 4 N	Beam 4 S	Beam 5 N	Units
Strength at time of Testing	10,500	10,500	8,600	8,600	9,200	10,700	7,500	7,500	7,600	psi

B.3 TRANSVERSE REINFORCEMENT PROPERTIES

Table B-4: Beam 1: Transverse Reinforcement Mechanical Properties

Beam 1 -- Transverse Reinforcement Properties				
	Bar Type	Nom. Area (in^2)	f_{sy} (ksi)	f_{su} (ksi)
1	R-rebar	0.20	61	101
2	R-rebar	0.20	65	93

Table B-5: Beam 2: Transverse Reinforcement Mechanical Properties

Beam 2 -- Transverse Reinforcement Properties				
	Bar Type	Nom. Area (in^2)	f_{sy} (ksi)	f_{su} (ksi)
1	R-rebar	0.20	61	101
2	R-rebar	0.20	67	109
3	R-rebar	0.20	66	108
4	R-rebar	0.20	68	111
5	R-rebar	0.20	65	109
6	R-rebar	0.20	65	109
7	R-rebar	0.20	66	110
8	R-WWR	0.20	87	96
9	R-WWR	0.20	87	96
10	R-WWR	0.20	88	97
11	R-WWR	0.20	80	97

Table B-6: Beam 3: Transverse Reinforcement Mechanical Properties

Beam 3 -- Transverse Reinforcement Properties				
	Bar Type	Nom. Area (in^2)	f_{sy} (ksi)	f_{su} (ksi)
1	R-rebar	0.20	68.3	107
2	R-rebar	0.20	63.25	103
3	R-rebar	0.20	64	101

Table B-7: Beam 4: Transverse Reinforcement Mechanical Properties

Beam 4 -- Transverse Reinforcement Properties				
	Bar Type	Nom. Area (in^2)	f_{sy} (ksi)	f_{su} (ksi)
1	R-rebar	0.20	64	101
2	R-rebar	0.20	61	99
3	R-rebar	0.20	64	102
4	S-rebar	0.31	59.5	99
5	S-rebar	0.31	60.8	101
6	C-rebar	0.20	63.36	106
7	C-rebar	0.20	68.02	106

Table B-8: Beam 5: Transverse Reinforcement Mechanical Properties

Beam 5 -- Transverse Reinforcement Properties				
	Bar Type	Nom. Area (in^2)	f_{sy} (ksi)	f_{su} (ksi)
1	R-rebar	0.31	63.5	102
2	R-rebar	0.31	65	105
3	R-rebar	0.31	63	102
4	R-rebar	0.31	63.5	102
5	S-rebar	0.44	69.5	114
6	S-rebar	0.44	70	114

B.4 PRESTRESSING STRAND PROPERTIES

Table B-9: Beam 1: Prestressing Reinforcement Mechanical Properties

Beam 1 -- Prestressing Strand Properties				
	Type	Nominal Area (in^2)	E_p - actual (linear) (ksi)	E_p - gauge (spiral) (ksi)
1	7-wire strand	0.153	28,100	29,900
2	7-wire strand	0.153	27,800	29,300
3	7-wire strand	0.153	27,300	30,100
4	7-wire strand	0.153	27,300	29,300
5	7-wire strand	0.153	28,000	31,300
Average			27,700	29,980

Table B-10: Beam 2: Prestressing Reinforcement Mechanical Properties

Beam 2 -- Prestressing Strand Properties				
	Type	Nominal Area (in^2)	E_p - actual (linear) (ksi)	E_p - gauge (spiral) (ksi)
1	7-wire strand	0.153	28,900	31,100
2	7-wire strand	0.153	28,700	30,400
3	7-wire strand	0.153	29,100	31,200
4	7-wire strand	0.153	28,800	30,600
5	7-wire strand	0.153	28,500	30,400
6	7-wire strand	0.153	28,400	30,900
Average			28,733	30,767

Table B-11: Beam 3: Prestressing Reinforcement Mechanical Properties

Beam 3 -- Prestressing Strand Properties				
	Type	Nominal Area (in^2)	E_p - actual (linear) (ksi)	E_p - gauge (spiral) (ksi)
1	7-wire strand	0.153	28,900	30,800
2	7-wire strand	0.153	28,900	30,900
3	7-wire strand	0.153	29,300	31,900
4	7-wire strand	0.153	28,700	31,500
Average			28,950	31,275

Table B-12: Beam 4: Prestressing Reinforcement Mechanical Properties

Beam 4 -- Prestressing Strand Properties				
	Type	Nominal Area (in^2)	E_p - actual (linear) (ksi)	E_p - gauge (spiral) (ksi)
1	7-wire strand	0.153	28,800	-- *
2	7-wire strand	0.153	28,800	-- *
3	7-wire strand	0.153	29,000	-- *
4	7-wire strand	0.153	29,600	-- *
Average			29,050	-- *

**Beam 4 contained no strain gauges attached to strand*

Table B-13: Beam 5: Prestressing Reinforcement Mechanical Properties

Beam 5 -- Prestressing Strand Properties				
	Type	Nominal Area (in^2)	E_p - actual (linear) (ksi)	E_p - gauge (spiral) (ksi)
1	7-wire strand	0.153	28,400	-- *
2	7-wire strand	0.153	29,000	-- *
3	7-wire strand	0.153	29,500	-- *
Average			28,967	-- *

**Beam 5 contained no strain gauges attached to strand*

APPENDIX C

Photo Documentation of all Shear Tests

This appendix provide detailed photographs showing all shear failures and any notable cracking which occurred in all shear tests performed during this research project. This is intended as a supplement to the material in Chapters 4 and 5.

Contents

C.1 Phase I Beams (Beams 1 through 3).....	139
C.2 Phase II Beams (Beams 4 and 5)	144

C.1 PHASE I BEAMS (BEAMS 1 THROUGH 3)

Beam 1 North Failure Shear = 659-kips

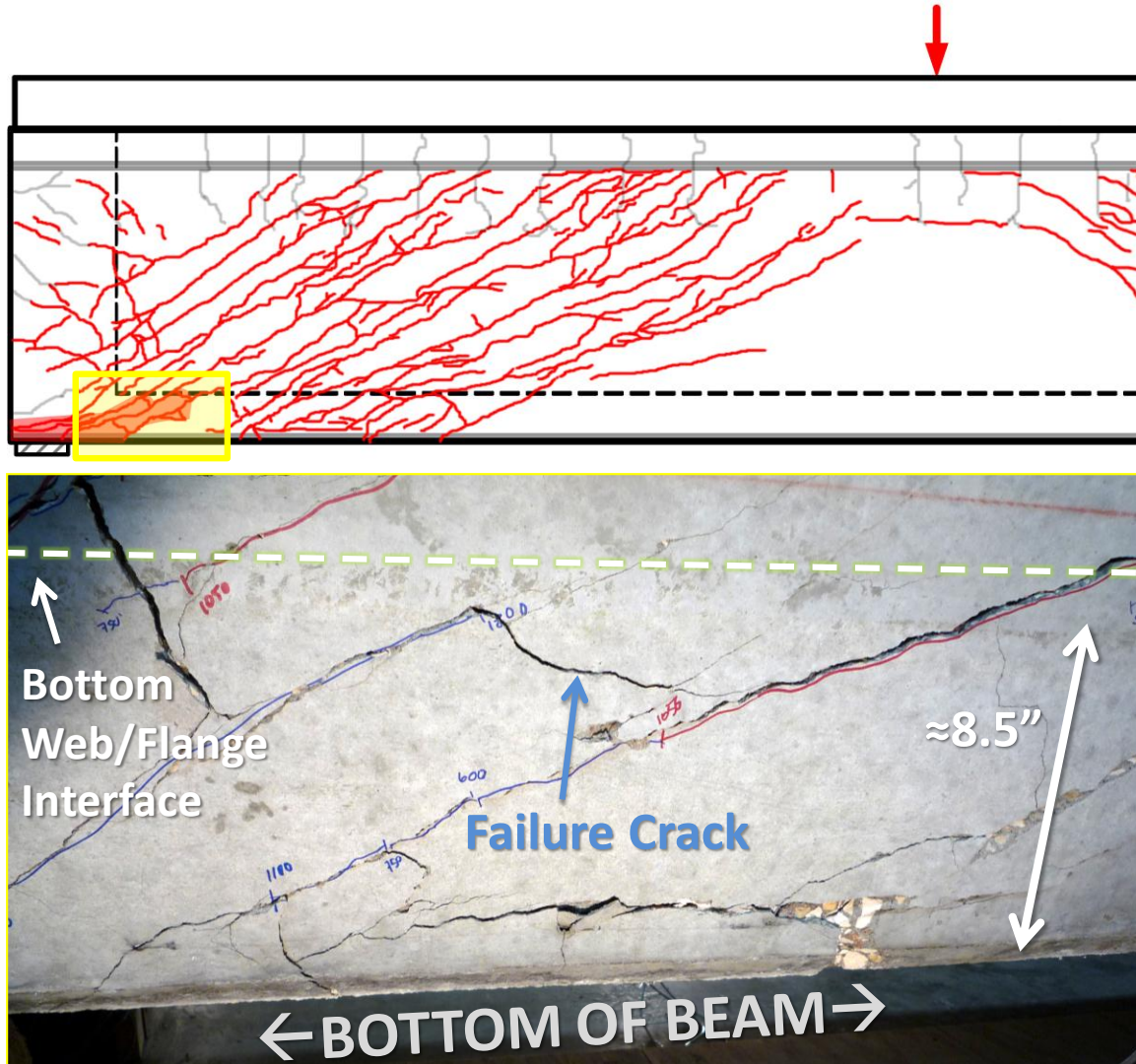


Figure C-1: Beam 1 North Failure

Beam 1 South Failure Shear = 612-kips

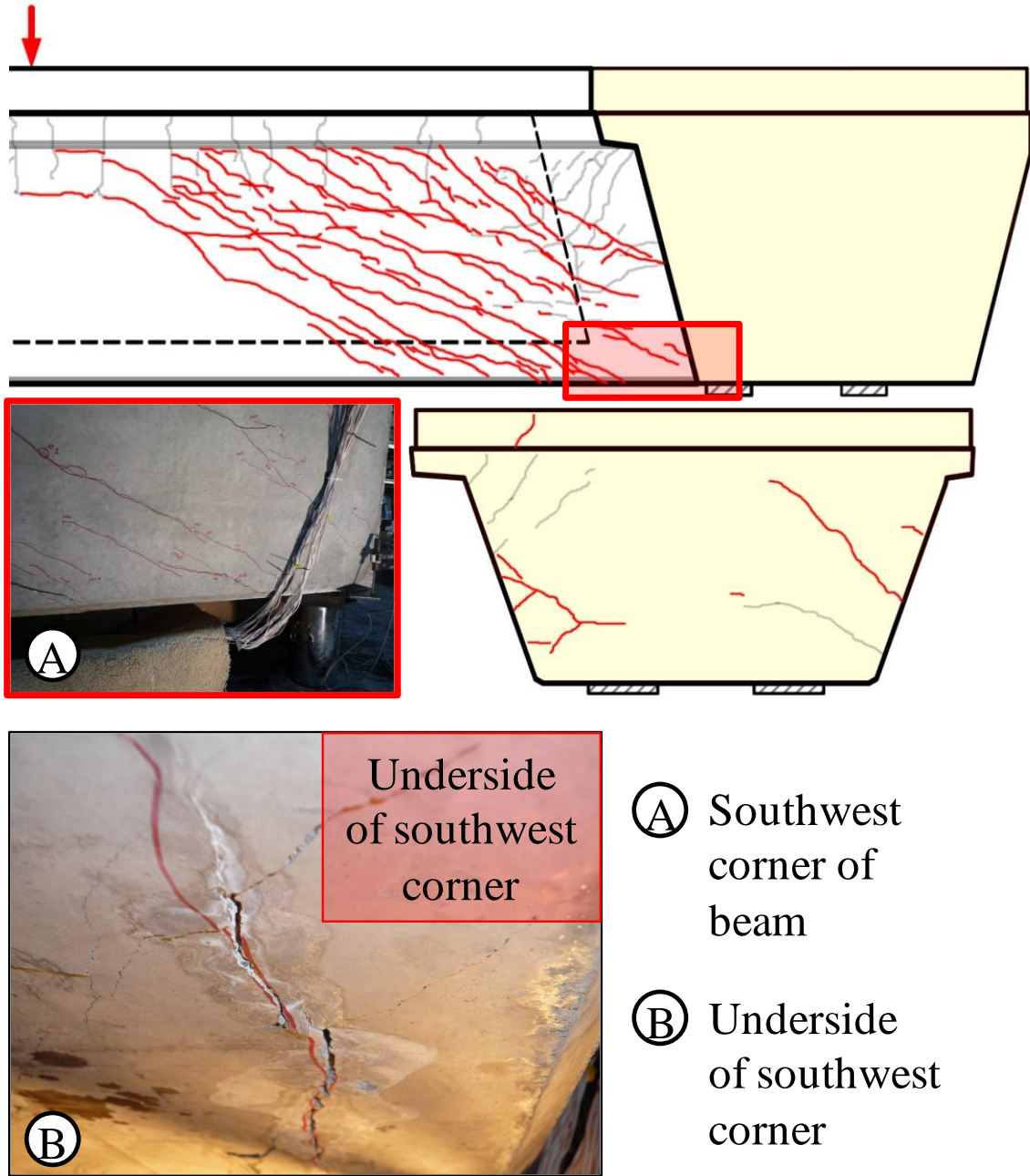


Figure C-2: Beam 1 South Failure (45-degree skewed end-block)

Beam 2 North Failure Shear = 610-kips

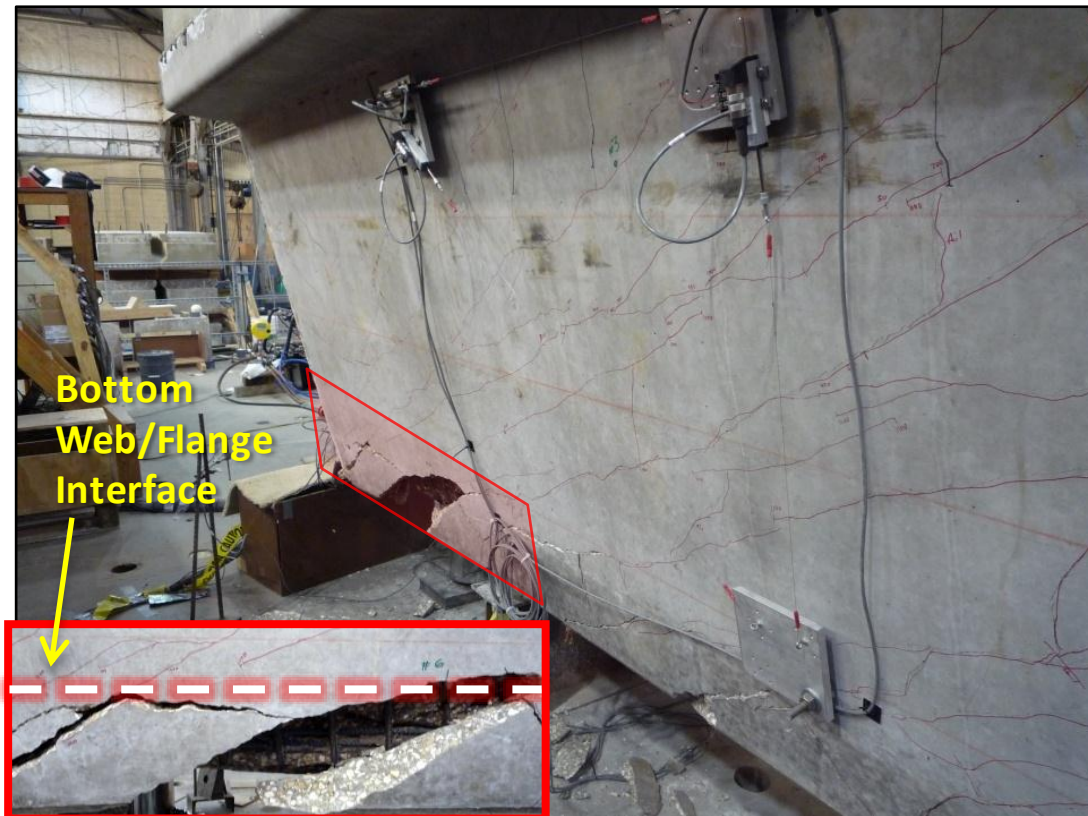
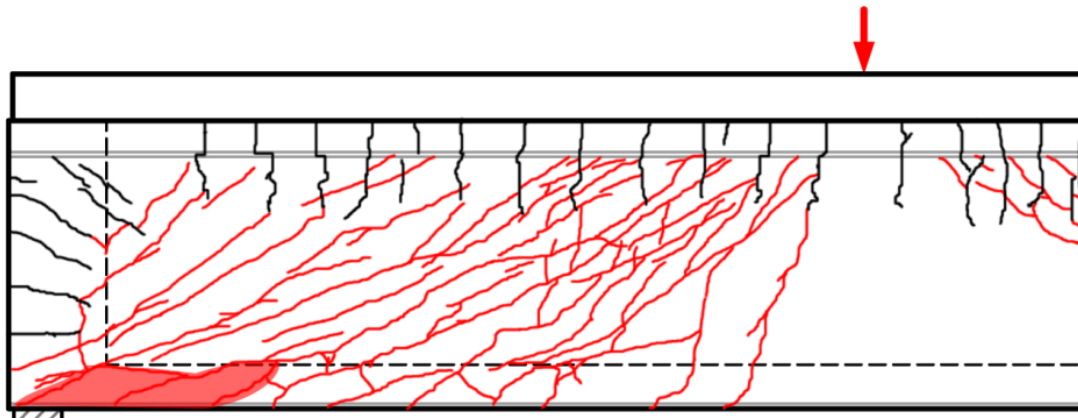


Figure C-3: Beam 2 North Failure

Beam 3 North Failure Shear = 655-kips

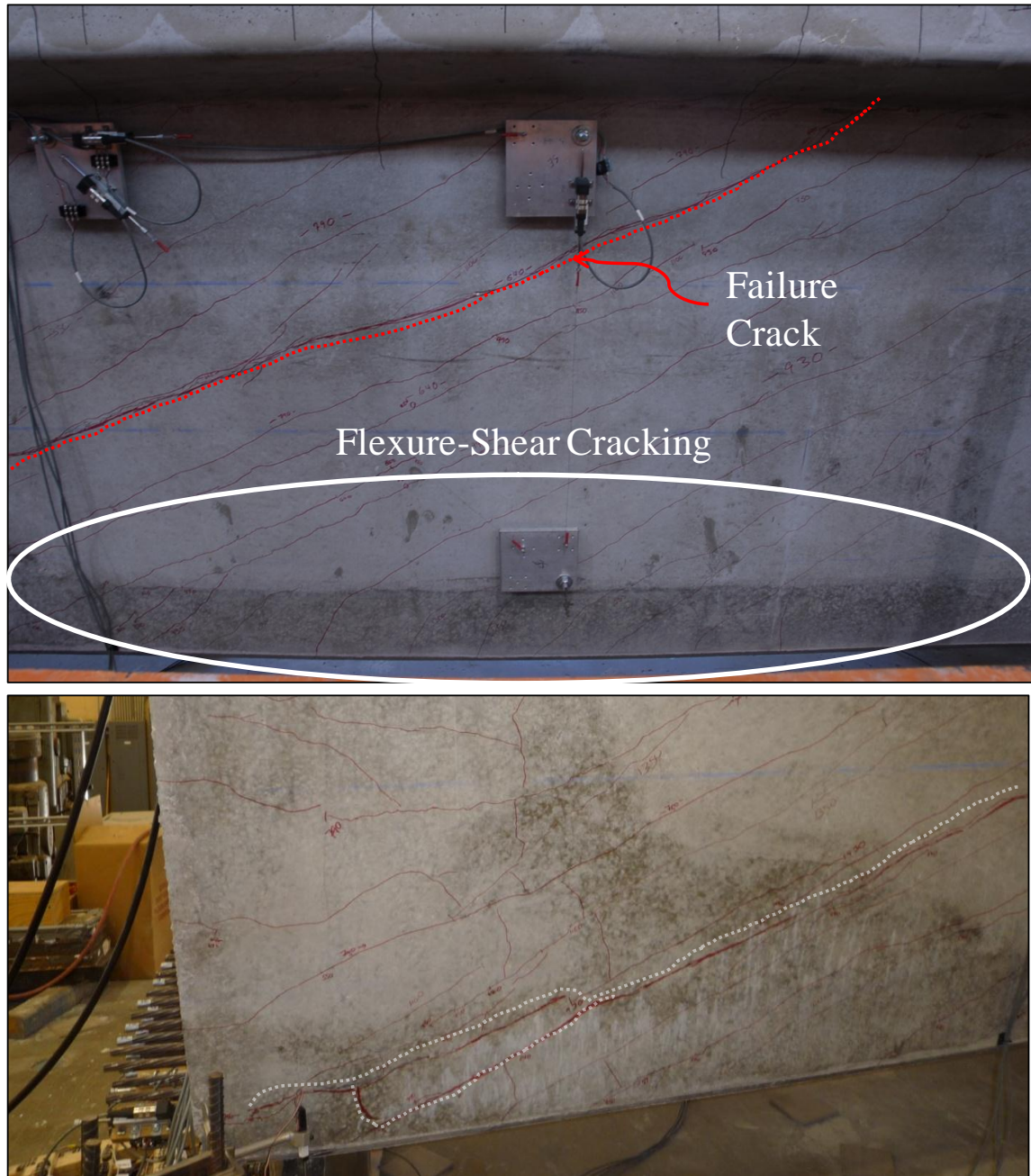


Figure C-4: Beam 3 North Failure

Beam 3 South Failure Shear = 663-kips

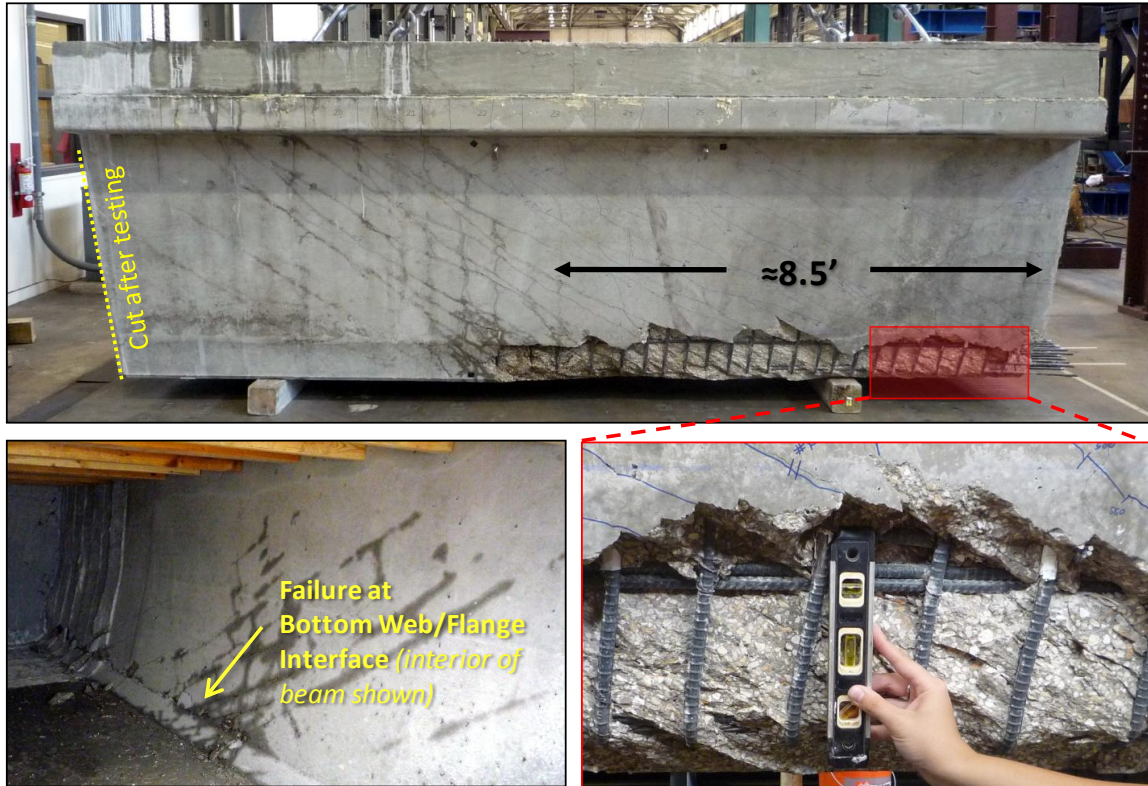


Figure C-5: Beam 3 South Failure



Figure C-6: Beam 3 South Time Lapse of Failure

C.2 PHASE II BEAMS (BEAMS 4 AND 5)

Beam 4 Failure Shear = 973-kips

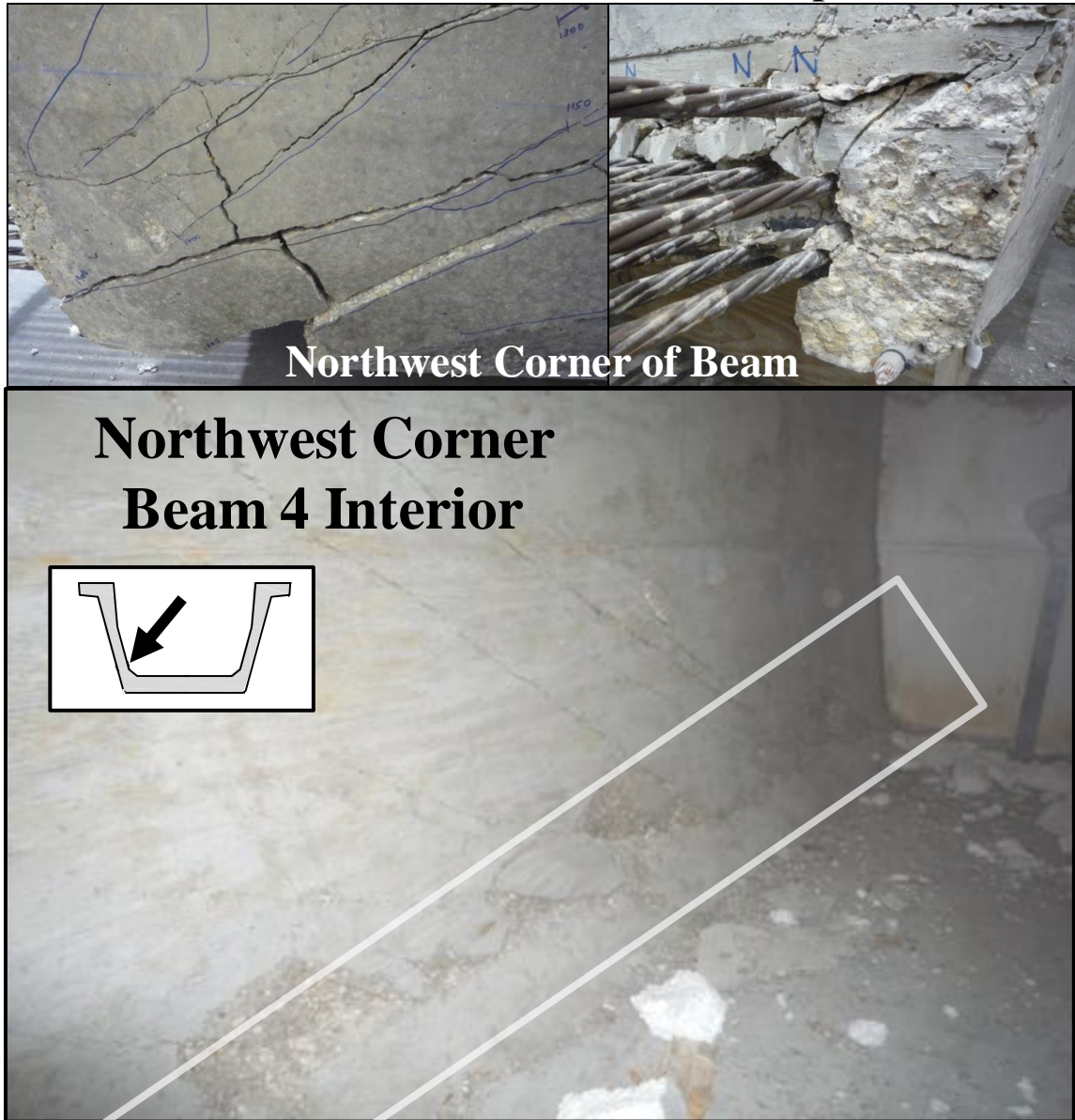


Figure C-7: Beam 4 North Failure

Beam 4 South not taken to Failure
Max Shear = 1191-kips

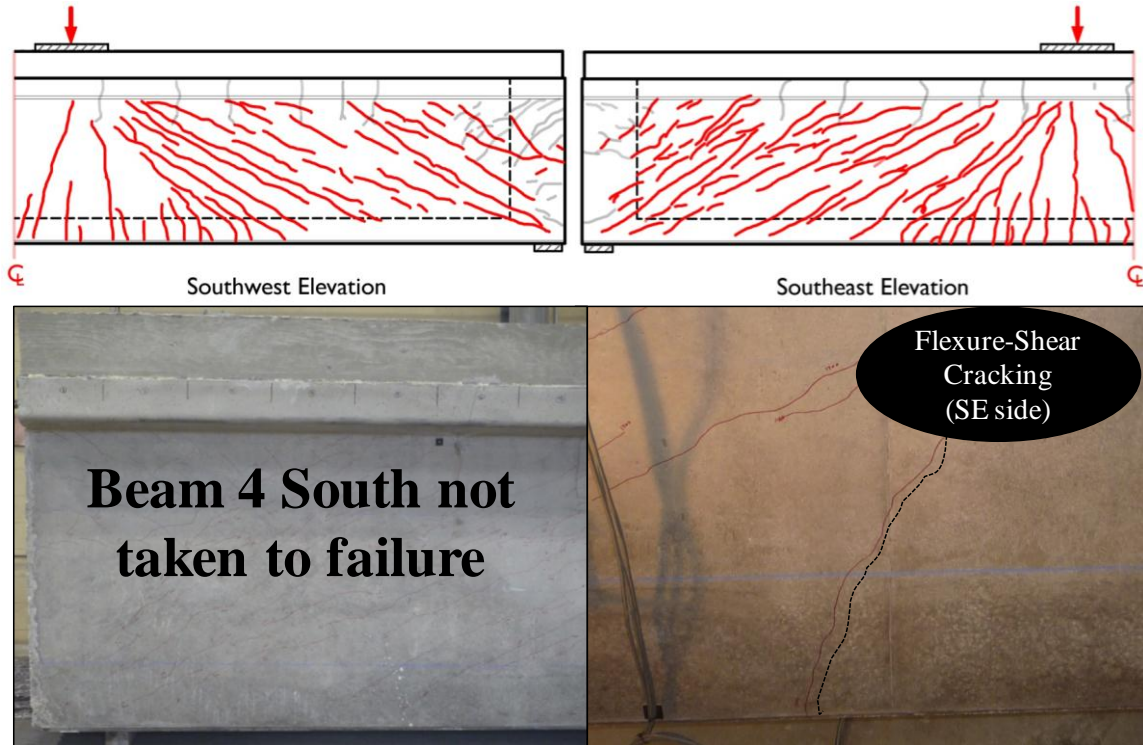


Figure C-8: Beam 4 South at Maximum Applied Load

Beam 5 Failure Shear = 1031-kips



Figure C-9: Beam 5 North Failure

APPENDIX D

Strain Gauge Data

This appendix will provide graphics depicting the data gathered from strain gauges attached to the transverse reinforcement in Beams 1 through 4 (Beam 5 did not contain internal instrumentation).

Contents

D.1	Transverse Reinforcement Strain at Web-to-Flange Interface	148
D.2	Transverse Reinforcement Strain at Mid-Depth of Web	152

D.1 TRANSVERSE REINFORCEMENT STRAIN AT WEB-TO-FLANGE INTERFACE

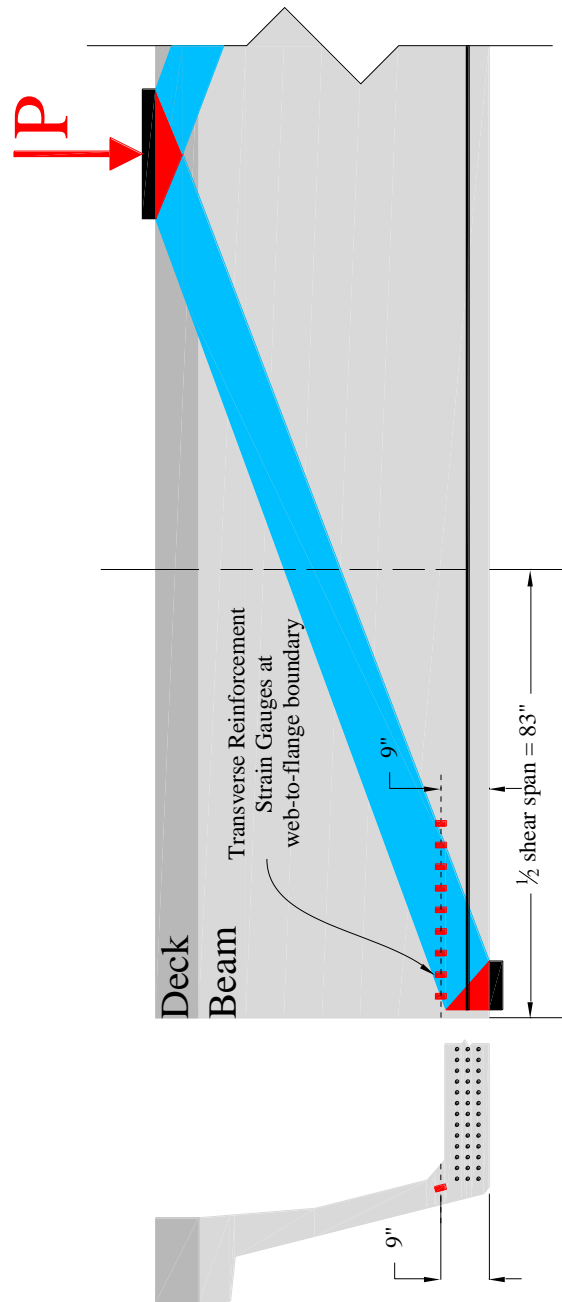


Figure D-1: Location of Strain Gaug Web-to-Flange Interface

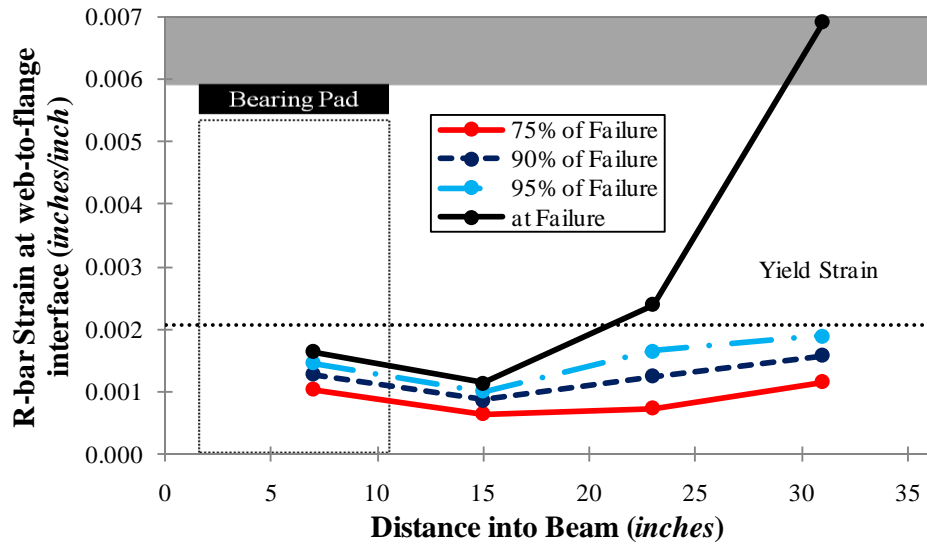


Figure D-2: Beam 1 North Reinforcement Strain at Web-to-Flange Interface

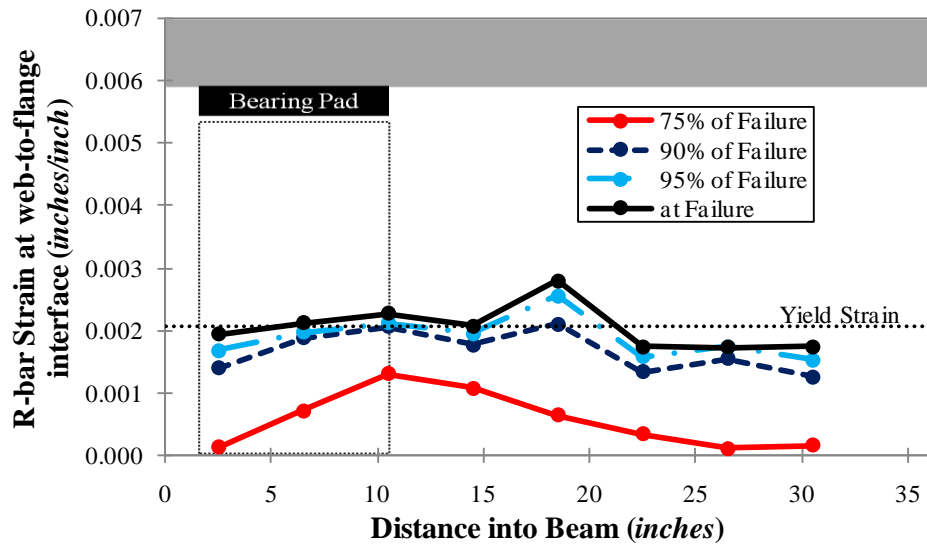


Figure D-3: Beam 2 North Reinforcement Strain at Web-to-Flange Interface

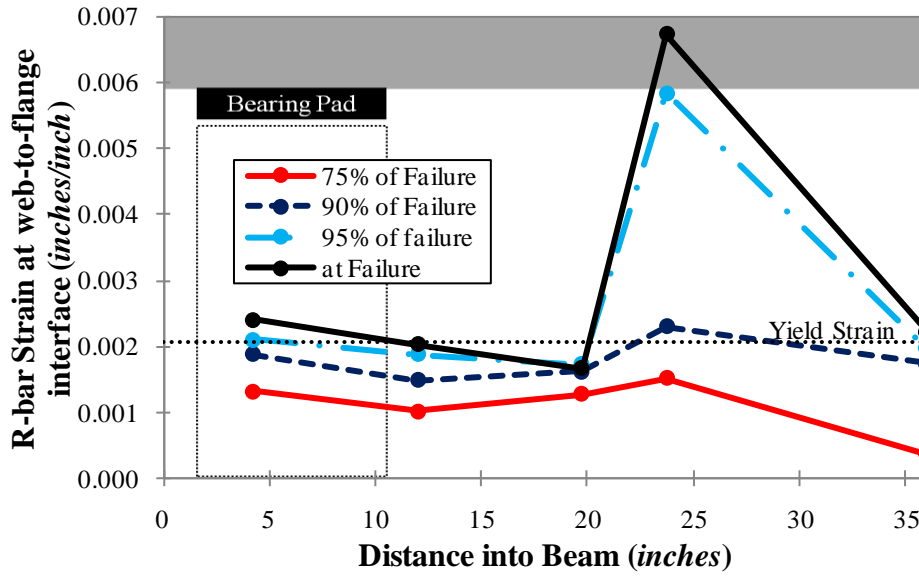


Figure D-4: Beam 3 North Reinforcement Strain at Web-to-Flange Interface

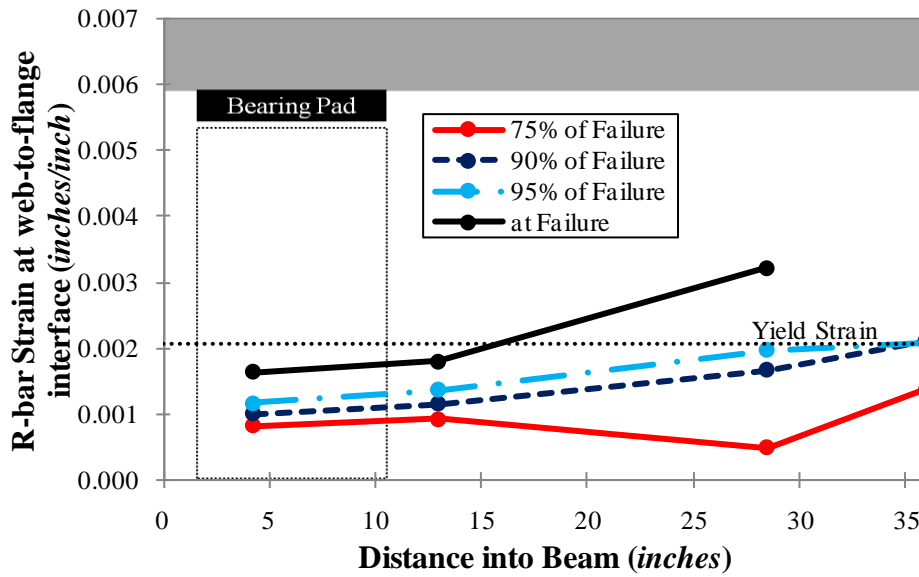


Figure D-5: Beam 3 South Reinforcement Strain at Web-to-Flange Interface

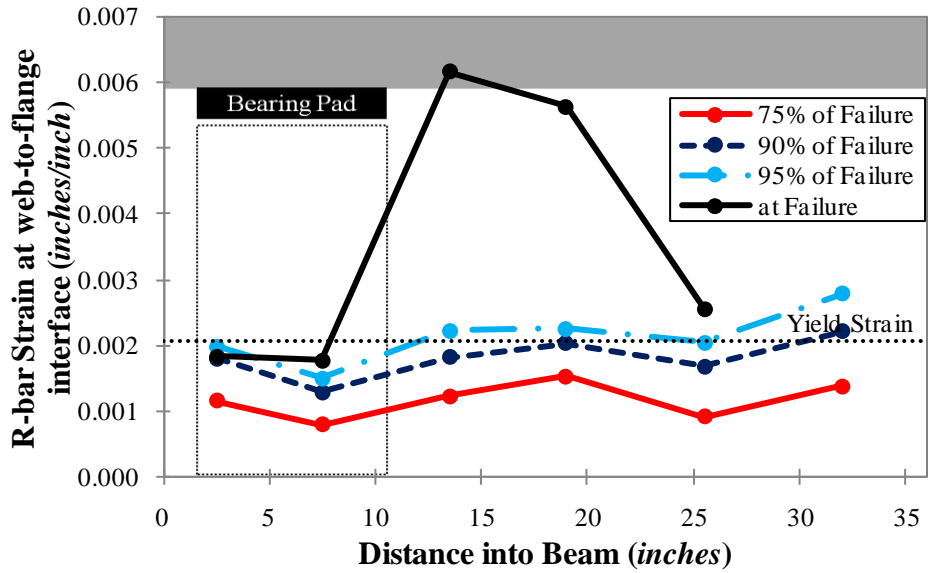


Figure D-6: Beam 4 North Reinforcement Strain at Web-to-Flange Interface

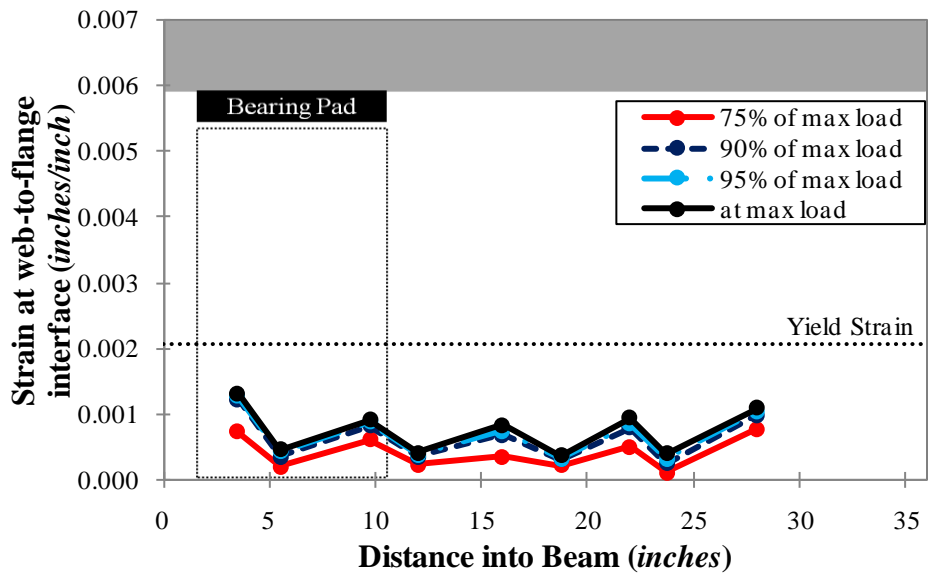


Figure D-7: Beam 4 South Reinforcement Strain at Web-to-Flange Interface

**Graph shows both #4 R-bars and #5 S-bars

D.2 TRANSVERSE REINFORCEMENT STRAIN AT MID-DEPTH OF WEB

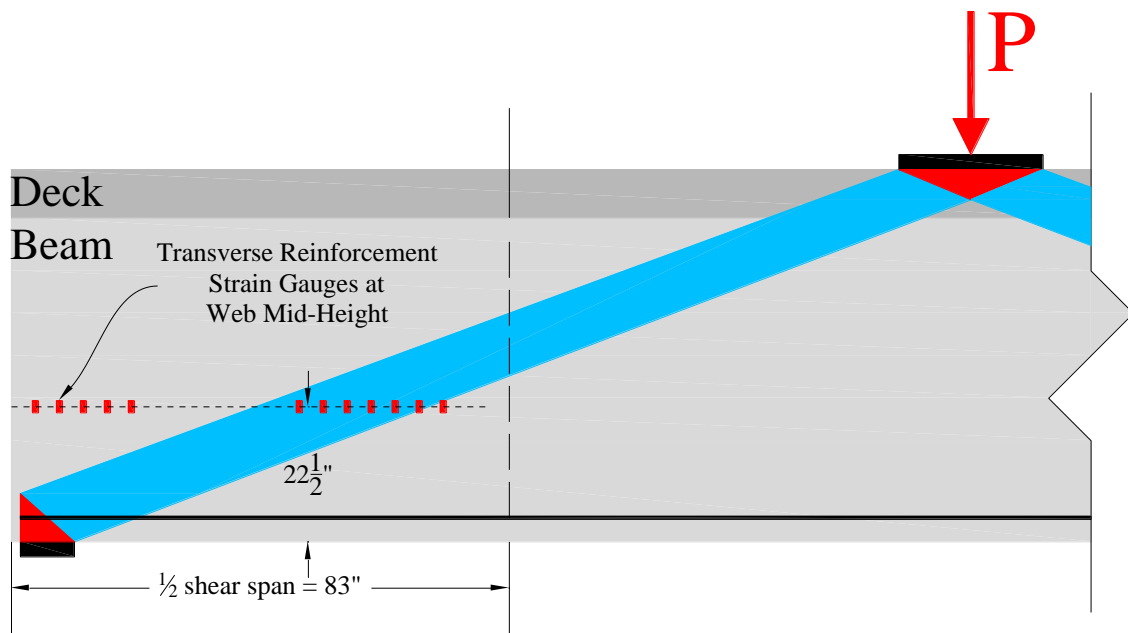


Figure D-8: Location of Shear Reinforcement Strain Gauges

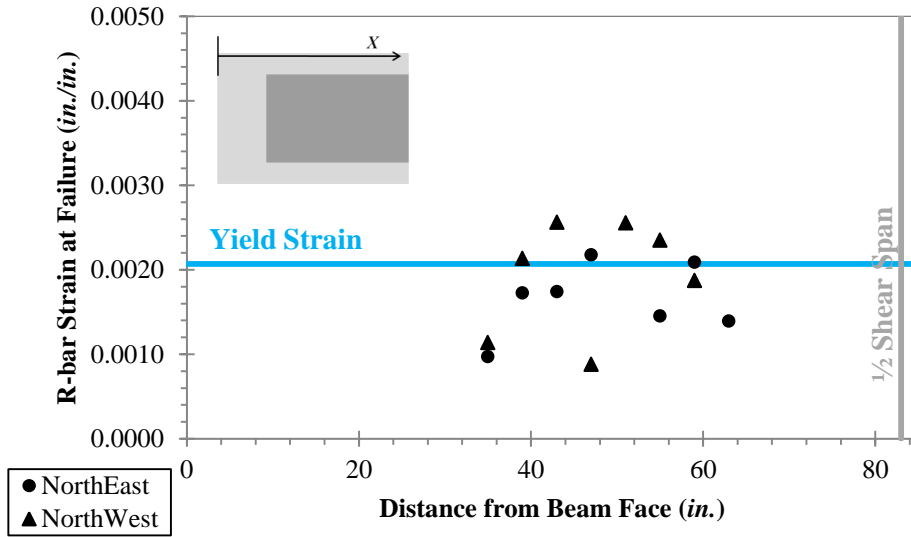


Figure D-9: Beam 1 North Reinforcement Strain at Web Mid-Depth at Failure

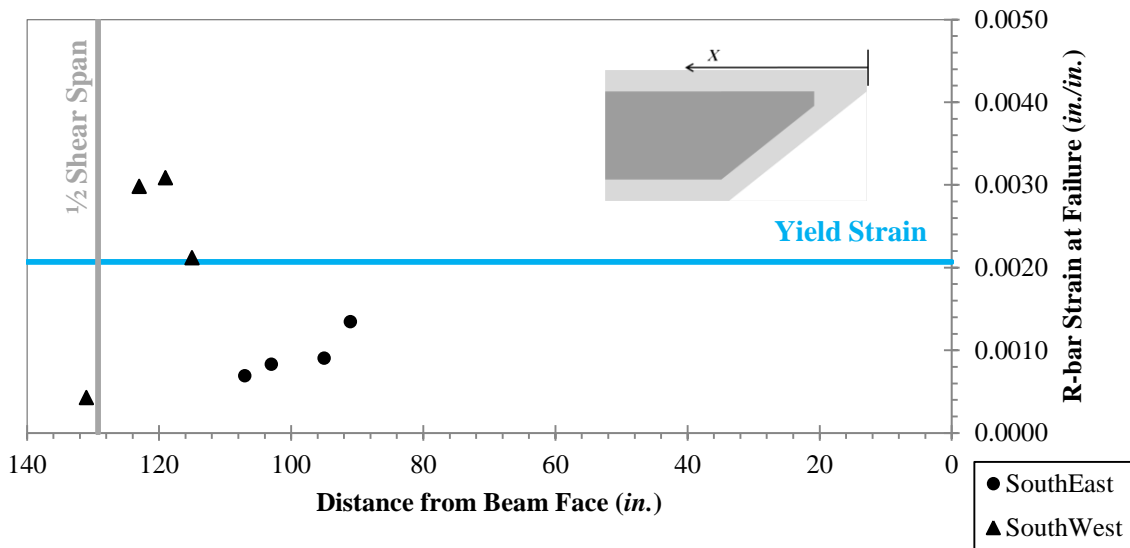


Figure D-10: Beam 1 South Reinforcement Strain at Web Mid-Depth at Failure

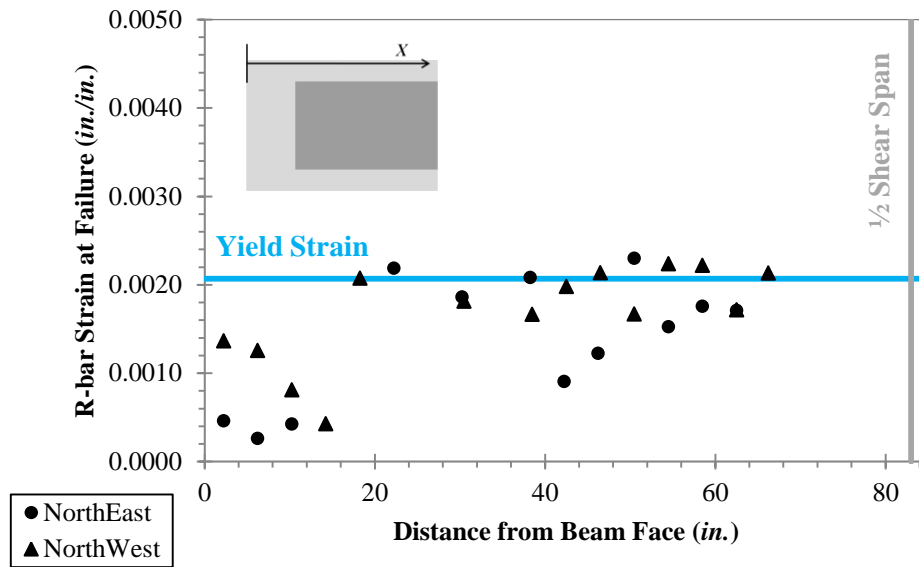


Figure D-11: Beam 2 North Reinforcement Strain at Web Mid-Depth at Failure

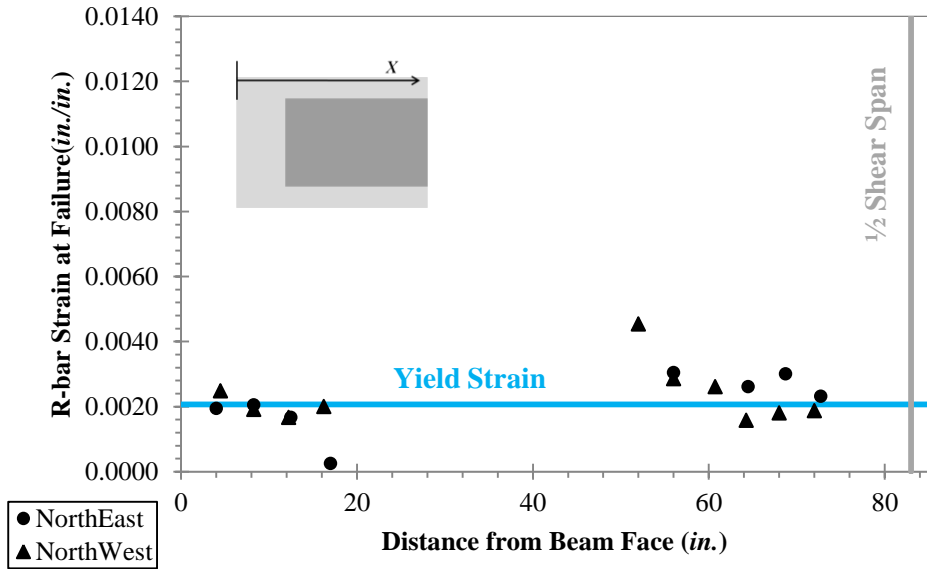


Figure D-12: Beam 3 North Reinforcement Strain at Web Mid-Depth at Failure

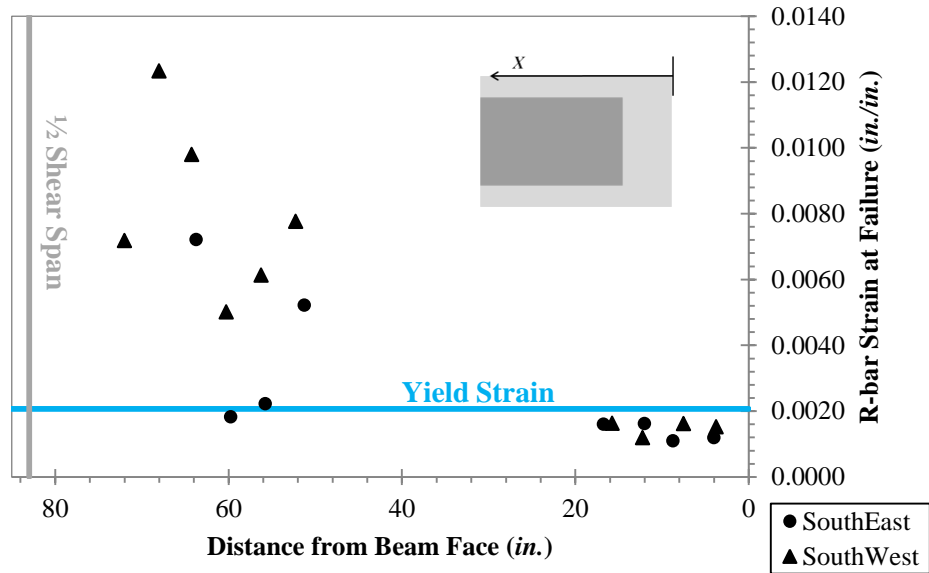


Figure D-13: Beam 3 South Reinforcement Strain at Web Mid-Depth at Failure

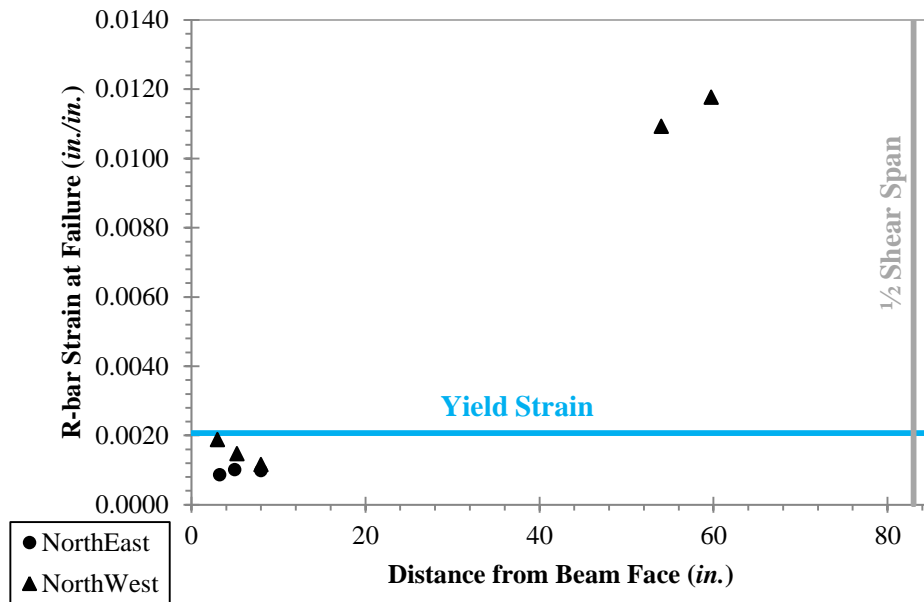


Figure D-14: Beam 4 North Reinforcement Strain at Mid-Depth of Web at Failure

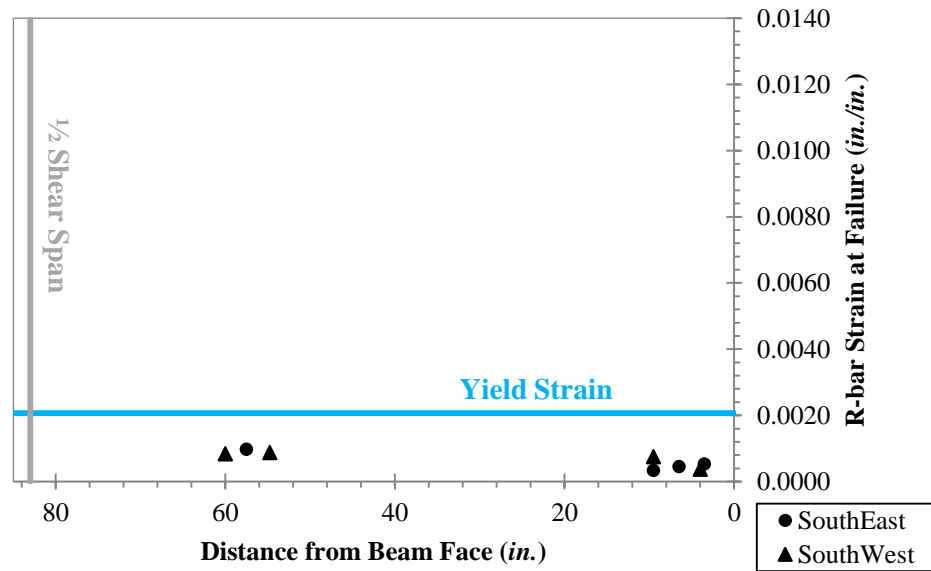


Figure D-15: Beam 4 South Reinforcement Strain at Mid-Depth of Web at Failure

APPENDIX E

Cross-Sectional Temperature Profiles

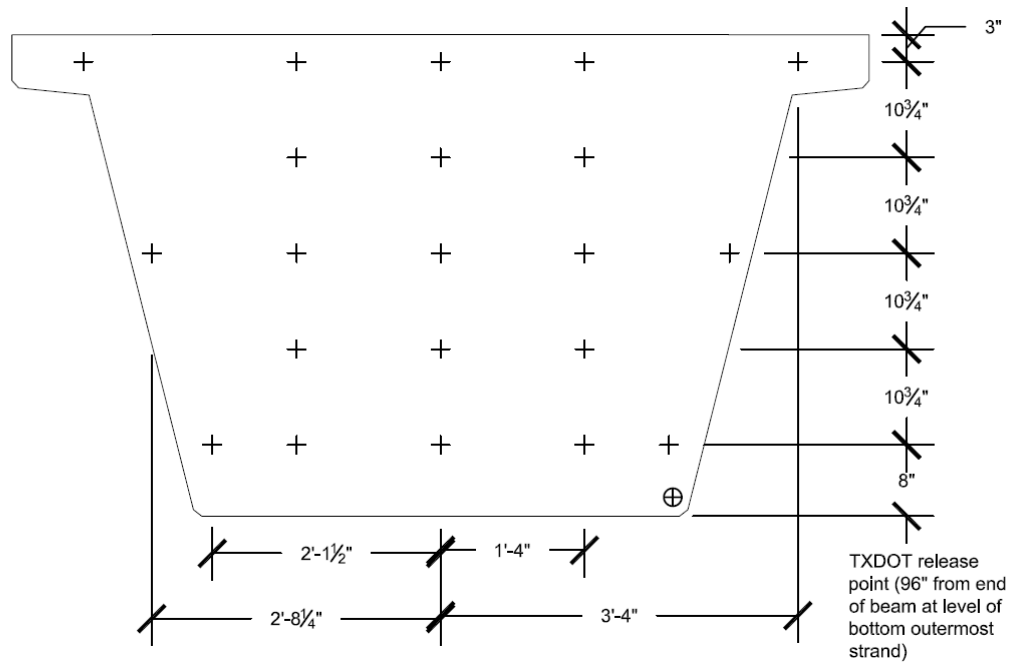
Contents

E.1	Introduction.....	158
E.2	Beam 1 temperature plots	159
E.3	Beam 2 temperature plots	163
E.4	Beam 3 temperature profiles.....	167
E.5	Beam 4 temperature profiles.....	171

E.1 INTRODUCTION

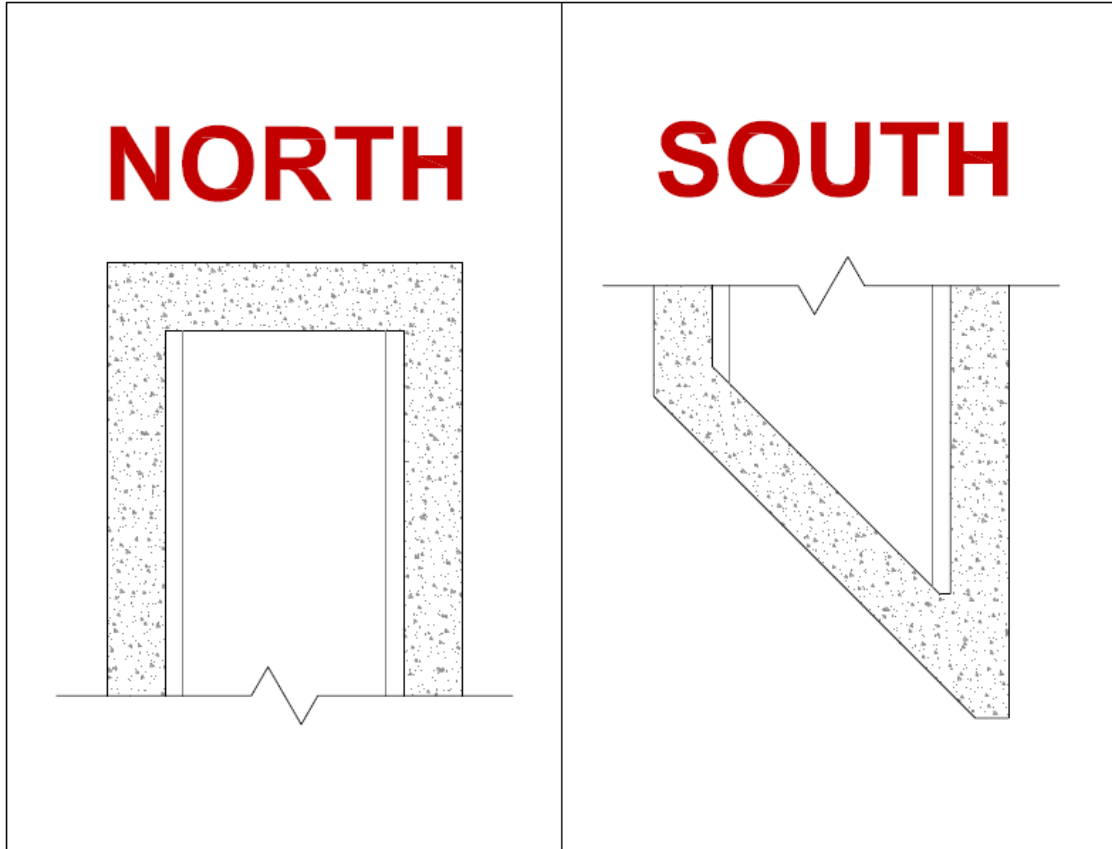
Appendix A contains the temperature profile plots for all beams cast at the Ferguson Structural Engineering Laboratory. The graphs interpolate between the actual thermocouple locations that recorded temperatures at the center of each end-block of the beam. These temperatures were affected by variables such as the inclusion of fly ash into the concrete mix, the material in which the concrete was formed, the overall geometry of the end-block, and the ambient temperature at the time of casting and curing. The general location for thermocouples in beams with zero degree skews is shown in Figure A-1; the actual horizontal coordinates will vary by the angle of the skew.

Figure E-1: Locations for Thermocouples in Beams with 90-degree End-Blocks



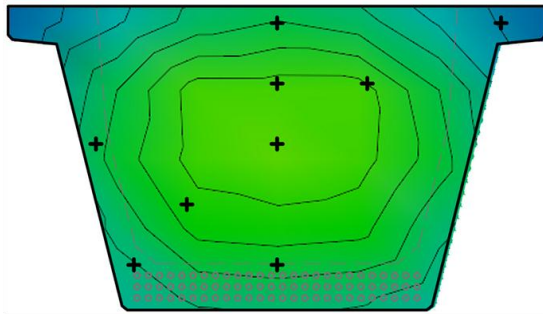
E.2 BEAM 1 TEMPERATURE PLOTS

Figure E-2: Beam 1 profile

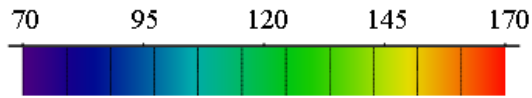


Beam 1: Maximum Temperature

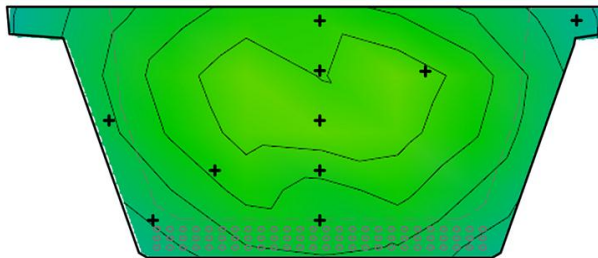
NORTH



Time since batching (hr.):	22
Ambient Temperature (°F):	71
Max. Temperature (°F):	137
Min. Temperature (°F):	100
Max. Temp. Differential (°F):	37
Formwork Material:	Steel
Contour Spacing (°F):	10
Skew angle (deg.):	0



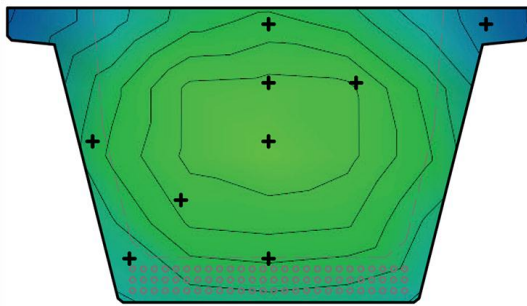
SOUTH



Time since batching (hr.):	21
Ambient Temperature (°F):	71
Max. Temperature (°F):	139
Min. Temperature (°F):	110
Max. Temp. Differential (°F):	29
Formwork Material:	Steel
Contour Spacing (°F):	10
Skew angle (deg.):	45

Beam 1: Differential Temperature

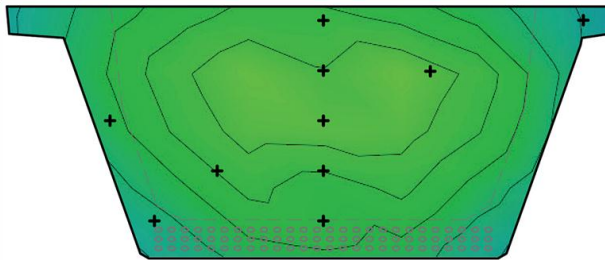
NORTH



Time after batching (hr.):	25
Ambient Temperature (°F):	73
Max. Temperature (°F):	136
Min. Temperature (°F):	98
Max. Temp. Differential (°F):	38
Formwork Material:	Steel
Contour Spacing (°F):	10
Skew angle (deg.):	0



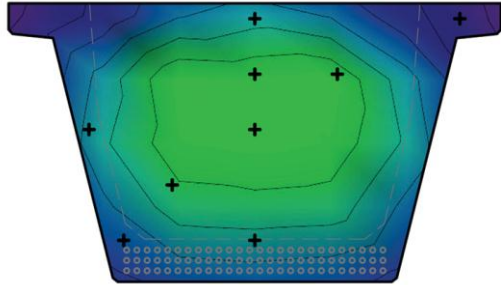
SOUTH



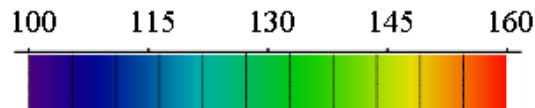
Time after batching (hr.):	25
Ambient Temperature (°F):	73
Max. Temperature (°F):	137
Min. Temperature (°F):	109
Max. Temp. Differential (°F):	28
Formwork Material:	Steel
Contour Spacing (°F):	10
Skew angle (deg.):	45

Beam 1: Prestress Release Temperature

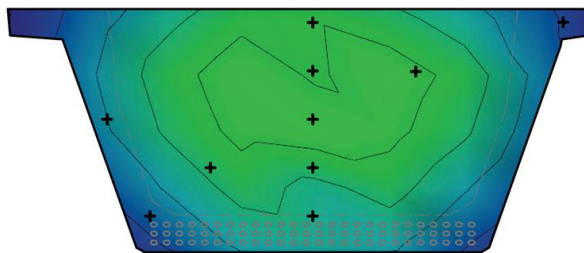
NORTH



Time since batching (hr.):	17
Ambient Temperature ($^{\circ}F$):	73
Max. Temperature ($^{\circ}F$):	135
Min. Temperature ($^{\circ}F$):	103
Max. Temp. Differential ($^{\circ}F$):	32
Formwork Material:	Steel
Contour Spacing ($^{\circ}F$):	6
Skew angle (deg.):	0



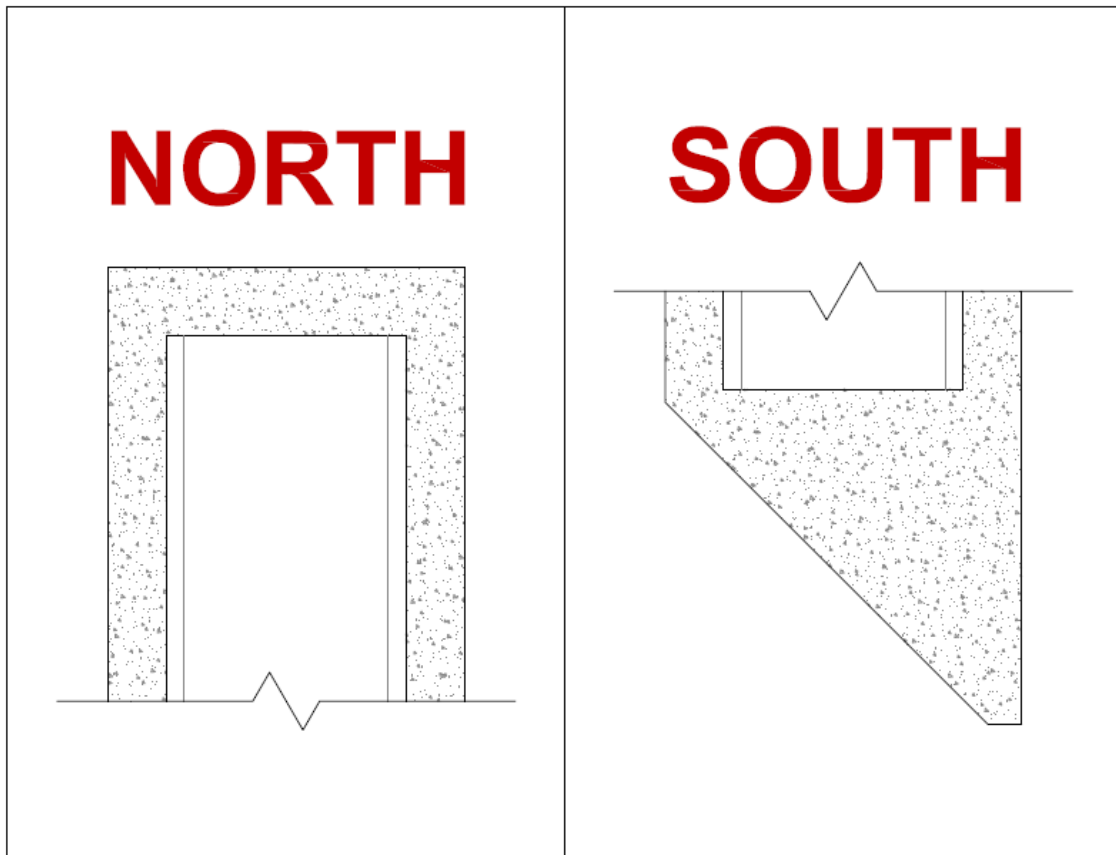
SOUTH



Time since batching (hr.):	17
Ambient Temperature ($^{\circ}F$):	73
Max. Temperature ($^{\circ}F$):	137
Min. Temperature ($^{\circ}F$):	114
Max. Temp. Differential ($^{\circ}F$):	23
Formwork Material:	Steel
Contour Spacing ($^{\circ}F$):	6
Skew angle (deg.):	45

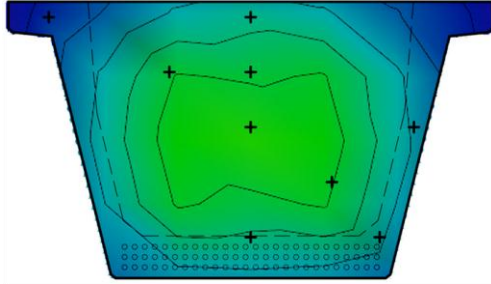
E.3 BEAM 2 TEMPERATURE PLOTS

Figure E-3: Beam 2 profile



Beam 2: Maximum Temperature

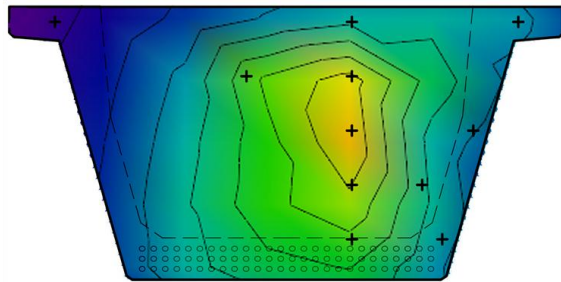
NORTH



Time since batching (hr.):	18
Ambient Temperature (°F):	74
Max. Temperature (°F):	142
Min. Temperature (°F):	113
Max. Temp. Differential (°F):	29
Formwork Material:	Steel
Contour Spacing (°F):	10
Skew angle (deg.):	0



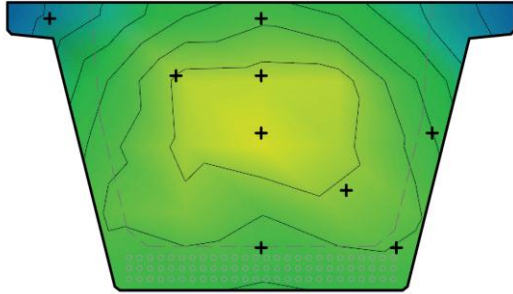
SOUTH



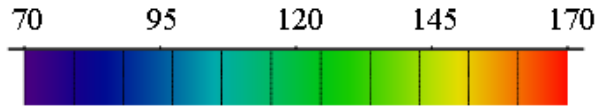
Time since batching (hr.):	25
Ambient Temperature (°F):	73
Max. Temperature (°F):	160
Min. Temperature (°F):	107
Max. Temp. Differential (°F):	53
Formwork Material:	Steel
Contour Spacing (°F):	10
Skew angle (deg.):	45

Beam 2: Differential Temperature

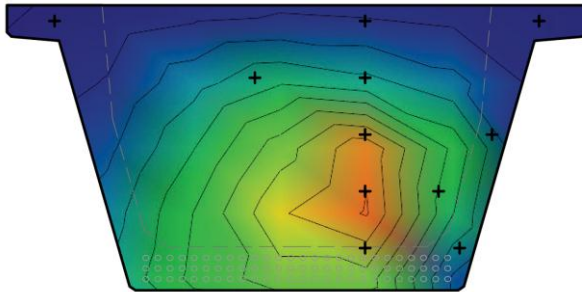
NORTH



Time since batching (hr.):	26
Ambient Temperature (°F):	74
Max. Temperature (°F):	142
Min. Temperature (°F):	108
Max. Temp. Differential (°F):	34
Formwork Material:	Steel
Contour Spacing (°F):	10
Skew angle (deg.):	0



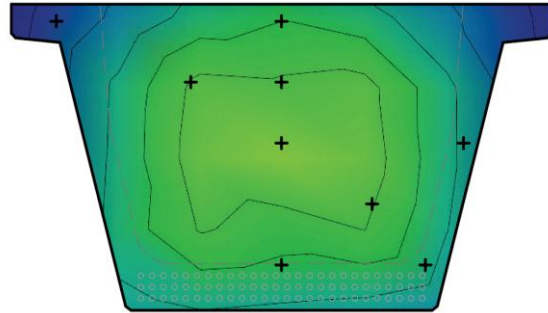
SOUTH



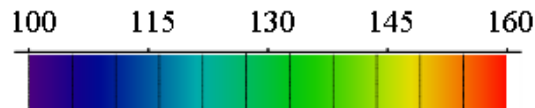
Time since batching (hr.):	10
Ambient Temperature (°F):	83
Max. Temperature (°F):	144
Min. Temperature (°F):	89
Max. Temp. Differential (°F):	55
Formwork Material:	Steel
Contour Spacing (°F):	10
Skew angle (deg.):	45

Beam 2: Prestress Release Temperature

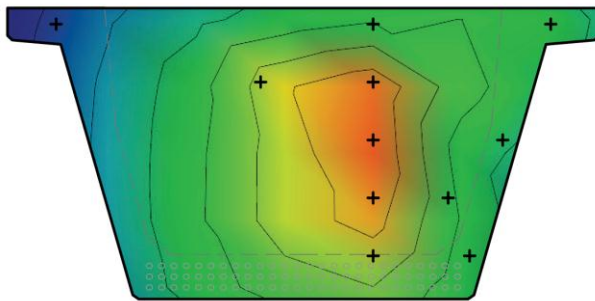
NORTH



Time since batching (hr.):	18
Ambient Temperature (°F):	73
Max. Temperature (°F):	142
Min. Temperature (°F):	112
Max. Temp. Differential (°F):	30
Formwork Material:	Steel
Contour Spacing (°F):	6
Skew angle (deg.):	0



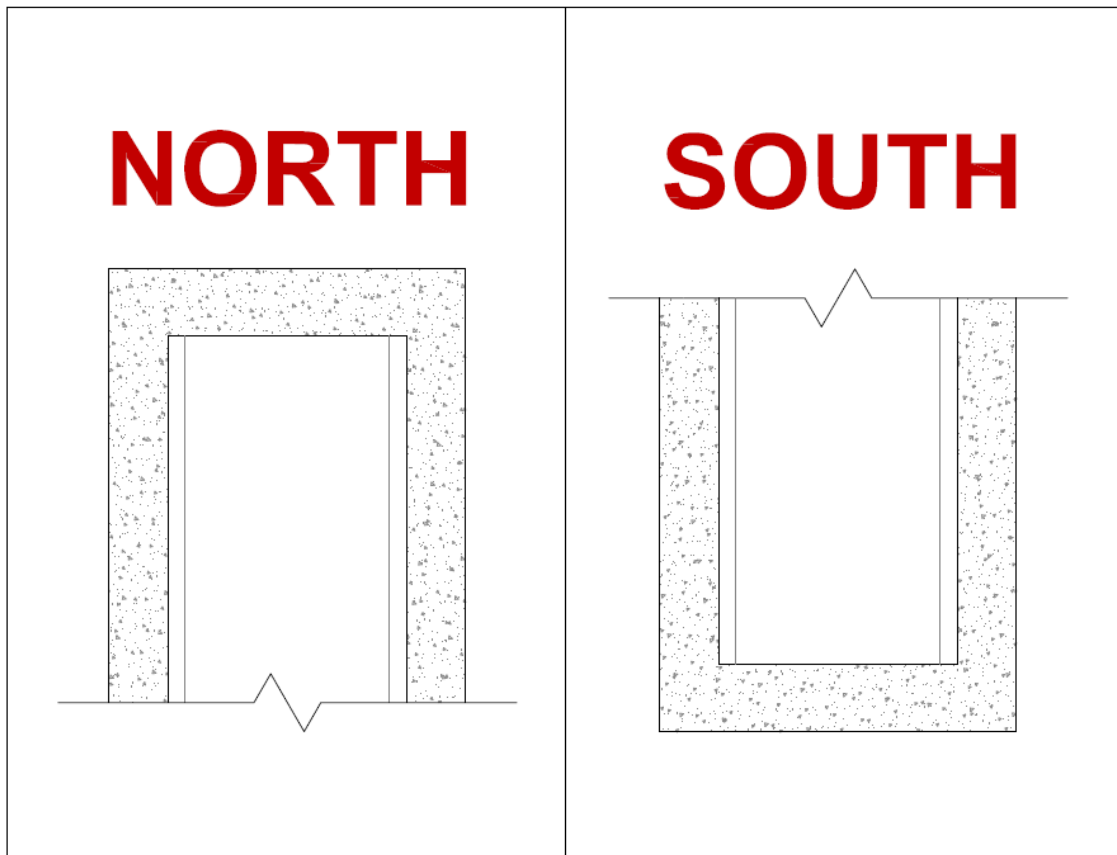
SOUTH



Time since batching (hr.):	18
Ambient Temperature (°F):	73
Max. Temperature (°F):	157
Min. Temperature (°F):	115
Max. Temp. Differential (°F):	42
Formwork Material:	Steel
Contour Spacing (°F):	6
Skew angle (deg.):	45

E.4 BEAM 3 TEMPERATURE PROFILES

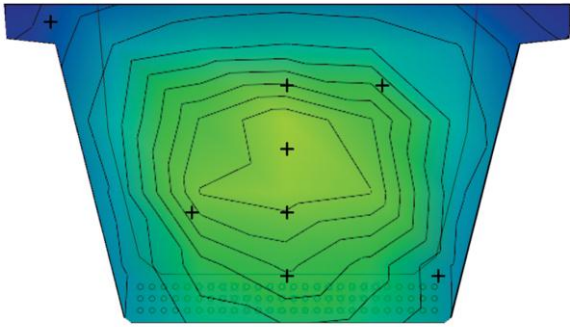

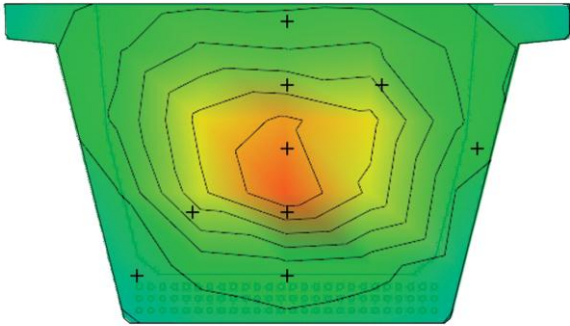
Figure E-4: Beam 3 profile



Beam 3: Maximum Temperature

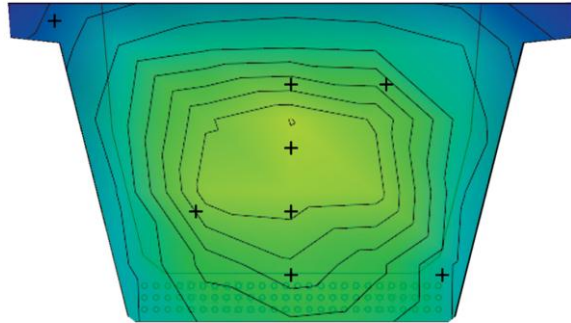
<u>NORTH</u>		Time since batching (hr.):	22
		Ambient Temperature ($^{\circ}F$):	101
		Max. Temperature ($^{\circ}F$):	165
		Min. Temperature ($^{\circ}F$):	113
		Max. Temp. Differential ($^{\circ}F$):	52
		Formwork Material:	Steel
		Contour Spacing ($^{\circ}F$):	10
		Skew angle (deg.):	0
<u>SOUTH</u>		Time since batching (hr.):	23
		Ambient Temperature ($^{\circ}F$):	99
		Max. Temperature ($^{\circ}F$):	184
		Min. Temperature ($^{\circ}F$):	135
		Max. Temp. Differential ($^{\circ}F$):	49
		Formwork Material:	Wood
		Contour Spacing ($^{\circ}F$):	10
		Skew angle (deg.):	0

Beam 3: Differential Temperature

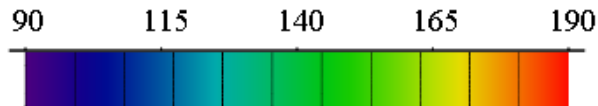
<u>NORTH</u>		Time since batching (hr.):	25
	Ambient Temperature ($^{\circ}F$):	99	
	Max. Temperature ($^{\circ}F$):	163	
	Min. Temperature ($^{\circ}F$):	111	
	Max. Temp. Differential ($^{\circ}F$):	52	
	Formwork Material:	Steel	
	Contour Spacing ($^{\circ}F$):	10	
	Skew angle (deg.):	0	
			
<u>SOUTH</u>		Time since batching (hr.):	25
	Ambient Temperature ($^{\circ}F$):	98	
	Max. Temperature ($^{\circ}F$):	180	
	Min. Temperature ($^{\circ}F$):	133	
	Max. Temp. Differential ($^{\circ}F$):	47	
	Formwork Material:	Wood	
	Contour Spacing ($^{\circ}F$):	10	
	Skew angle (deg.):	0	

Beam 3: Prestress Release Temperature

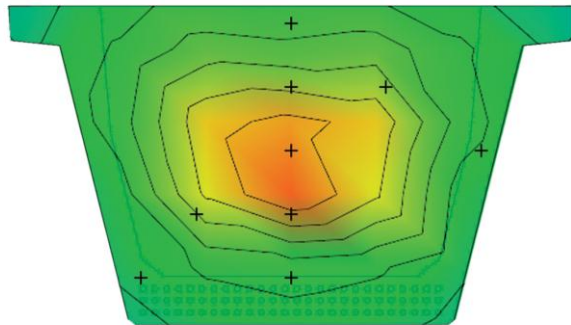
NORTH



Time since batching (hr.):	20
Ambient Temperature (°F):	95
Max. Temperature (°F):	164
Min. Temperature (°F):	114
Max. Temp. Differential (°F):	50
Formwork Material:	Steel
Contour Spacing (°F):	10
Skew angle (deg.):	0



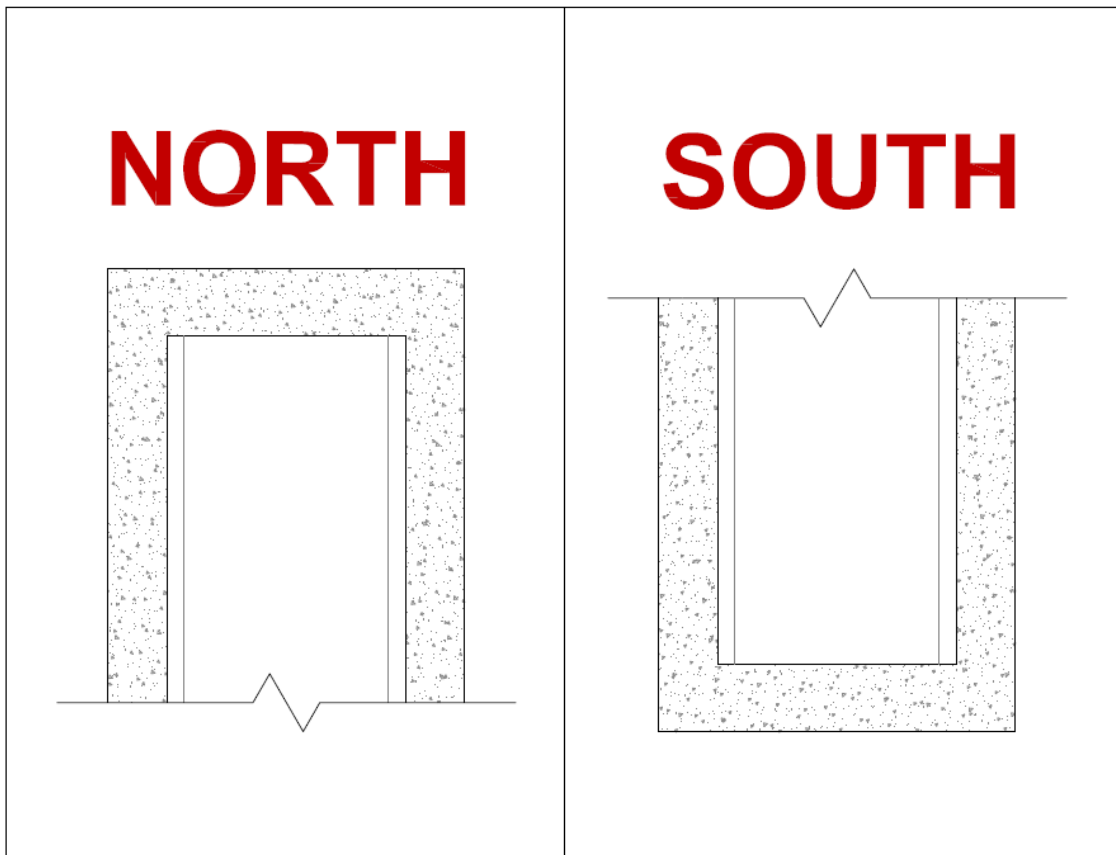
SOUTH



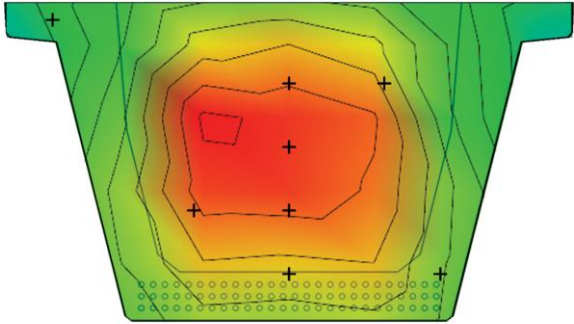
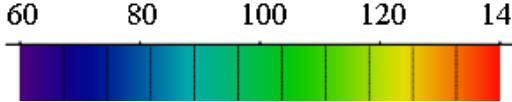
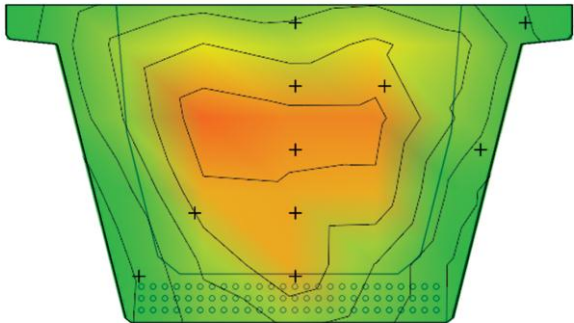
Time since batching (hr.):	20
Ambient Temperature (°F):	95
Max. Temperature (°F):	183
Min. Temperature (°F):	137
Max. Temp. Differential (°F):	46
Formwork Material:	Steel
Contour Spacing (°F):	10
Skew angle (deg.):	0

E.5 BEAM 4 TEMPERATURE PROFILES

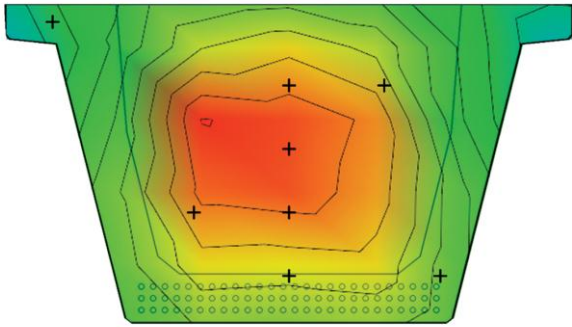

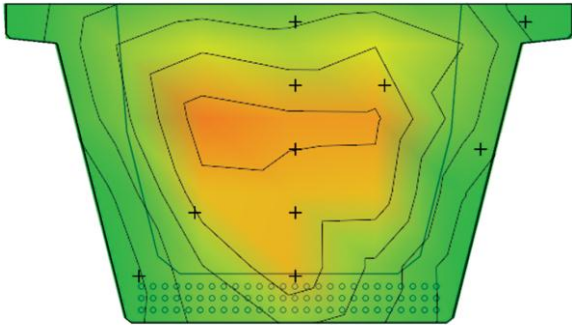
Figure E-5: Beam 4 profile



Beam 4: Maximum Temperature

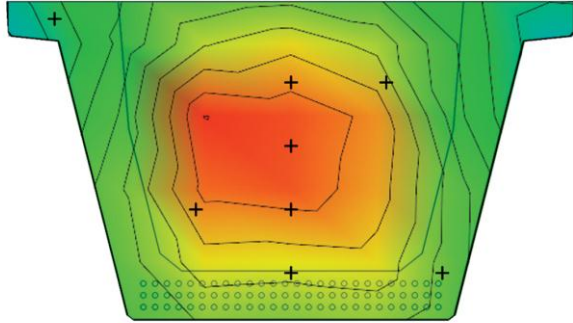
<u>NORTH</u>		Time since batching (hr.):	31
	Ambient Temperature (°F):	67	
	Max. Temperature (°F):	131	
	Min. Temperature (°F):	102	
	Max. Temp. Differential (°F):	29	
	Formwork Material:	Steel	
	Contour Spacing (°F):	8	
	Skew angle (deg.):	0	
			
<u>SOUTH</u>		Time since batching (hr.):	26
	Ambient Temperature (°F):	73	
	Max. Temperature (°F):	139	
	Min. Temperature (°F):	95	
	Max. Temp. Differential (°F):	44	
	Formwork Material:	Wood	
	Contour Spacing (°F):	8	
	Skew angle (deg.):	0	

Beam 4: Differential Temperature

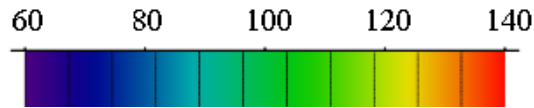
<u>NORTH</u>	
	Time since batching (hr.): 36
	Ambient Temperature (°F): 77
	Max. Temperature (°F): 137
	Min. Temperature (°F): 92
	Max. Temp. Differential (°F): 45
	Formwork Material: Steel
	Contour Spacing (°F): 8
	Skew angle (deg.): 0
	
<u>SOUTH</u>	
	Time since batching (hr.): 29
	Ambient Temperature (°F): 69
	Max. Temperature (°F): 135
	Min. Temperature (°F): 101
	Max. Temp. Differential (°F): 34
	Formwork Material: Wood
	Contour Spacing (°F): 8
	Skew angle (deg.): 0

Beam 4: Prestress Release Temperature

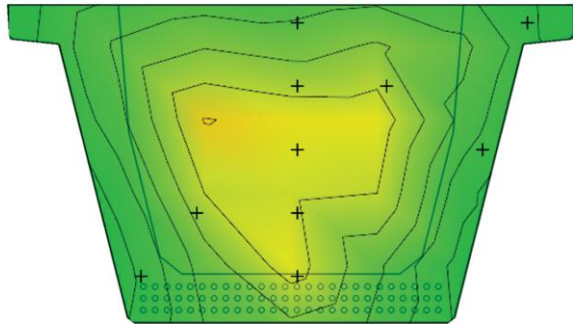
NORTH



Time since batching (hr.):	37
Ambient Temperature (°F):	77
Max. Temperature (°F):	137
Min. Temperature (°F):	113
Max. Temp. Differential (°F):	24
Formwork Material:	Steel
Contour Spacing (°F):	8
Skew angle (deg.):	0



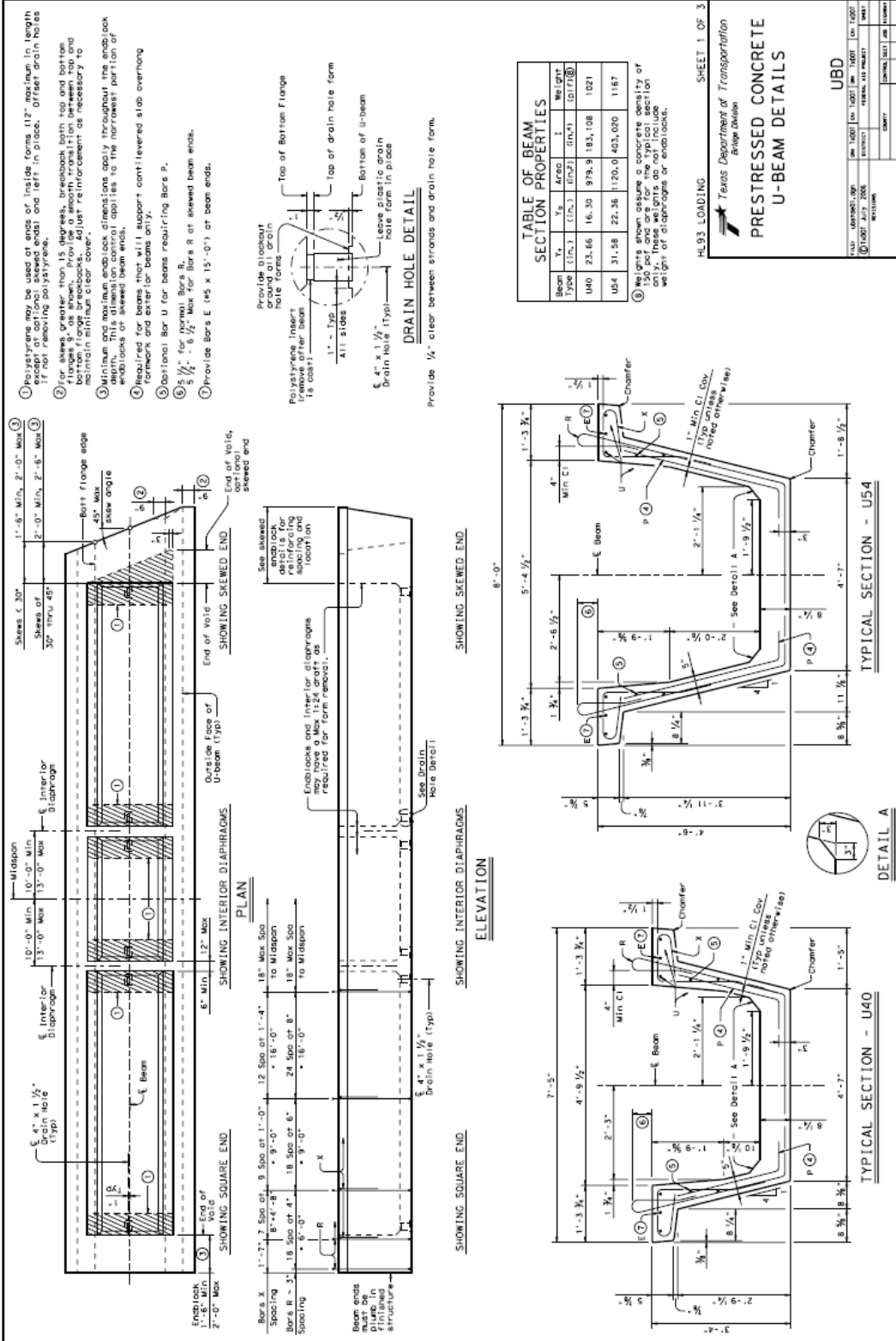
SOUTH



Time since batching (hr.):	37
Ambient Temperature (°F):	77
Max. Temperature (°F):	130
Min. Temperature (°F):	98
Max. Temp. Differential (°F):	32
Formwork Material:	Steel
Contour Spacing (°F):	8
Skew angle (deg.):	0

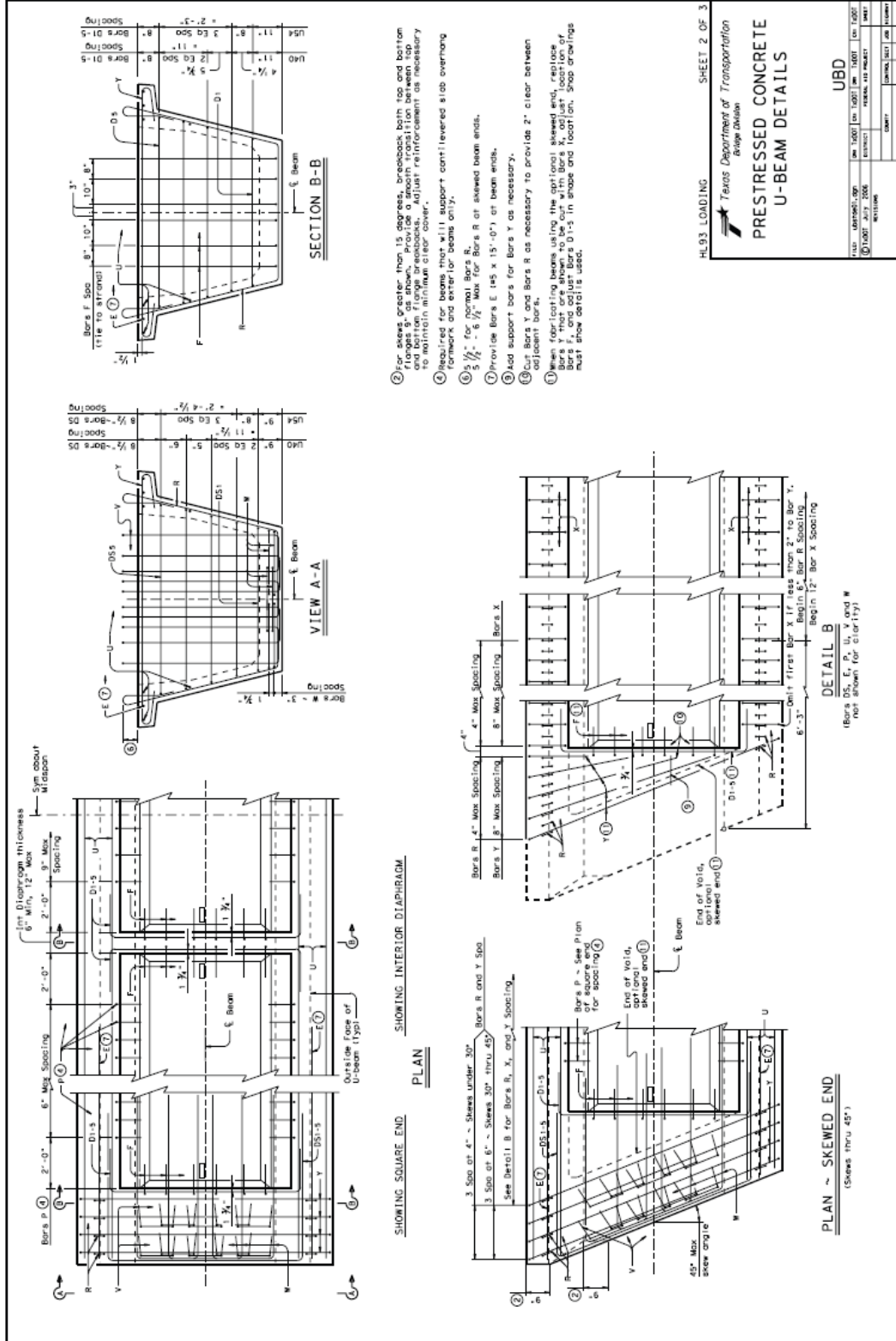
APPENDIX F

Texas Department of Transportation Standard U-Beam Drawings



HL93 LOADING SHEET 1 OF 3
 Texas Department of Transportation
 Bridge Division
PRESTRESSED CONCRETE U-BEAM DETAILS
 UBD
 DATE: 01/00/07
 DRAWN BY: J. W. BERRY
 CHECKED BY: J. W. BERRY
 PROJECT: 10000000000000000000
 SHEET NO.: 10000000000000000000

DISCLAIMER
 DATE
 THE USE OF THIS STANDARD IS GOVERNED BY THE TEXAS ENGINEERING PROFESSION BOARD'S REGULATIONS AND THE BOARD'S POLICY ON LIABILITY. THE BOARD AND ITS ENGINEERS ASSUME NO LIABILITY FOR THE CONSTRUCTION OF THIS STANDARD OR OTHER COMMENTS OR INFORMATION RESULTING OR OTHERWISE RESULTING FROM ITS USE.



DISCLAIMER: The use of this drawing is governed by the Texas Engineering Practice Act. The engineer assumes no responsibility for the construction of this structure to other than the extent of the design shown on this drawing. The engineer is not responsible for incorrect results or omissions resulting from the use of this drawing.

DATE: 10/10/00
 DRAWN BY: J. L. WILSON
 CHECKED BY: J. L. WILSON
 TITLE: PRESTRESSED CONCRETE U-BEAM DETAILS

- ① For skew greater than 15 degrees, breakback both top and bottom flanges 5' as shown. Provide a smooth transition between top and bottom flanges. Adjust reinforcement as necessary to obtain minimum clearances.
- ② Reinforce for beams that will support cantilevered slab overhang formwork and enter for beams only.
- ③ 5/8" for normal Bars R.
- ④ Provide Bars E (45 x 15'-0") at beam ends.
- ⑤ Add support bars for Bars Y as necessary.
- ⑥ Cut Bars U and Bars R as necessary to provide 2" clear between adjacent beams using the adjacent skewed end. Reinforce Bars Y that are shown to be cut with Bars R, adjust location of Bars F, and adjust Bars D1-5 in shape and location. Shop drawings must show details used.

HL93 LOADING SHEET 2 OF 3

Texas Department of Transportation
 Engineering Division

**PRESTRESSED CONCRETE
 U-BEAM DETAILS**

DATE: 10/10/00	BY: J. L. WILSON	DATE: 10/10/00
DESIGNED BY: J. L. WILSON	CHECKED BY: J. L. WILSON	DATE: 10/10/00
SCALE: AS SHOWN	PROJECT: HL93 LOADING	SHEET: 2 OF 3

UBD

Beam Length - 3"

2'-5" Min. LOD

BARS U (#5)

Bars u may be placed with multiple segments, provided the length of each segment is less than 10 ft in length and 40 ft Min C-C spacings.

BARS V (#4)
(ISOMETRIC VIEW)

USA, LMO
3'-8" x 4'-10"
1'-2" x 1'-2" x 3'-0" x 4'-0"
Lap (Typ)
Min. Reversals

BARS W (#4)

USA, LMO
2'-0" x 3'-0" x 2'-0" x 3'-0" x 2'-0" x 3'-0" x 2'-0" x 3'-0"

BARS Y (#4)

USA, LMO
3'-0" x 4'-10" x 3'-0" x 4'-10" x 3'-0" x 4'-10"

BARS X (#4)

USA, LMO
3'-0" x 4'-10" x 3'-0" x 4'-10" x 3'-0" x 4'-10"

BARS P (#4)

USA, LMO
3'-0" x 4'-10" x 3'-0" x 4'-10" x 3'-0" x 4'-10"

BARS F (#4)

USA, LMO
3'-0" x 4'-10" x 3'-0" x 4'-10"

BARS R (#4)

USA, LMO
3'-0" x 4'-10" x 3'-0" x 4'-10"

BARS DS-1.5 (#4)

USA, LMO
3'-0" x 4'-10" x 3'-0" x 4'-10"

BARS D-1.5 (#4)

USA, LMO
3'-0" x 4'-10" x 3'-0" x 4'-10"

GENERAL NOTES:

Reinforcing steel shall be placed in accordance with the Texas Department of Transportation (TxDOT) Standard Specifications for Construction of Highway Bridges and Structures, 2013 Edition, unless otherwise noted. The use of this drawing is governed by the Texas Engineering Experiment Station (TEES) Terms and Conditions. The user of this drawing shall be responsible for the coordination of this drawing with the relevant Texas Department of Transportation (TxDOT) Standard Specifications for Construction of Highway Bridges and Structures, 2013 Edition, and any other documents or drawings resulting from this use.

DISCLAIMER:

The user of this drawing shall be responsible for the coordination of this drawing with the relevant Texas Department of Transportation (TxDOT) Standard Specifications for Construction of Highway Bridges and Structures, 2013 Edition, and any other documents or drawings resulting from this use.

HL93 LOADING SHEET 3 OF 3

**PRESTRESSED CONCRETE
U-BEAM DETAILS**

Texas Department of Transportation
Bridge Division

UBD

REV	DATE	BY	CHKD	APP'D
10	10/27/2016	WJT/DAK	JAC/JAC	
09	10/27/2016	WJT/DAK	JAC/JAC	
08	10/27/2016	WJT/DAK	JAC/JAC	
07	10/27/2016	WJT/DAK	JAC/JAC	
06	10/27/2016	WJT/DAK	JAC/JAC	
05	10/27/2016	WJT/DAK	JAC/JAC	
04	10/27/2016	WJT/DAK	JAC/JAC	
03	10/27/2016	WJT/DAK	JAC/JAC	
02	10/27/2016	WJT/DAK	JAC/JAC	
01	10/27/2016	WJT/DAK	JAC/JAC	

DISCLAIMER
The use of this standard is governed by the Texas Engineering Practice Act. The user assumes all liability for the consequences of its application. The user shall be responsible for the consequences of its application. The user shall be responsible for the consequences of its application.

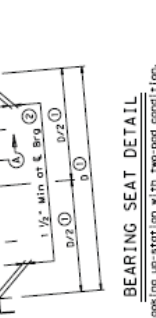
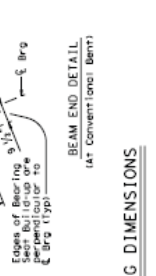
DATE	REVISED BY	DATE	REVISED BY
10/07/2008	WILLIAM	10/07/2008	WILLIAM

- Measured along ϵ of Bearing.
- Reinforce bearing seat bulldogs greater than 1/2" from ϵ of concrete structure, 300 as per 1909.
- See Estimating, Quantities and Bearing Seat Elevation sheet for right and left elevations and locations.
- Unless noted otherwise in the plans.
- Locate permanent mark here.
- Fabricated pad top surface slope must not vary from plan bearing pad taper by more than $(\frac{1}{16} \text{ length}) \text{ IN/IN}$.
- Use 0.195" thick steel (unless parallel to the bottom surface of the pad, except the top laminate) and a customer bearing pad must receive the same bearing pad taper. Refer to the Fabricator's Report of bearing pad taper, and or amount of all bearings will be developed by the bearing fabricator. Permanently mark each bearing with the bearing layout to the fabricator of furnishing and installing elastomeric bearings. Is included in unit price bid for Pressurized Concrete U-Beams.

GENERAL NOTES:
Shop drawings for approval are required. Finish Bearing Surface with a wood float and free of all loose material before placing bearing pads. Reinforcement bars in the beams and a customer bearing pad must receive the same bearing pad taper. Refer to the Fabricator's Report of bearing pad taper, and or amount of all bearings will be developed by the bearing fabricator. Permanently mark each bearing with the bearing layout to the fabricator of furnishing and installing elastomeric bearings. Is included in unit price bid for Pressurized Concrete U-Beams.

BEARING SEAT DIMENSION "D" (4)

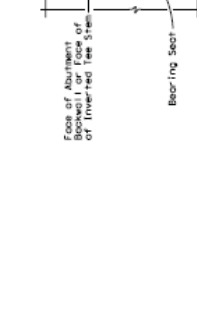
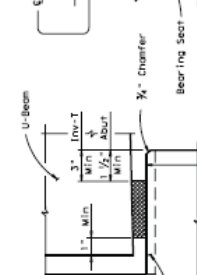
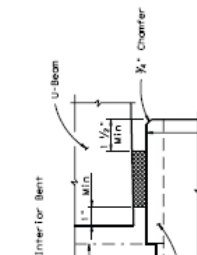
BEAM ANGLE	70°
75° thru 80°	4'-0"
80° thru 85°	5'-0"
85° thru 90°	5'-6"



BEARING DIMENSIONS

BEAM END DETAIL (AT CONVENTIONAL BENT)

BEAM END DETAIL (AT Abutment Backwall or Inverted Tee Stem)



BEARING PAD DETAILS

ONE-PAD DETAIL Type U2-N* Bearing

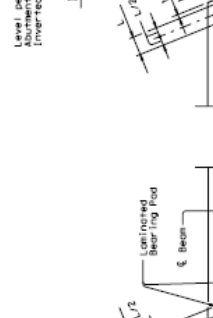
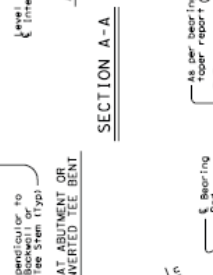
ONE-PAD DETAIL Type U1-N* Bearing

ONE-PAD DETAIL Type U2-N* Bearing

ONE-PAD DETAIL Type U1-N* Bearing

TABLE OF ELASTOMERIC BEARING PAD DIMENSIONS (ALL U-BEAM TYPES)

W	One-Pad (Type U1-N*) (6)		Two-Pad (Type U2-N*) (6)	
	L	T	W	L
32"	9"	2 1/2"	16"	9"



BEARING PAD DETAILS

ONE-PAD DETAIL Type U2-N* Bearing

ONE-PAD DETAIL Type U1-N* Bearing

ONE-PAD DETAIL Type U2-N* Bearing

ONE-PAD DETAIL Type U1-N* Bearing

Notes: The use of Polypropylene (natural fibers) for the manufacture of bearing pads is not permitted.

HL-93. LOADING

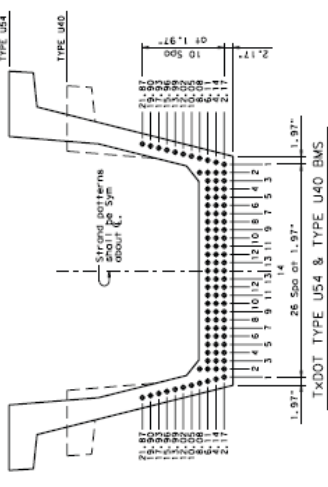
Texas Department of Transportation
Texas Division

ELASTOMERIC BEARING AND BEARING SEAT DETAILS
PRESTR. CONC U-BEAMS

UBEB

DATE	REVISED BY	DATE	REVISED BY
10/07/2008	WILLIAM	10/07/2008	WILLIAM

STRUCTURE	SPAN NO.	BEAM TYPE	PRESTRESSING STRINGS		DESIGNED STRAND PATTERNS (STRAIGHT STRANDS)		CONCRETE		OPTIONAL DESIGN								
			STRENGTH INC.	SIZE (mm)	TOTAL NO.	END "A" (mm)	END "B" (mm)	DESIGNED STRANDS	NUMBER OF STRANDS	MINIMUM RELAXATION STRAIN (%)	28 DAY STRENGTH (MPa)	SLIP TEST (MPa)	MINIMUM CAPACITY (kN)	DESIGN CAPACITY (kN)	LONGITUDINAL POSITION		



TXDOT TYPE U54 & TYPE U40 BMS

GENERAL NOTES:
 Designed in accordance with AASHTO LRFD Specifications. Fabricator shall be responsible for determining strand placement in field. All reinforcing bars shall be Grade 60. When shown on this sheet, the fabricator has the option of using a different strand size than that shown. All optional design submissions and shop drawings must be signed, sealed and dated by a registered Professional Engineer, no greater than that of the design engineer, and shall contain a relative humidity of 75 percent. Optional designs must meet or conform to the design beam as low as possible on the 1.97" grid system. Fill row "2, 11", then row "4, 14", then row "6, 11", etc., beginning each row in the cut position and, distributing uniformly as required. All strands, including those in the web, must be adequately distributed across the section. Do not use lap splices. Do not use devices to prevent do not debar strands in position "1". Distribute debarred strands working inward, with debarbing staggered in each row. Increase debarred strands up to plastic tubing along entire span. Plastic tubing may be used provided the seal of the tubing is sufficiently tight to prevent moisture from entering the strands. Wrapping of strands with tape to provide debarbing is not permitted. Full-length debarred strands are not permitted in strong positions. Full-length debarred strands in row "2, 11" and internal vibrator cables cannot exceed 1% diameter for first stage, full-length debarred strands for the design beam must be low relaxation strands. Strand placement and spacing of strands is based on exact conversions from a metric grid spacing of 50mm.

① Portion of full HL 93

HL 93 - LOADING
 Texas Department of Transportation
 Bridge Division
PRESTRESSED CONCRETE U-BEAMS
 (DESIGN DATA)

UBND

DATE: 07/10/08
 DRAWN BY: [blank]
 CHECKED BY: [blank]
 DESIGNED BY: [blank]

1	DATE	BY	CHKD	APP'D
2				
3				
4				
5				
6				
7				
8				
9				
10				
11				
12				
13				
14				
15				
16				
17				
18				
19				
20				

REFERENCES

- AASHTO. *LRFD Bridge Design Specifications*. Washington D.C.: American Association of State and Highway Transportation Officials, 1994.
- AASHTO. *LRFD Bridge Design Specifications*. Washington D. C.: American Association of State and Highway Transportation Officials, 2009 Interim.
- AASHTO. *LRFD Bridge Design Specifications*. Washington, D.C.: American Association of State Highway and Transportation Officials, 2007.
- ACI 318. *Building Code Requirements for Structural Concrete*. Farmington Hills: American Concrete Institute, 2008.
- ACI-ASCE Joint Committee 445. *Recent Approaches to Shear Design of Structural Concrete*. Farmington Hills: American Concrete Institute, 2000.
- Avendaño, Alejandro Raul. *Shear Strength and Behavior of Prestressed Concrete Beams*. Austin: University of Texas at Austin, 2008.
- Birkeland, Philip W., and Halvard W. Birkeland. "Connections in Precast Concrete Construction." *Journal of the American Concrete Institute*, March 1966: 345-368.
- Hawkins, Neil M., and Daniel A. Kuchma. *NCHRP Report 579: Application of LRFD Bridge Design Specifications to High-Strength Structural Concrete Shear Provisions*. National Cooperative Highway Research Program, Washington D.C.: Transportation Research Board, 2007.
- Hawkins, Neil M., Daniel A. Kuchma, Robert F. Mast, M. Lee Marsh, and Karl-Heinz Reineck. *NCHRP Report 549: Simplified Shear Design of Structural Concrete Members*. National Cooperative Highway Research Program, Washington, D.C.: Transportation Research Board, 2005.
- Hovell, Catherine, Alejandro Avendaño, David Dunkman, Andrew Moore, Oguzhan Bayrak, and James Jirsa. *Behavior of Texas U-Beams and Box-Beams at Prestress*

- Transfer and Under Shear Loads (Interim Report)*. University of Texas at Austin, Austin: Center for Transportation Research, 2010.
- Llanos, Gustavo, Brandon E. Ross, and H. R. Hamilton III. *Shear Performance of Existing Prestressed Concrete Dridge Girders*. Final Report, Tallahassee: Florida Department of Transportation, 2009.
- Nagle, Thomas J., and Daniel A. Kuchma. *Nontraditional Limitations on the Shear Capacity of Prestressed Concrete Girders*. Urbana: University of Illinois, 2007.

VITA

Andrew Michael Moore was born to Linda and Paul Moore on June 17th, 1984 in Little Rock, Arkansas. He grew up in Little Rock and graduated from Little Rock Catholic High School. Afterwards he studied at and received his Bachelors of Science in Engineering from The University of Arkansas at Fayetteville.

After graduating Andrew enrolled at The University of Texas at Austin and worked towards his master's degree in structural engineering as a graduate research assistant at the Ferguson Structural Engineering Laboratory. He obtained his Masters of Science in Engineering in December of 2010 and will continue to work towards his doctoral degree at The University of Texas at Austin.

Permanent address: 1209 Fawnwood Rd.
 Little Rock, AR 72227

ammoore84@gmail.com

This thesis was typed by the author.